

**Membrane/adsorption hybrid processes for water
purification and lupanine isolation from lupin beans
debittering wastewater**

Ana Teresa Afonso Parente Mota

Thesis to obtain the Master of Science Degree in

Bioengineering and Nanosystems

Supervisors:

Prof. Frederico Castelo Alves Ferreira

Dr. Teresa Sofia Araújo Esteves

Examination Committee

Chairperson: Prof. Gabriel António Amaro Monteiro

Supervisor: Prof. Frederico Castelo Alves Ferreira

Members of the Committee: Prof. Carlos Alberto Mateus Afonso

Eng. Renata Alexandra Ferreira Loureiro

December 2017

*“The very nature of science is discoveries,
and the best of those discoveries are the ones you don’t expect.”*

— Neil deGrasse Tyson

Resumo

A lupanina é um alcalóide de quinolizidina presente nos tremoços. Este composto pode ser utilizado para sintetizar um ligando quiral essencial para síntese assimétrica (esparteína). A lupanina é uma molécula tóxica e confere um sabor amargo aos tremoços. Na indústria alimentar, foi desenvolvido um processo de “desintoxicação” para remover o referido alcalóide dos tremoços a fim de garantir a segurança do seu consumo. Este processo utiliza uma quantidade significativa de água limpa e origina águas residuais ricas em lupanina. Nesta tese foi explorada uma abordagem multidisciplinar para isolar a lupanina presente nas águas residuais dos tremoços. Um processo viável começa com uma centrifugação para remoção de sólidos em suspensão seguido de duas filtrações: uma ultrafiltração para reduzir a quantidade de (macro)moléculas e uma nanofiltração para redução do volume da água residual e concentração de lupanina no retentado. Depois, uma resina de troca iônica com grupos funcionais ácidos (Dowex MAC-3) foi selecionada para isolar a lupanina a partir do retentado da nanofiltração. A recuperação da lupanina da resina é feita com uma solução de NaOH em água, seguida de uma extração líquido-líquido com diclorometano. Polímeros de impressão molecular foram sintetizados usando a lupanina como “template”, de modo a que pudessem ser incluídos como última operação unitária do processo para isolar este alcalóide. O polímero mais eficiente para a lupanina foi obtido utilizando ácido itacónico como monómero funcional.

Palavras-chave

Águas residuais de desintoxicação dos tremoços, lupanina, ultrafiltração, nanofiltração, resina, extração líquido-líquido, polímero de impressão molecular.

Abstract

Lupanine is a quinolizidine alkaloid (QA) that can be found in white lupin beans. This compound can be utilized to synthesize an essential chiral ligand for asymmetric synthesis (sparteine). Lupanine is considered to be toxic and confer a bitter taste to the beans. The food industry developed a “debittering” process for removing this alkaloid from these beans so that their consumption is safe. This process of lupin beans “debittering” uses large amounts of fresh water and yields wastewater that is rich in lupanine. In this thesis, a multidisciplinary approach was explored to isolate lupanine from the lupin beans debittering wastewater. A viable process starts with a centrifugation to remove suspended solids followed by two filtration steps, ultrafiltration to remove the (macro)molecules, and a nanofiltration for wastewater volume reduction and lupanine concentration in the retentate. Then, a weak acid cation exchanger resin (Dowex MAC-3) was selected to isolate lupanine from the nanofiltration retentate. Lupanine recovery from the resins was done using a solution of NaOH in water, followed by a liquid-liquid extraction with dichloromethane. Molecularly Imprinted Polymers (MIPs) were synthesized using lupanine as a template, to be included as the last unit operation of the process to isolate the alkaloid. The most efficient MIP for lupanine was obtained using itaconic acid as the functional monomer.

Keywords

Lupin beans debittering wastewater, lupanine, ultrafiltration, nanofiltration, resin, liquid-liquid extraction, molecularly imprinted polymer.

Acknowledgments

Quero agradecer aos meus orientadores, professor Frederico e Teresa pela oportunidade que me deram de participar neste projeto, por todo o acompanhamento, pela confiança, dedicação e por tudo o que me ensinaram durante esta fase essencial para a conclusão do mestrado.

Ao Flávio pelas incontáveis vezes em que me ajudou, por toda a disponibilidade, generosidade, simpatia e otimismo. Foi sem dúvida uma pessoa incansável, e sem ele muito daquilo que fiz não teria sido possível. Obrigada por tudo o que me ensinaste, por tantas vezes me teres animado com a tua boa disposição e por me mostrares que tudo tem um lado bom.

Ao professor Carlos Afonso da Faculdade de Farmácia, por ter sido sempre tão prestável, pela sua simpatia, conselhos e por todo o interesse que sempre mostrou no meu trabalho.

À Raquel da Faculdade de Farmácia por ter sido sempre tão querida comigo, e por se ter sempre mostrado disponível para me ajudar no que fosse preciso.

À Sara por tão rapidamente se ter tornado uma amiga importante para mim. Por ter tido paciência para aturar as minhas lamúrias, e por me ter apoiado sempre, sobretudo nos momentos mais críticos e stressantes. Obrigada por tantas vezes me teres feito rir quando a disposição para isso não era a melhor.

Aos meus colegas de laboratório, Ricardo, Luís e Rui Pedro, pela simpatia e por se terem mostrado sempre tão prestáveis.

À Marisa por ter sido sempre uma amiga tão querida, paciente, pela preocupação e pelos conselhos que me deu, essenciais sobretudo na fase final desta tese.

Por último, mas não menos importante, quero agradecer à minha família, especialmente aos meus pais e à minha irmã pelo apoio incondicional, pela paciência e por me ensinarem que tudo se consegue com trabalho e dedicação.

Gostaria também de agradecer financiamento da Fundação para a Ciência e Tecnologia (FCT) através de projecto "**Biorg4WasteWaterVal+: Bioorganic Novel Approaches for Food Processing WasteWater Treatment and Valorisation: Lupanine Case Study**" (**WaterWorks2014, ID 278**), bem como scholarship SFRH/BPD/116767/2016 e iBB-Institute for Bioengineering and Biosciences (FCT reference: UID/BIO/04565/2013 and POL2020 reference 007317).

Table of Contents

Resumo	v
Palavras-chave	v
Abstract.....	vii
Keywords	vii
Acknowledgments	ix
Table of Contents	xi
List of Abbreviations	xiv
List of Figures	xv
List of Tables	xix
1. Objectives and Thesis Outline.....	1
2. Introduction.....	2
2.1 Lupanine.....	2
2.1.1. Natural occurrence	2
2.1.2. Adverse health effects.....	3
2.1.3. Industrial lupin beans debittering process.....	3
2.1.4. Pharmaceutical interest.....	4
2.1.5. Sparteine: a valuable chiral ligand that can be obtained from lupanine.....	4
2.2. Chirality.....	7
2.2.1. Stereoisomers: enantiomers and diastereoisomers.....	7
2.2.2. Optical isomers and biological systems	7
2.2.3. Resolution of enantiomers.....	8
2.3. Extraction of lupanine from white lupin beans leaching waters	10
2.3.1. Membrane processes: ultrafiltration and nanofiltration	10
2.3.2. Resins: ion exchangers and polymeric adsorbents.....	12
2.3.3. Liquid-liquid extractions with organic solvents	14
2.3.4. Molecularly Imprinted Polymers	19
2.3.4.1. Synthesis of MIPs.....	19
2.3.4.2. Chiral MIPs	25
2.3.4.3. Applications	28

2.4. Degradation of lupanine	29
3. Materials and Methods	30
3.1. Materials and Reagents	30
3.1.1. Lupanine quantification.....	30
3.1.2. Liquid-liquid extractions	30
3.1.3. Resins.....	30
3.1.4. Nanofiltration and Ultrafiltration	31
3.1.5. Molecularly Imprinted Polymers	31
3.1.6. Enzymatic assays	32
3.2. Methods.....	33
3.2.1. Lupanine quantification and calibration curves	33
3.2.2. Chemical Oxygen Demand (COD)	33
3.2.3. Liquid-liquid extractions	36
3.2.4. Resins.....	36
3.2.5. Nanofiltration and Ultrafiltration	37
3.2.6. Molecularly Imprinted Polymers	38
3.2.7. Enantiomeric Excess	39
3.2.8. Enzymatic Assays	40
4. Results and discussion.....	41
4.1. Improvement of unit operations: membranes, organic solvents and resins.....	41
4.1.1. Membrane-based processes.....	41
4.1.1.1. Ultrafiltration and nanofiltration membranes assessment	42
4.1.1.2. Nanofiltration membrane performance: recirculation and concentration studies with NF270	45
4.1.2. Extraction of lupanine with organic solvents	51
4.1.2.1. Screening of the best solvents: % extraction	51
4.1.2.2. COD retained.....	53
4.1.2.3. Water contamination.....	54
4.1.2.4. Environmental impact, waste and human health	55
4.1.2.5. Final decisions for liquid-liquid extractions	55
4.1.3. Extraction of lupanine with resins.....	56
4.1.3.1. Screening of the best resins: % binding	56

4.1.3.2. Regeneration assays and lupanine recovery	59
4.1.3.3. Binding isotherms	61
4.1.3.4. COD retained.....	63
4.1.3.5. Recyclability.....	64
4.1.3.6. Final remarks on resins selection to isolate lupanine.....	65
4.2. Molecularly Imprinted Polymers for lupanine	66
4.2.1. Screening of monomers using racemic lupanine	66
4.2.2. Chiral MIP for lupanine resolution	69
4.2.3. MIPs regeneration and lupanine recovery.....	70
4.3. Enzymatic transformation of lupanine	72
4.4. Lupanine Recovery Process	73
5. Conclusions and Future Work.....	77
6. References	78
Annexes.....	A
A. Calibration curves.....	A
B. Chromatograms.....	B
C. Recirculation experiments	D
D. Langmuir and Freundlich Isotherms.....	D

List of Abbreviations

ACN	Acetonitrile
AIBN	Azobis(isobutyronitrile)
COD	Chemical Oxygen Demand
CSP	Chiral Stationary Phase
DCM	Dichloromethane
ee	Enantiomeric excess
EGDMA	Ethylene Glycol Dimethacrylate
EtOH	Ethanol
HCl	Hydrochloric Acid
HPLC	High Performance Liquid Chromatography
IA	Itaconic Acid
KOH	Potassium Hydroxide
MAA	Methacrylic Acid
MeOH	Methanol
MIBK	Methyl Isobutyl Ketone
MIP	Molecularly Imprinted Polymer
MMA	Methyl Methacrylate
MTBE	Methyl <i>tert</i> -Butyl Ether
MWCO	Molecular weight cut-off
NaOH	Sodium Hydroxide
NF	Nanofiltration
NIP	Non-Imprinted Polymer
NIPAM	N-isopropylacrylamide
PBS	Phosphate Buffer Solution
QA	Quinolizidine Alkaloid
rpm	Revolutions per minute
UF	Ultrafiltration

List of Figures

Figure 1. Structure of lupanine and sparteine [3].	2
Figure 2. Main intermediates of the biosynthetic pathway of QAs. Adapted from [10].	2
Figure 3. Structure of acetylcholine (natural ligand of the neuroreceptor) and lupanine. The chemical group indicated in each molecule corresponds to the binding site [6].	3
Figure 4. Reduction of (-)-lupanine to (+)-sparteine using LiAlH_4 in THF [15].	5
Figure 5. Reaction of nitromethane with 4-nitrobenzaldehyde using copper(II)-(-)-sparteine complexes [18].	5
Figure 6. Reaction of dimethylhydrazones using (-)-sparteine complexes to obtain a chiral α -alkylated ketone [19].	5
Figure 7. Sequential steps to obtain (S)-boroproline (indicated as (S)-7) using (-)-sparteine complexes. Adapted from [20].	6
Figure 8. (-)- and (+)-enantiomer of lupanine [15].	7
Figure 9. Example of a lipase-catalyzed transesterification of a secondary alcohol using isopropenyl acetate as acyl donor in toluene [30].	9
Figure 10. Possible types of fouling and concentration polarization phenomenon [40].	11
Figure 11. General structure of (A) a styrene (on the left) divinylbenzene (on the right) copolymer and (B) a polyacrylic polymer, that are used as matrix of both adsorbent and ion exchange resins.	12
Figure 12. Chemical structure of XAD-16 resin.	14
Figure 13. Generic structure of ginkgolic acids (GAs) and the compounds used as dummy templates [56].	21
Figure 14. Illustration of possible intermolecular interactions between atrazine (A) and triethylmelamine (B) with MAA and EDMA. R corresponds to $-\text{C}(\text{CH}_3)=\text{CH}_2$ and R' corresponds to $-\text{C}_2\text{H}_4\text{-OCO-C}(\text{CH}_3)=\text{CH}_2$ [57].	22
Figure 15. Structure of MAA and TfMAA [53].	23
Figure 16. Structure of ethylene glycol dimethacrylate [53].	23
Figure 17. Chemical structure of common initiators: (61) Azobisisobutyronitrile (AIBN); (62) azobisdimethylvaleronitrile (ADVN); (63) 4,40-azo(4-cyanovaleric acid) (ACID); (64) benzoylperoxide (BPO); (65) dimethylacetal of benzyl (BDK); (66) potassium persulfate (KPS) [59].	24
Figure 18. Predicted mechanism for lupanine hydrolysis at high hydrostatic pressure [76].	29
Figure 19. Variation of permeate flux with % concentration, during the ultrafiltration of 400 mL of lupin beans debittering water. The % concentration is the ratio between the volume of permeate over volume of feed.	42

Figure 20. Variation of permeate flux with % concentration, during the nanofiltration of 400 mL of lupin beans debittering water, and the nanofiltration of 250 mL of permeate from the ultrafiltration experiment. The % concentration is the ratio between the volume of permeate over volume of feed.	44
Figure 21. Variation of permeate flux with time of recirculation, after filtration of 400 mL of lupin beans wastewater to obtain 100 mL that were then recirculated. Two experiments were made: the first one for around 13 hours, at 420 mL/min. and the other one for around 17 hours at 600 mL/min. Both experiments were performed at 20 bar, using NF270.....	45
Figure 22. Variation of permeate flux with % concentration, during the nanofiltration of 1500 mL of lupin beans debittering water. The % concentration is the ratio between the volume of permeate over volume of feed. The arrows signalize the depressurizations of the filtration cell.....	47
Figure 23. Lupanine concentration in the retentate and permeate during the nanofiltration of 1500 mL of lupin beans debittering water, at 20 bar and 420 mL/min.	48
Figure 24. Conductivity and pH values registered for both permeate and retentate during the concentration of 1500 mL of lupin beans debittering wastewater.	48
Figure 25. Variation of permeate flux with % concentration, during the nanofiltration of 670 mL of lupin beans debittering water, immediately after the recirculation experiment at 20 bar and 600 mL/min. The % concentration is the ratio between the volume of permeate over volume of feed. The arrows signalize the depressurizations of the filtration cell.	49
Figure 26. Lupanine concentration in the retentate and permeate during the nanofiltration of 670 mL of lupin beans debittering water, at 20 bar and 420 mL/min.	50
Figure 27. % extraction calculated according to equation 14 for lupin beans debittering wastewater and a solution of pure lupanine.	52
Figure 28. % COD retained calculated according to equation 15, for the extractions with the best five solvents and lupin beans debittering wastewater. COD values determined for the aqueous phase recovered after the two successive extractions.....	53
Figure 29. % binding and Q values obtained for each resin. Each different color represents the classification of each resin (15 ion exchangers and 3 polymeric adsorbents). Amb. Is an abbreviation for Amberlite.	57
Figure 30. % binding for the eighteen resins that were tested using a solution of pure lupanine in water (3.2 g/L) and lupin beans debittering wastewater. IRC50 and IRC86 were not included because these resins are no longer commercially available and Dowex MAC-3 has analogous characteristics (binding and regeneration results were similar), so it was used to replace the other two.	58
Figure 31. % recovery for the acidic resins and the polymeric one, using five different solutions. The vertical line signalizes the resins with % binding higher than 90% (on the left) and the resins with % binding between 60 and 70% (on the right).....	60
Figure 32. Freundlich, Langmuir and adsorption isotherms obtained for XAD-16.	62

Figure 33. Freundlich, Langmuir and adsorption isotherms obtained for Dowex MAC-3.	62
Figure 34. % binding and % recovery for the XAD-16 and MAC-3 assays with debittering wastewater, for 3 cycles.	64
Figure 35. Possible hydrogen bonding (dashed lines) and ionic interactions between lupanine and IA, MAA (A) and possible hydrogen bonding (dashed lines between lupanine and NIPAM (B). For MAA, R = CH ₃ and for IA R = H ₂ C-COOH.	67
Figure 36. Binding results for NIPs and MIPs obtained with the monomers indicated and two solutions of racemic lupanine in dichloromethane (0.1 and 1 g/L).	68
Figure 37. % regeneration obtained for the MIPs obtained with MAA and IA.	70
Figure 38. Results from the enzymatic assays with lupanine in PBS. The reactions were allowed to occur for approximately 5 days, and a sample was recovered every day for lupanine quantification. A control test tube containing only lupanine dissolved in PBS was placed in the same conditions as the tubes containing the enzymes.	72
Figure 39. (A) δ -lactam ring structure (present in lupanine) and (B) β -lactam ring hydrolyzed by β -lactamases.	72
Figure 40. Suggested process to extract lupanine from lupin beans debittering wastewater. This process starts with a centrifugation to remove the solid particles, then the supernatant is subjected to an ultrafiltration to reduce the concentration of macromolecules. The resultant permeate will be used as feed of a nanofiltration, and the resultant retentate is applied to XAD-16, that is regenerated with ethanol.	73
Figure 41. Suggested process to extract lupanine from lupin beans debittering wastewater. This process starts with a centrifugation to remove the solid particles, then the supernatant is subjected to an ultrafiltration to reduce the concentration of macromolecules. The resultant permeate will be used as feed of a nanofiltration, and the retentate is the applied to MAC-3, that is regenerated with NaOH 10% in water. After regeneration, a liquid-liquid extraction with DCM is done, and the organic phase is applied to MIPs.	74
Figure 42. Sequence of filtrations that compose the first part of the process to recover lupanine. The approximate volume values obtained in each fraction are indicated, considering an initial value of 3500 L. membrane areas were calculated for 24 hours and considering the fluxes indicated.	76
Figure 43. Calibration curve for concentrations between 0.00145 and 2 g/L.	A
Figure 44 Calibration curve for concentrations higher than 2 g/L and equal or lower than 14 g/L.	A
Figure 45. Typical chromatogram obtained for a solution of lupanine in water (approximately 3 g/L). the arrow signalizes the peak correspondent to lupanine.	B
Figure 46. Typical chromatogram obtained for phase 3. The arrow signalizes the peak correspondent to lupanine.	B

Figure 47. Chromatogram obtained for the injection of a sample after the binding assays with the IA NIP. Both (L)-(-)- and (D)-(+)-lupanine retention times (t_r) are indicated.C

Figure 48. Chromatogram obtained for the injection of a sample after the binding assays with the IA chiral MIP. Both (L)-(-)- and (D)-(+)-lupanine retention times (t_r) are indicated.C

Figure 49. Langmuir linear regression obtained for XAD-16, by representing each c_e/q_e values as a function of c_e values. The equation of the linear regression and the value of R^2 are also indicated. E

Figure 50. Langmuir linear regression obtained for Dowex MAC-3, by representing each c_e/q_e values as a function of c_e values. The equation of the linear regression and the value of R^2 are also indicated. .. E

Figure 51. Freundlich linear regression obtained for XAD-16, by representing each c_e/q_e values as a function of c_e values. The equation of the linear regression and the value of R^2 are also indicated. F

Figure 52. Freundlich linear regression obtained for Dowex MAC-3, by representing each c_e/q_e values as a function of c_e values. The equation of the linear regression and the value of R^2 are also indicated.G

List of Tables

Table 1. Lupanine and COD concentration of each phase of the industrial debittering process. Data from [12].	4
Table 2. Classification (ion exchangers or adsorbents), functional groups, ionic forms and polymer structure of the matrix for each one of the eighteen commercial resins tested in the present study. The molecular structure of the functional groups is indicated. The functional groups and ionic forms do not apply to polymeric resins, which is indicated as “NA” – “non-applicable”.	13
Table 3. List of the organic solvents that were used in the present study with the corresponding structure and relative density values.	15
Table 4. List of the organic solvents that were used in the present study with the corresponding boiling point, polarity, solubility in water, solubility of water in and $\log_{10}Kow$ values. Kow is the n-octanol/water partition coefficient and it is obtained by the ratio between the concentration of solvent in n-octanol and the concentration of solvent in water.	16
Table 5. List of the organic solvents that were used in the present study with the corresponding aquatic impact score and ecotoxicological class for two trophic levels (fish and invertebrates) assigned according to the following values: (1) very toxic ($LC50 < 1 \text{ mg.L}^{-1}$), (2) toxic ($LC50 < 10 \text{ mg.L}^{-1}$), (3) harmful ($LC50 < 100 \text{ mg.L}^{-1}$), (4) not harmful ($LC50 > 100 \text{ mg.L}^{-1}$). $LC50$ represents the lethal concentration of each solvent in the water to kill 50% of population, after exposure for 4 hours [50]. Air impact score, POCP, vapor pressure and odor threshold values are also indicated.	17
Table 6. Incineration., recycling, biotreatment, VOC emissions, health hazard and exposure potential scores attributed to the organic solvents that were used in the present study [47].	18
Table 7. Examples of chiral MIPs produced with chiral monomers and racemic templates. Both monomer and template structures are indicated. The observations correspond to the main conclusions of the studies and the references are indicated in the last column.	26
Table 8. Examples of chiral MIPs produced with non-chiral monomers and chiral templates. Both monomer and template structures are indicated. The observations correspond to the main conclusions of the studies and the references are indicated in the last column.	27
Table 9. List of enzymes and the correspondent CAS number and company.	32
Table 10. COD, lupanine concentration, pH and conductivity values obtained for each fraction recovered after ultrafiltration of 400 mL of lupin beans wastewater. COD rejection was calculated according to equations 8 and 9.	43
Table 11. COD, lupanine concentration, pH and conductivity values obtained for each fraction recovered after nanofiltration of 400 mL of lupin beans wastewater. Lupanine and COD rejection were calculated according to equations 10 and 11.	43

Table 12. COD, lupanine concentration, pH and conductivity values obtained for each fraction recovered after nanofiltration of 250 mL of permeate from the ultrafiltration. Lupanine and COD rejection were calculated according to equations 10 and 11.	43
Table 13. Lupanine concentration for both permeate and retentate recovered after the filtration of 100 mL and both permeate and retentate recovered after the recirculation experiments.	46
Table 14. COD values obtained for the aqueous phase recovered after two extractions with 4 mL of distilled water and 2 mL of each organic solvent (twice).	54
Table 15. % COD retained and absolute values of COD for Dowex MAC-3 and XAD-16 (100 and 300 mg/mL).....	63
Table 16. Structure and molecular weight of the five monomers used to synthesize MIPs with racemic lupanine.	66
Table 17. Binding and enantiomeric excess results obtained after the binding assays with the chiral MIP produced with IA and L-(-)-lupanine as template.	69
Table 18. Conductivity and pH values for both permeate and retentate recovered after the filtration of 100 mL and both permeate and retentate recovered after the recirculation experiments.	D
Table 19. Langmuir parameters (q_{\max} and K_L) for both XAD-16 and Dowex MAC-3, calculated from the equation of the linear regressions (Figures 49 and 50).....	E
Table 20. Freundlich parameters (n and K_F) for both XAD-16 and Dowex MAC-3, calculated from the equation of the linear regressions (Figures 51 and 52).....	G

1. Objectives and Thesis Outline

The four main objectives of this thesis were defined as follows:

(1) - Optimization of specific unit operations that can be used to create a process to efficiently extract lupanine from lupin beans debittering wastewater:

- a) Eighteen resins were tested for lupanine binding and subsequent recovery with different regeneration solutions;
- b) Nine different organic solvents were studied to do a liquid-liquid extraction of lupanine from the wastewater;
- c) A nanofiltration membrane performance was analyzed through concentration and recirculation studies;
- d) An ultrafiltration membrane performance was also assessed.

(2) - Synthesis of MIPs for racemic lupanine using five different monomers. The MIPs were then tested and the most efficient monomer was selected to synthesize a chiral MIP using L-(-)-lupanine as template, as an attempt to create an enantioselective unit operation.

(3) - Enzymatic transformation of lupanine was also explored using ten lipases, an esterase and a penicillin amidase.

(4) - Considering the best conditions obtained in (1), two processes comprising some of the unit operations above mentioned were suggested and discussed to obtain pure lupanine.

The introduction of this thesis (Section 2.) highlights important features regarding lupanine, including the natural occurrence of this compound, and provides also an explanation on its importance to the pharmaceutical industry despite its toxicity. Since lupanine is an enantiomeric compound, this first section includes also some highlights on chirality in general, including resolution of enantiomers. Then, each unit operation of the predicted process to efficiently isolate lupanine from the lupin beans debittering wastewater is introduced, with relevant information about nanofiltration and ultrafiltration, resins and liquid-liquid extractions. The last section of the introduction is about molecularly imprinted polymers (MIPs), and describes the main components that are necessary to obtain these polymers (template, cross-linker, functional monomer, porogen and initiator) and some of the main polymerization strategies are also described. There is a sub-section about chiral MIPs and finally some applications of MIPs in general are presented.

Section 3. provides a description of the materials and methods used during this project. The results and correspondent discussion are in Section 4. The thesis ends with Section 5. containing the main conclusions and suggestions for future work.

2. Introduction

2.1 Lupanine

Quinolizidine alkaloids (QAs) are natural compounds with a ring structure and a nitrogen atom, derived from lysine. Lupanine is one of the most common QAs [1]. They are metabolites that give the plants some resistance to pathogens and also to herbivores as they confer a bitter taste, in addition to their toxicity [2,3,4].

2.1.1. Natural occurrence

QAs like lupanine and sparteine (Figure 1) are characteristic compounds present in *Lupinus* species. There are around 400 known *Lupinus* species, but only four of them are of interest to the food industry, because of their high protein content: *L. albus* (white lupin), *L. luteus* (yellow lupin), *L. angustifolius* (narrow leaf lupin) and *L. mutabilis* (Andean lupin) [5].

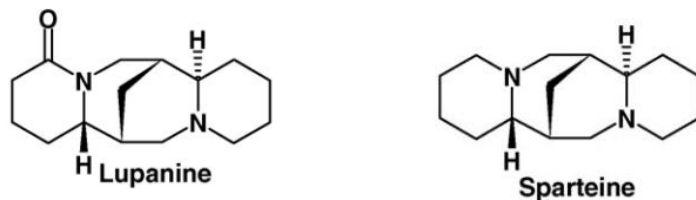


Figure 1. Structure of lupanine and sparteine [3].

Most alkaloids, including QAs, confer bitter taste and constitute important defence mechanisms of plants. Bitterness perception is a common feature of many toxic compounds, so most of the animals (both herbivores and carnivores) react with repulsion to bitter taste. The presence of these toxic compounds is important to avoid predators [6,7,8].

Regarding biosynthesis, L-lysine is the precursor for all quinolizidine alkaloids [7]. The first step of the biosynthetic pathway of lupanine is the conversion of L-lysine into cadaverine (Figure 2) by an enzyme catalysed decarboxylation [7,9]. Then, there is an oxidative deamination of cadaverine allowing the formation of 5-aminopentanal which is cyclized to Δ^1 -piperideine, a Schiff base. This intermediate is modified by condensation, hydrolysis and methylation in order to produce lupanine [10].

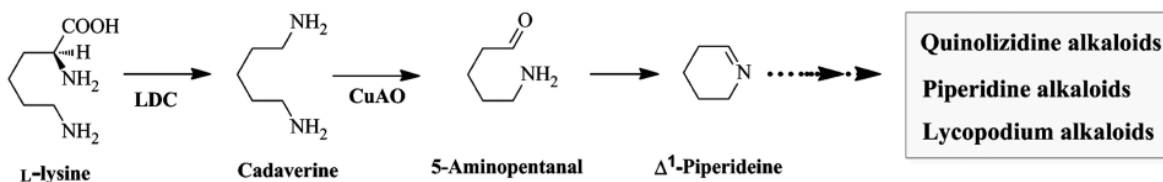


Figure 2. Main intermediates of the biosynthetic pathway of QAs. Adapted from [10].

2.1.2. Adverse health effects

QAs are neurotoxins that affect nicotinic and muscarinic acetylcholine receptors and ion channels [11]. Therefore, a significant amount of these compounds has to be removed from lupin beans before ingestion.

There are some neurological, cardiovascular and gastrointestinal symptoms attributed to the ingestion of high levels of QAs. For example, cases of people suffering from weakness, palpitations, nausea, abdominal pain and respiratory depression after eating lupin seeds that were not previously debittered have been reported [1]. The symptoms described result from anticholinergic effects, since QAs interfere with neuroreceptors, ion channel and signal transduction, thus affecting neurotransmission [1,8]. In particular, lupanine can bind to two acetylcholine receptors: muscarinic acetylcholine receptor and nicotinic acetylcholine receptor. This QA will bind to the neuroreceptor instead of the natural ligand (Figure 3), blocking the physiologic response. Also, lupanine is a muscular sodium channel blocker causing hyperpolarisation and a more negative membrane potential of the neuron. Thus, the neuron will not be capable of triggering an action potential [8].

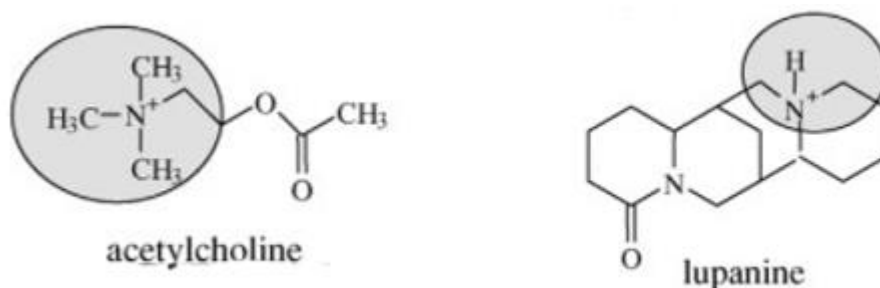


Figure 3. Structure of acetylcholine (natural ligand of the neuroreceptor) and lupanine. The chemical group indicated in each molecule corresponds to the binding site [6].

2.1.3. Industrial lupin beans debittering process

Traditional debittering process involves boiling the lupin beans which allows the QAs to be released into the water [12]. The alkaloid content of the beans is reduced from 1-2% (10-20 g/kg) to 0.05% (0.5 g/kg) [1]. Lupanine content in *L. albus* beans corresponds to 1.4% (14 g/kg plant material) [5]. Therefore, since hundreds of tons of white beans are debittered per year, a high amount of water rich in QAs, especially lupanine, is disposed as wastewater [13].

The industrial lupin beans debittering process from which the debittering wastewater used in this study was utilized comprises four stages: hydration, cooking, resting and sweetening. During hydration (phase 1), the lupin beans are left to swell in water, for 14 hours (around 784 kg of water intake per ton of dry lupin beans). Then, the swollen beans are boiled (phase 2), and the QAs start to be released from the beans to the boiling water. After cooking, there is a resting phase (phase 3) during which the boiled beans are cooled down by being left inside a tank (total volume equal to 6600 L) that is filled with fresh water (800 L water per 800 kg lupin beans), for 3 to 5 days. QAs, especially lupanine, are mainly released during phase 3. In the end, the tank is emptied and sweetening takes place (phase 4). Sweetening consists in washing the beans with fresh water, in a continuous way for around 40 hours

(flow between 1400 and 1900 L/h) [12]. Table 1 contains the approximate values for lupanine concentration and COD in each phase of the industrial process:

Table 1. Lupanine and COD concentration of each phase of the industrial debittering process. Data from [12].

Phase		Lupanine (g/L)	COD (g O ₂ /L)
Hydration (1)		0.000 ± 0.000	0.005
Cooking (2)		1.674 ± 0.009	23.0
Resting (3)		3.444 ± 0.019	30.0
Sweetening (4)	After 15 hours	0.943 ± 0.003	8.5
	After 25 hours	0.468 ± 0.001	4.7
	After 40 hours	0.045 ± 0.002	1.0

Lupin beans debittering wastewater referred throughout this thesis corresponds to phase 3 (resting), since this is the phase with higher lupanine concentration.

2.1.4. Pharmaceutical interest

There are evidences showing that lupanine may also be a compound of pharmaceutical interest, especially due to the fact that it may have a hypoglycemic effect as it can enhance insulin secretion [13]. For example, an *in vitro* study with isolated β -cells from rats showed that this QA enhanced the release of insulin by a mechanism involving glucose [14]. The secretion of insulin induced by glucose starts with the synthesis of mitochondrial ATP. The ATP is used to close ATP-dependent K⁺ channels (K_{ATP} channels) that will lead to the opening of Ca²⁺ channels. This sequence of steps promotes the exocytosis of granules containing insulin. Lupanine directly inhibits K_{ATP} channels, increasing glucose-induced insulin release [11].

2.1.5. Sparteine: a valuable chiral ligand that can be obtained from lupanine

Lupanine is chemically related to sparteine, and it can be converted into the latter through a reduction reaction (Figure 4). Each lupanine enantiomer can be obtained by crystallization of a racemic mixture with (+)-dibenzoyltartaric acid to produce (-)-lupanine, or (-)-dibenzoyltartaric acid to produce (+)-lupanine [15].

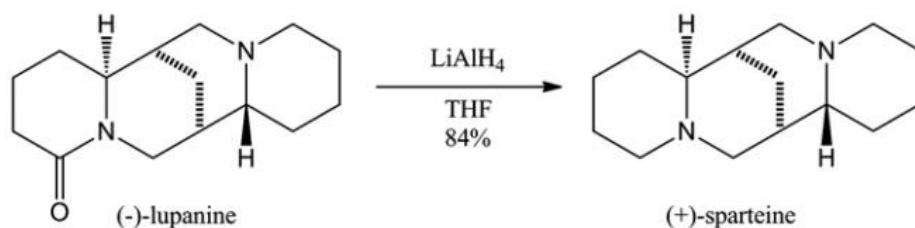


Figure 4. Reduction of (-)-lupanine to (+)-sparteine using LiAlH_4 in THF [15].

Sparteine is a very important chiral ligand for asymmetric synthesis. Optically active compounds can be obtained using systems that incorporate chiral diamines. (-)-sparteine is the most investigated chiral diamine that is used with organolithium reagents in stereoselective deprotonation, oxidation, reduction, substitution and addition reactions to obtain chiral compounds. The great majority of synthesis reactions involves one or more steps that are based on these lithium reagents [16, 17].

In particular, asymmetric Henry reactions, that are based on the formation of a C-C bond between nitroalkanes and aldehydes or ketones, can generate enantiomeric compounds when performed in the presence of a complex formed by (-)-sparteine and copper(II) that work as catalyst (Figure 5) [18].

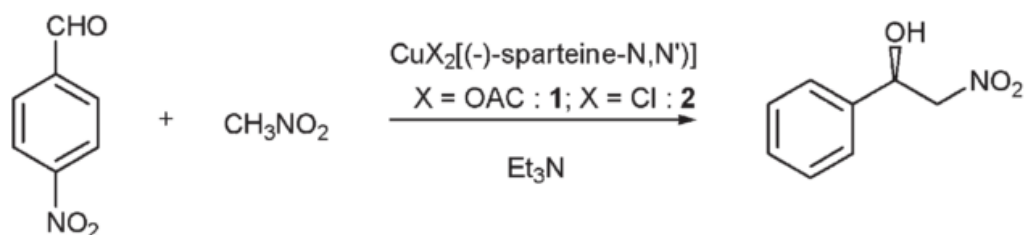


Figure 5. Reaction of nitromethane with 4-nitrobenzaldehyde using copper(II)-(-)-sparteine complexes [18].

The asymmetric alkylation of ketones is also important in organic chemistry, to obtain α -functionalized ketones, that are present in many optically active drugs and natural products. Sparteine was successfully utilized as chiral ligand to produce chiral α -alkylated ketones from non-chiral dimethylhydrazones (Figure 6) [19].

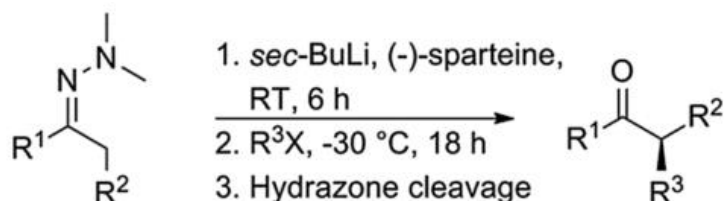


Figure 6. Reaction of dimethylhydrazones using (-)-sparteine complexes to obtain a chiral α -alkylated ketone [19].

Another interesting application of sparteine as chiral mediator was the production of (S)-boroproline from N-Boc-pyrrolidine, with a (-)-sparteine-mediated lithiation as the first step of the reaction

(Figure 7.). The boroproline compounds are important as inhibitors of dipeptidylpeptidase IV (DPP4), a serine protease that is involved in diabetes mellitus type 2 [20].

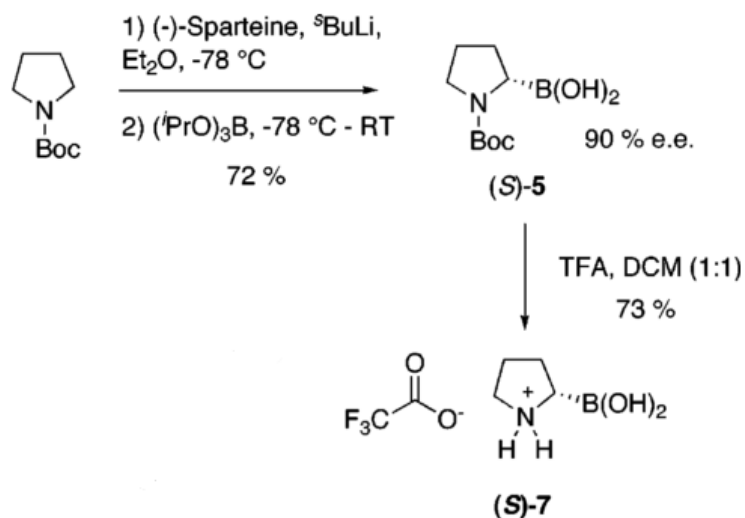


Figure 7. Sequential steps to obtain (S)-boroproline (indicated as (S)-7) using (-)-sparteine complexes. Adapted from [20].

For a certain period, (-)-sparteine was unavailable in the market and some hypothesis were raised as an attempt to explain why this compound was no longer commercially available. It was thought that maybe there was only one producer of this compound that stop making it or that a pharmaceutical company acquired all the (-)-sparteine that was available because it was needed for a given chemical reaction. This alkaloid can be isolated from a plant (Scotch broom) but it is a cumbersome process [21]. Its synthesis, although already described, is very complex [21, 22]. Some researchers started to look for alternatives, for example, some tertiary amines for ring opening polymerizations or some sparteine surrogates that could be used instead of sparteine for organolithium reactions [21, 23]. Instead, it was suggested that lupanine could be a useful compound to obtain sparteine [21].

2.2. Chirality

An important feature of lupanine is its chirality (Figure 8). The current section is dedicated to chirality. Some important concepts, such as *enantiomer* and *diastereoisomer*, are clarified. The importance of studying these molecules is briefly explained, and some methods to the resolution of enantiomers are also described.

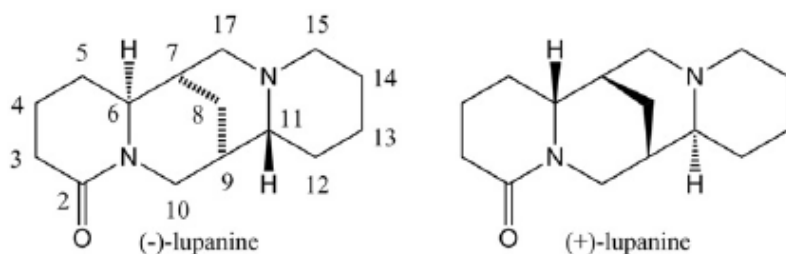


Figure 8. (-)- and (+)-enantiomer of lupanine [15].

2.2.1. Stereoisomers: enantiomers and diastereoisomers

Stereoisomers are molecules that have the same molecular formula, with the atoms connected in the same sequence but with different spatial arrangement. The term “stereoisomers” includes both enantiomers and diastereoisomers.

Enantiomers (also referred to as optical isomers) are non-superimposable mirror images, which means that the position of each atom of a structure of a given molecule and its mirror image will not match if it is placed over the other. Every compound that is not superimposable on its mirror image is called a chiral compound. These chiral molecules are said to be optically active because they are able to rotate the plane of polarization of polarized-light as it passes through them. An enantiomer can be termed dextrorotatory (*d*) or levorotatory (*l*) if the plane of polarization is rotated to the right or to the left, respectively. A racemic mixture corresponds to an equimolar mixture of two enantiomers and in this case, the net rotation of polarized light is zero.

When a chiral compound contains a carbon atom bound to four different groups (an asymmetric carbon atom), it is called a stereogenic or chiral center. Usually, an enantiomer has only one chiral center whereas a diastereoisomer contains more than one chiral centers.

Any stereoisomer compounds that are not enantiomers (meaning that they are not superimposable or they are not mirror images of one another) are called diastereoisomers.

The two enantiomers of a compound are characterized by identical chemical properties (because they have similar arrangements of atoms in space), differing only in their interactions with other chiral objects [24, 25].

2.2.2. Optical isomers and biological systems

Chirality is a characteristic of almost half of the drugs that are on the market, and in most cases only one of the enantiomers exhibits the desired pharmacologic effect (this enantiomer is called

eutomer). The inactive enantiomer (called *distomer*) can have no effect, but in some cases it can be an antagonist or it can even be related to toxic effects [26].

Enantiomeric compounds do not have any physical differences, but they can have different effects on living organisms. That is the reason why pharmaceutical industries need to synthesize only the active enantiomer of a given drug. Enantiomers can be distinguished by their bioactivity or rate of reaction [27].

Two enantiomers show similar physical and chemical properties unless they are in a chiral environment. If a given drug has two enantiomers, each one must be considered a different drug because they can behave differently *in vivo* due to the chirality existent in biological systems. For example, the binding site of an enzyme determines which of the two enantiomers is the active one. If only one of them has a three-dimensional arrangement of atoms that can be aligned with the binding site, this will be the eutomer. The distomer has the same groups as the eutomer but their arrangement does not allow interaction with specific regions of the binding site [28]. It is well known that there are various racemic drugs and very often only one enantiomer is active. In some cases, the non-effective enantiomer is toxic or can cause several side effects.

Each enantiomer of the same drug can be used to treat different diseases, for example, (S)-(-)-enantiomer of timolol is used to treat angina, whereas the (R)-(+)-enantiomer is used to treat glaucoma. Penicillamine corresponds to a distinct case, since the (S)-(-)-enantiomer is utilized to treat copper poisoning and the (R)-(+)-enantiomer is toxic. L-3,4-dihydroxyphenylalanine is used to treat Parkinson's disease, but only the (S)-(-)-enantiomer has the desired function. (R)-(+)-enantiomer contributes to side effects [24].

2.2.3. Resolution of enantiomers

The resolution of a chiral compound consists in the separation of its enantiomers. Diastereomeric resolution is a classical method in which the compound is converted to a cation or anion that will form a salt with a chiral counter-ion, that is a pure enantiomer. The chiral counter-ion corresponds to the chiral resolving agent that will combine with each enantiomer, allowing the formation of two diastereomeric salts. For example, if a chiral base, *B* is added to a racemic mixture of a given acid, *dA*, then two diastereomeric salts will be formed: *dA.B* and *lA.B*. As mentioned previously, the two enantiomers have similar physical and chemical properties. On the contrary, pairs of diastereomers can have different solubilities, according with the solvent matrix. Thus, crystallization can then be used to separate the less soluble salt. The less soluble diastereomeric salt must contain the enantiomer of interest, so it is sometimes necessary to replace the chiral resolving agent by its enantiomer that does not exist in nature. However, if the solubility of *dA.B* is higher than the solubility of *lA.B*, that does not imply that *dA.dB* has a lower solubility of *lA.dB* in the solvent matrix, being *B* the resolving agent [29]–[31].

The resolution of two enantiomers can also be achieved by means of an enzymatic reaction. The enzymatic resolution of chiral compounds is defined as the use of the selectivity of enzymes to

react with only one of the enantiomers from a racemic mixture [32]. When the two enantiomers react at different rates with an enzyme, the one that reacts faster will be converted to the product faster [4]. For example, lipases have been widely used to the resolution of racemates, especially through catalysis

of transesterification reactions. In the presence of an acyl group donor, an appropriate solvent and a racemic mixture, these enzymes can selectively transfer only one enantiomer to the corresponding ester. The second enantiomer remains intact (Figure 9) [30, 33].

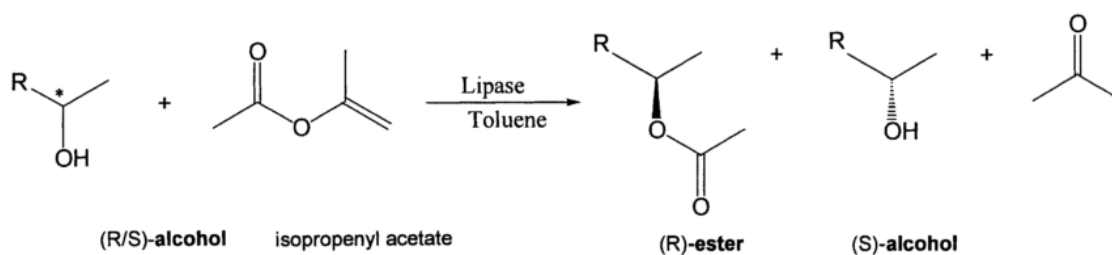


Figure 9. Example of a lipase-catalyzed transesterification of a secondary alcohol using isopropenyl acetate as acyl donor in toluene [30].

Currently, the methods of enantiomeric resolution are based on chromatographic techniques, such as high performance liquid chromatography (HPLC), gas chromatography (GC), capillary electrochromatography (CEC) or thin layer chromatography (TLC), using a chiral stationary phase (CSP). CSPs can be made of polysaccharides, proteins and DNA, cyclodextrins and molecularly imprinted polymers [26, [34]. Polysaccharides, for example, cellulose or amylose are immobilized on silica particles and used as CSPs [35]. Stereoselective DNA aptamers were also tested as CSPs. These short oligonucleotides have been shown to have great stereospecificity and stability during enantiomeric separation [36]. Cyclodextrins are natural sugar compounds used as chiral selectors. A hydrophobic interior cavity and hydrophilic edges characterize these compounds. Inside the cavities, it is possible to introduce some molecules which is an important feature for chiral separations. Also, the hydrophilic edges can be chemically modified to increase the solubility or to improve the enantioselectivity of these complexes [37]. Chiral MIPs are obtained through a polymerization reaction, using chiral template molecules. This process allows to produce cavities similar to chiral template molecules, suitable for enantioseparation [34].

2.3. Extraction of lupanine from white lupin beans leaching waters

Osmotic evaporation was described for lupanine isolation from *L. albus* leaching waters. The wastewater was concentrated by osmotic evaporation, followed by lupanine extraction with an organic solvent (diethyl ether). In osmotic evaporation, a diluted aqueous solution (in this case, the lupin beans wastewater) was separated from a concentrated osmotic solution (NaCl or CaCl₂ solutions) by a hydrophobic porous membrane. The membrane is hydrophobic, so it cannot be wetted by the water, which allows to create a vapor-liquid interface on the pores. The difference in vapor pressure (that is the driving force for water vapor transport) is a result of the difference in water activity between the aqueous solution and the concentrated osmotic solution. This procedure allowed to recovery 18.5% of the lupanine that was present in the concentrate of obtained after the osmotic evaporation process. The main limitation was the low water flux that was registered [38].

A previous academic study performed also in our team at iBB-IST provided the preliminary information for the development of a process to recover lupanine from lupin beans debittering wastewater. The membrane-based process suggested included an ultrafiltration followed by a nanofiltration step. Resins and liquid-liquid extractions were then also studied as viable options to be part of the process. Several ultrafiltration and nanofiltration membranes were assessed and characterized. This study allowed to select an appropriate nanofiltration membrane (NF270) but none of the ultrafiltration membranes was adequate for this process. Preliminary tests regarding some resins and organic solvents were also performed to extract lupanine [12].

2.3.1. Membrane processes: ultrafiltration and nanofiltration

Membrane filtration can be classified into four general categories, according to the pore sizes: microfiltration (50 nm – 1 µm), ultrafiltration (5 – 20 nm), nanofiltration (1 – 5 nm) or reverse osmosis (essentially non-porous, and most of the solutes are retained) [39]. Both nanofiltration and ultrafiltration are pressure-driven membrane processes, which means that when pressure is applied, the solvent and some solute molecules of the feed pass through the pores of the membrane, and will be part of the permeate. Other molecules will be rejected by the membrane and will remain in the retentate [40].

Cut-off is an important parameter for membrane characterization. It is defined as the lowest molecular weight value for which 90% of the solute is retained by the membrane (for example, for a membrane that has a molecular weight cut-off (MWCO) of 3500 Da, i.e the rejection of a solute with a molecular weight (MW) of 3500 Da will be 90%). However, molecular size must not be the only parameter that is considered to decide if a given solute is able to pass through the membrane. The interaction of the solutes with the membrane, or their shape are also important. A globular protein and a flexible polymer may have the same molecular weight but different rejections [40]. Rejection curve shape also matters, as membranes with the same MWCO can actually have very different rejection curves allowing either easy permeation of smaller solutes for sharp curves or making separation between small and large molecules more challenging using membranes that present less steeply rejection curves.

Membrane fouling is defined as the deposition of particles, macromolecules, salts or colloids, for example, on the surface of the membrane and it can be reversible or irreversible. Temperature, pH, ionic strength and interactions such as hydrogen bonding or dipole-dipole interactions are important factors for fouling susceptibility. It is responsible for a flux decline, maintenance and membrane replacement due to its degradation over time [40, 41].

In general, there are four different types of fouling mechanisms (Figure 10): adsorption (that results from specific interactions established between the membrane and the solutes in the feed solution), partial or full pore blocking, cake layer formation (in which several layers are formed on the membrane surface due to particles deposition) and gel layer formation (caused by the concentration polarization phenomenon) [41].

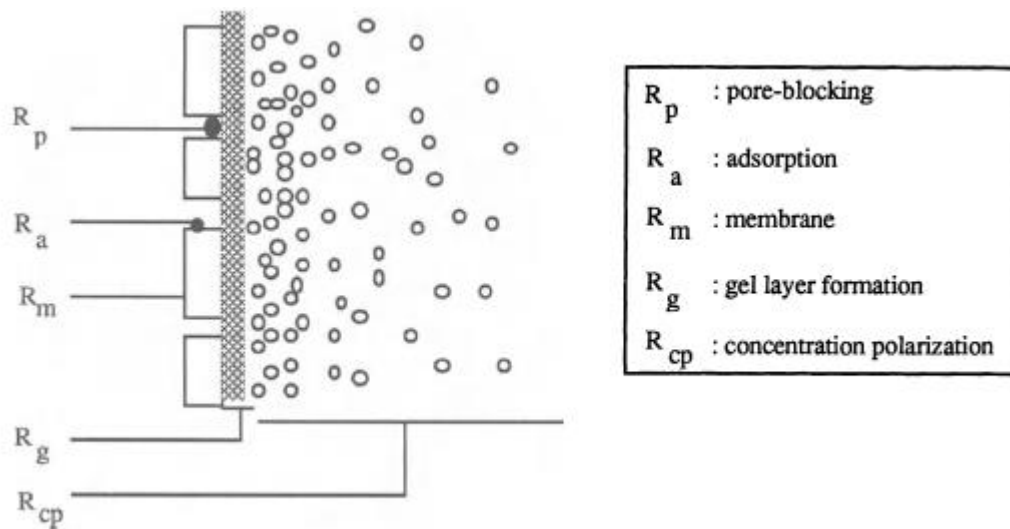


Figure 10. Possible types of fouling and concentration polarization phenomenon [40].

Besides fouling, concentration polarization and osmotic pressure are also important phenomena that contribute to flux decline over time. The first one is a result of the accumulation of solutes near the membrane at the feed side, that will cause a higher concentration on the membrane surface than in the bulk solution. Also, during the nanofiltration process, the osmotic pressure will increase because the solutes will become more concentrated, leading to a decrease of the permeate flux [39–41].

Fouling is classified into four types: organic (that results from the deposition or adsorption of proteins or polysaccharides, for example), colloidal (associated to the accumulation of metal oxides or salt precipitates), scaling (that is caused by the presence of calcium sulfate or carbonate, for example, that will form mineral deposits that precipitate from the feed to the membrane surface) and biofouling (that results from the adhesion and growth of microorganisms). Organic, inorganic and colloidal fouling occur after a short period of time, whereas biofouling becomes important only after the other three [39, 41].

Membrane properties (functional groups, morphology and charges), feed stream characteristics (type and concentration of foulants, pH, ionic strength) and operational conditions (permeate flux, cross flow velocity, temperature and pressure) are crucial to understand fouling issues [39, 41].

Although fouling is inevitable after a certain time, some strategies can be adopted to prevent its severe effects on the membrane. For example, feed pre-treatment before the nanofiltration can be used to reduce the quantity of fouling agents. This can be achieved through centrifugation, coagulation, flocculation and/or precipitation. The cross-flow velocity and the pressure are also important factors. For example, if the pressure is decreased and the cross-flow velocity is increased, the performance of the membrane will be better. During nanofiltration, fouling can be reduced by avoiding concentration polymerization using air sparging, pulsating flow or low frequency ultrasonic irradiation. Some chemicals may also be added during the process to reduce membrane fouling. For example, antiscalting agents, oxidizing biocides or cleaning agents (such as EDTA) have already been used. However, these cleaning agents can change membrane surface properties or membrane pore size [41].

2.3.2. Resins: ion exchangers and polymeric adsorbents

Resins are classified into two types: ion exchangers or polymeric adsorbents. Both are made of styrene-divinylbenzene or acrylic cross-linked polymers (Figure 11.) [42, 43].

Ion exchange resins contain immobilized acid or base groups that exchange positive or negative counter ions (so-called cation and anion exchanger resins, respectively) [42]. In the case of polymeric adsorbents, the interactions between the compounds and the resin are based on hydrogen bonding, hydrophobic or van der Waals interactions [43].

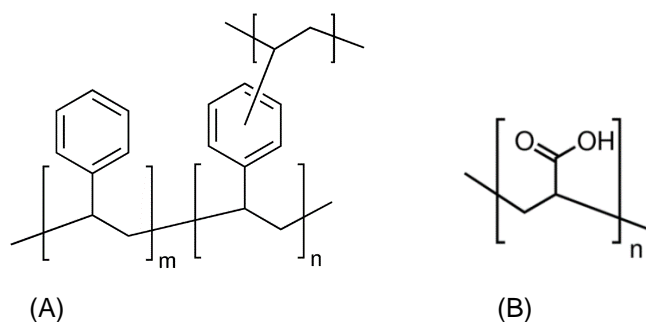


Figure 11. General structure of (A) a styrene (on the left) divinylbenzene (on the right) copolymer and (B) a polyacrylic polymer, that are used as matrix of both adsorbent and ion exchange resins.

Ion exchange resins are generally used to water demineralization or to remove heavy metals from wastewater. Some more specific applications include starch and sucrose hydrolysis or salts removal from fruit juices [42]. Adsorbent resins are commonly used in the pharmaceutical industry for the purification of amino-acids, peptides, antibiotics or vitamins [43].

These resins are cheap, both binding and regeneration are, in general, simple steps and the regeneration chemicals are also not expensive. However, there are some disadvantages such as the adsorption of organic matter that will reduce the loading capacity of the resins. The resin itself may contain non-ionized organic matter because of the manufacture process. Also, the polymer structure will degrade over time, and old resins may contain organic fragments that will contaminate the sample. The

chlorine that is present in the water is a problem because it will cause the oxidation and damage the structure of the resin [42, 44].

Eighteen commercial resins were tested for lupanine binding. The following table contains the classification, functional group and ionic form (for ion exchange resins) and the matrix composition:

Table 2. Classification (ion exchangers or adsorbents), functional groups, ionic forms and polymer structure of the matrix for each one of the eighteen commercial resins tested in the present study. The molecular structure of the functional groups is indicated. The functional groups and ionic forms do not apply to polymeric resins, which is indicated as “NA” – “non-applicable”.

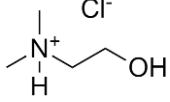
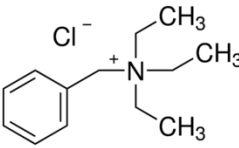
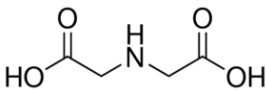
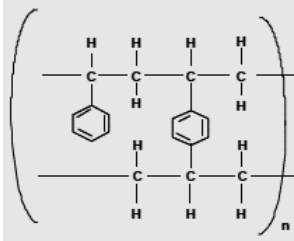
Classification	Resin	Functional Group	Ionic Form	Matrix
Strong acid cation exchanger	AG 50W-X2	Sulfonic acid (-R-SO ₃)	Hydrogen (H ⁺)	Polystyrene cross-linked with 2% divinylbenzene
	AG 50W-X8			Polystyrene cross-linked with 8% divinylbenzene
	Amberlyst 36			Polystyrene cross-linked with divinylbenzene
	Amberlyst 16			
	Purolite PD206			
Strong base anion exchanger	Amberlite IRA 400	Quaternary ammonium (NR ₄ ⁺)	Chloride (Cl ⁻)	Polystyrene
	Amberlite IRA 458			Polyacrylic
	Amberlite IRA 410	Dimethyl ethanol ammonium 		Styrene cross-linked with divinylbenzene copolymer
	Dowex 1X8-50	Trimethyl benzyl ammonium 		Polystyrene
	Amberlite CG-400	Quaternary ammonium (-CH ₂ N ⁺ (CH ₃) ₃)		Styrene cross-linked with divinylbenzene copolymer
Weak base anion exchanger	Amberlite IRA 68	Tertiary ammonium (NHR ₃ ⁺)	Free base	Crosslinked acrylate

Table 2. (continuation) Classification (ion exchangers or adsorbents), functional groups, ionic forms and polymer structure of the matrix for each one of the eighteen commercial resins tested in the present study. The molecular structure of the functional groups is indicated. The functional groups and ionic forms do not apply to polymeric resins, which is indicated as “NA” – “non-applicable”.

Classification	Resin	Functional Group	Ionic Form	Matrix
Weak acid cation exchanger	Amberlite IRC 86	Carboxylic acid (-R-COOH)	H ⁺	Polyacrylic
	Amberlite IRC 50			
	Dowex MAC-3*			
Chelating cation exchanger	IRC 7481	Iminodiacetic acid 	Sodium (Na ⁺)	Polyacrylic
Polymeric adsorbent	Amberlite XAD-16	NA	NA	Hydrophobic polyaromatic  Figure 12. Chemical structure of XAD-16 resin.
	Amberlite XAD-7			Polyacrylic ester
	Amberlite XAD-1			Polystyrene-divinilbenzene

* Dowex MAC-3 is the alternative resin to IRC 50 and IRC 86, since these two are no longer commercially available. Binding and recovery assays showed similar results.

2.3.3. Liquid-liquid extractions with organic solvents

Liquid-liquid extractions are based on the different solubility of a given solute in two distinct solvents, that will promote the passage of the compound of interest from one solvent to the other. Four simple steps are needed to perform a liquid-liquid extraction: (i) firstly, an extractant is added to the diluent (that contains the solute of interest); (ii) then, the diluent and the extractant are mixed to promote the movement of the solute from the original solution to the extractant solvent until equilibrium is reached; (iii) the mixture is then allowed to stand for formation of two phases, and (iv) finally the two phases are separated.

Some requirements should be taken into account when choosing the extractants: specific selectivity of the extractant for the solute and high solubility of the solute in the extractant;; low solubility of the extractant in the diluent; ; diluent and extractant must have different densities to facilitate formation of two phases; easy separation of the solute from the extractant (e.g. by distillation of the extractant); toxicity and environmental impact of both solvents has to be considered [45].

In the case of the present study, lupanine is dissolved in an aqueous matrix (lupin beans debittering wastewater) and nine different solvents (hydrocarbons, ethers, ketones and alcohols) were tested. Tables 3 and 4 contain important parameters that will be referred in the discussion (Section 4.1.2.5.).

Table 3. List of the organic solvents that were used in the present study with the corresponding structure and relative density values.



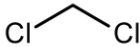
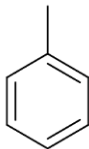
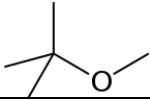
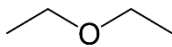
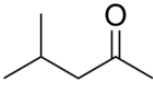
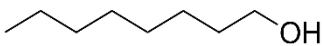

Class	Organic solvent	Structure	Density (water = 1)
Hydrocarbons	Hexane		0.70
	Heptane		0.68
Halogenated hydrocarbon	Dichloromethane (DCM)		1.30
Aromatic hydrocarbon	Toluene		0.87
Ethers	Methyl <i>tert</i> -butyl ether (MTBE)		0.70
	Diethyl ether		0.70
Ketone	Methyl isobutyl ketone (MIBK)		0.80
Alcohols	1-octanol		0.83
	1-butanol		0.81

Table 4. List of the organic solvents that were used in the present study with the corresponding boiling point, polarity, solubility in water, solubility of water in and log₁₀Kow values. Kow is the n-octanol/water partition coefficient and it is obtained by the ratio between the concentration of solvent in n-octanol and the concentration of solvent in water.

Solvent	Boiling point[46] (°C)	Polarity (water = 100) [46]	Solubility in water[46] (25 °C; w/w) [46]	Solubility of water in (25 °C; w/w) [46]	Log ₁₀ Kow (w/w) [46]
Dichloromethane	40	30.9	1.3	0.20	1.25
Toluene	111	9.9	0.052	0.033	2.69
1-octanol	195	54.3	0.6	4.8	-
1-butanol	118	60.2	7.3	20.4	0.88
MTBE	55	14.8	4.3	1.4	0.94
MIBK	117	27	1.7	1.9	1.31
Diethyl ether	35	11.7	6.9	1.3	0.77
Heptane	98	1.2	0.0003	0.010	3.50
Hexane	69	0.9	0.0010	0.011	3.80

GlaxoSmithKline's (GSK) solvent guide allows to determine how "green" a given solvent is. The solvents are ranked according to waste disposal, environment, human health and safety issues. A score is attributed in each category, from 1 (less green) to 10 (more green). Each of these scores is then combined to give an overall score called composite score [47, 48].

The environmental impact of a solvent is related to aqueous and air impact of the solvent. The aqueous impact is associated with acute and chronic environmental toxicity. For example, if a solvent is very toxic to aquatic species, it will have a low score. The biodegradation is also important. The air impact is associated with the photochemical ozone creation potential (POCP), and also with the ratio of vapor pressure to odor threshold [47].

POCP is a parameter that is used to classify a given solvent according to its capacity to generate ozone[49]. The solvents are classified from 0 to 100: 0 is attributed to the most stable compounds and 100 is the maximum value (it is attributed to ethylene) [46]. Higher values of this parameter lead to significant penalizations of the correspondent compounds (lower scores) [47].

Air impact score is a combination of the scores attributed to POCP and vapor pressure to odor threshold ratio [47]. The odor threshold represents the minimum concentration of a solvent that can be detected by the human nose [46]. Solvents with higher values of vapor pressure to odor threshold ratio have lower odor scores. Solvents with a high ratio of vapor pressure to odor threshold have low score [47].

Table 5. List of the organic solvents that were used in the present study with the corresponding aquatic impact score and ecotoxicological class for two trophic levels (fish and invertebrates) assigned according to the following values: (1) very toxic ($LC_{50} < 1 \text{ mg.L}^{-1}$), (2) toxic ($LC_{50} < 10 \text{ mg.L}^{-1}$), (3) harmful ($LC_{50} < 100 \text{ mg.L}^{-1}$), (4) not harmful ($LC_{50} > 100 \text{ mg.L}^{-1}$). LC_{50} represents the lethal concentration of each solvent in the water to kill 50% of population, after exposure for 4 hours [50]. Air impact score, POCP, vapor pressure and odor threshold values are also indicated.

Solvent	Ecotoxicological class [50] (fish)	Ecotoxicological class [50] (invertebrates)	Aquatic Impact [47]	POCP [46]	Vapor pressure [46] (21 °C; mmHg)	Odor threshold [46] (ppm)	Vapor Pressure: Odor Threshold Ratio (mmHg/ppm)	Air Impact [46]
DCM	4	4	8	0.9	37.6	250	0.15	6
Toluene	2	3	7	56	23.2	40	0.58	2
1-octanol	3	2	5	-	0.14	0.5	0.28	4
1-butanol	4	4	9	55	4.8	5000	0.001	3
MTBE	4	4	7	-	206	-	-	5
MIBK	4	4	9	63.3	16.5	8	2.06	3
Diethyl ether	4	4	5	60	462	1	462	3
Heptane	-	-	3	53	40	150	0.27	5
Hexane	-	-	3	42	128	-	-	5

The waste score is also an important issue, and it is related with incineration, recycling, biotreatment and volatile organic compound (VOC) emissions. The incineration is related with solubility, emissions to air and enthalpy of combustion of each solvent. If a solvent can be easily separated from water, it will have a high recycling score. The solvents that require greater oxidation, that are volatile or that are miscible with water are penalized in the biotreatment score. VOC emissions score is related with spillages during transport or storage (lower scores are attributed to solvents with low boiling points) (tables 5 and 6.) [47].

Human health problems are divided into two categories: health hazard and exposure potential. The health hazard score is based on risk phrases and the exposure potential is a combination of an upper limit on the concentration of a hazardous substance in a workplace (occupational exposure limits) and the saturation concentration (table 6.) [47].

Table 6. Incineration., recycling, biotreatment, VOC emissions, health hazard and exposure potential scores attributed to the organic solvents that were used in the present study [47].

Solvent	Incineration	Recycling	Biotreatment	VOC emissions	Health hazard	Exposure potential
Dichloromethane	2	10	4	1	1	2
Toluene	10	7	6	7	7	6
1-octanol	9	7	8	10	7	10
1-butanol	6	7	5	8	7	7
MTBE	7	8	4	2	7	4
MIBK	7	8	5	7	7	6
Diethyl ether	7	7	3	1	10	4
Heptane	10	4	5	6	10	6
Hexane	10	8	4	3	7	4

2.3.4. Molecularly Imprinted Polymers

Molecular imprinting is a technique that allows to create specific binding sites for a given target molecule. Three main components are required: a template, a monomer and a cross-linking agent. The monomer must be carefully chosen because the formation of the cavities with the desired shape, functionality and selectivity is strongly dependent on the stabilization of the complex formed by the monomer and the template during polymerization. The stabilization of this complex depends on the interaction established between the target molecule and certain functional groups carried by the monomer. The nature of the interactions can be classified, in general, as covalent or non-covalent interactions [51–53].

2.3.4.1. Synthesis of MIPs

A. Covalent approach

The covalent approach is based on the formation of reversible covalent bonds between the template and the monomer. There is a chemical step, independent of the polymerization, to allow the formation of the covalent bonds between the template and the monomer [53]. After the polymerization with the cross-linker, there is a chemical cleavage step [54].

This approach has some advantages, for example, a reduced number of non-specific bindings is obtained and there is a significant amount of functional binding sites [55]. Also, there are low non-specific interactions because the functional monomer residues are only near the specific cavities created with the template [53].

However, covalent approach is less utilized to obtain MIPs because the number of monomers that are able to establish reversible covalent bonds with the template are reduced [54]. The chemical process needed to associate the template and the monomer, before polymerization and also to release the template, after formation of the binding sites makes this process more complex. It is associated to low template recovery [53].

B. Non-covalent approach

The most frequently used approach to prepare MIPs is the one based on non-covalent interactions between the template and the functional monomer. Firstly, an interaction between those two components is induced and then there is a polymerization step with the cross-linking agent. In this case, the molecules of interest (the template and the target) interact with the polymer via ionic or hydrogen bonding, for example [54].

This method is the most used because it is very flexible since there are many functional monomers available to establish non-covalent interactions with many compounds. There are no chemical reactions involved, so the imprinting process is simpler. The interactions are easily reversed, since hydrogen bonding is the preferable interaction established between the two components and it can be easily disrupted by using a solution containing an acid, a base or methanol [53, 54].

Although this is a simpler and more practical approach, it has some drawbacks such as the need of a hydrophobic environment to stabilize the interactions between the template and the monomer and the

use of an excess of monomers that causes non-specific interactions. Also, the presence of a single group of interaction in the compound of interest will decrease the efficiency of the imprinting process because the molecular recognition capacity will be reduced [54, 55].

The heterogeneity of the binding sites and non-specific interactions between target molecules and the monomer, or between the monomers and the cross-linking agent due to spreading of large quantities of free monomers around the polymer are significant drawbacks. The percentage of functional binding sites relatively to the amount of template that is used during the polymerization process is very low (less than 15% of the template produces functional cavities) [53, 55].

C. Methods to obtain MIPs

Bulk polymerization is the most frequently used method to obtain a MIP. Firstly, there is the polymerization reaction and after that, the polymer that is obtained is mechanically grinded. In the end, the particles are sieved into the desired size ranges. Although this is a simple and fast method to produce a MIP, due to the sieving steps, the particles obtained are irregular in size and shape. There is a significant loss of the initial bulk polymer (50 to 75%) and some cavities are destroyed leading to a decrease in the loading capacity of the polymer [54].

Some different polymerization techniques have been used to obtain spherical particles, such as precipitation, multi-step swelling, suspension and grafting [52, 54].

In the case of precipitation polymerization, template monomer and cross-linker are dissolved in a solution. The polymer grows until a certain critical mass, when it becomes insoluble and precipitates [52]. There is no need to grind or sieve because spherical particles are obtained, and the recognition ability of the cavities is significant [34].

Multi-step swelling polymerization consists in the use of pre-formed particles that are suspended in water and swell due to the addition of an organic solvent. Then, the three components (monomers, cross-linker and template) are added to the solution and they are incorporated in the particles [52]. This technique allows to control the diameter of the spherical particles, but requires complicated procedures and reaction conditions. Also, the use of aqueous emulsions decreases the selectivity of the MIP due to the polarity of the environment [34].

There is also suspension polymerization, in which all components are dissolved in an organic solvent, forming a solution that is added to an immiscible solvent. The system is stirred in order to promote the formation of droplets, allowing the reaction to occur [52]. In this case, aggregates of spherical particles are obtained. The continuous phase is composed of perfluorocarbons instead of water to avoid interference with the non-covalent interactions. However, the use of this special solvent makes this method less practical and applicable [34].

Grafting is another technique that consists in the utilization of silica particles. All components needed for polymerization are adsorbed within the particles, the reaction starts and, in the end, the silica is removed [52].

D. Template

The template is a molecule that is used to originate the molecular imprinting. It can be any given compounds, such as amino acids, carbohydrates, alkaloids (atrazine, ephedrine, nicotine) and also more complex molecules, for example drugs or hormones [52, 54].

When molecular imprinting targets are natural compounds that are rare or difficult to produce, their massive utilization has high costs associated. Furthermore, the target may be inappropriate to use in huge concentrations due to its toxicity. Thus, the so-called “dummy templates” can be used instead of the target compound during the imprinting process. These molecules bear functional groups that are able to interact with the functional monomer (by hydrogen bonding, ion-pair formation or dipole-dipole interactions) in a similar way as the target [56, 57].

Dummy templates may be already existent compounds or they may be designed and synthesized from the structural skeleton of the target molecule. These compounds are selected based on the interaction of the target with the functional monomer. The conformation effects between the analyte and the cavities that are generated during the imprinting process are also important aspects to achieve both proper affinity and sufficient recovery [56, 58].

An imprinting process to quantify atrazine (an herbicide) was the first reported case of a MIP being prepared with dummy templates (Figure 13). The removal process of atrazine after polymerization is time-consuming and it is very hard to completely remove this template. Three non-agrochemical compounds were used as dummy templates for the imprinting process to avoid contamination of environmental samples to be analysed [57]. More recently, dummy templates were described for selective removal and enrichment of ginkgolic acids (allergenic compounds present in *Ginkgo biloba* L. leaves). In this case, two dummy templates with similar structural characteristics to ginkgolic acids (Figure 14) were designed and synthesized. The imprinted polymers obtained showed high selectivity and affinity to the original target [56].

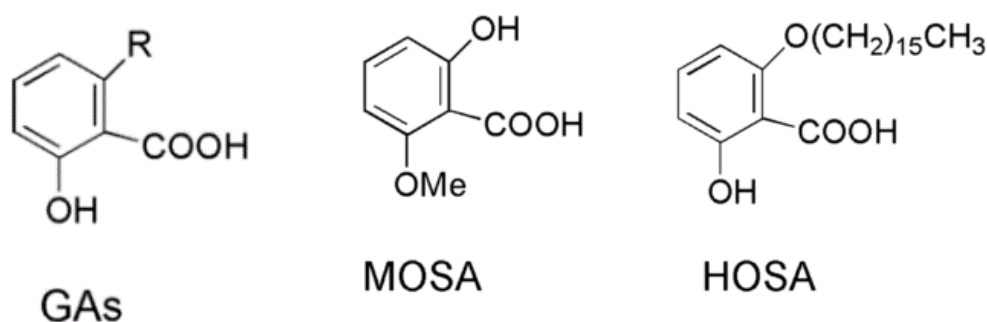


Figure 13. Generic structure of ginkgolic acids (GAs) and the compounds used as dummy templates [56].

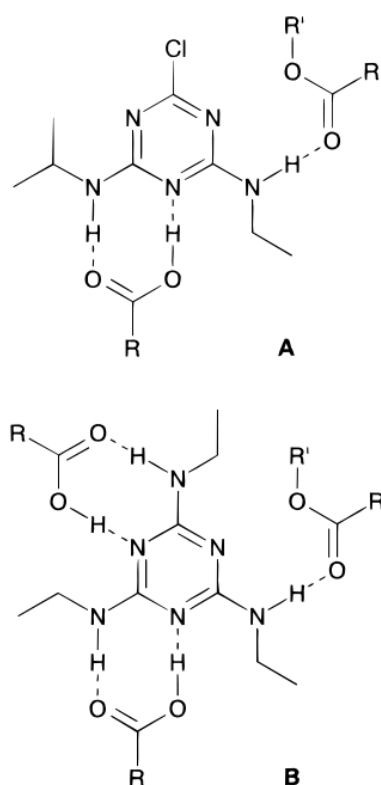


Figure 14. Illustration of possible intermolecular interactions between atrazine (A) and triethylmelamine (B) with MAA and EDMA. R corresponds to $-\text{C}(\text{CH}_3)=\text{CH}_2$ and R' corresponds to $-\text{C}_2\text{H}_4-\text{OCO}-\text{C}(\text{CH}_3)=\text{CH}_2$ [57].

E. Monomers

The functional monomer is a crucial component since it will stabilize the complex formed with the template during the polymerization process and will also allow the selective interaction between the MIP and the target. These interactions are possible because of the functional groups carried by the monomer [52, 53]. It is important to mention that a monomer contains two main “units”: the “recognition unit” that comprises the chemical groups such as hydroxyl, carbonyl or amide groups that interact with both the template and the target, and also a “polymerizable unit” that is responsible for the polymerization process, in general, a carbon-carbon double bond [59].

There are several monomers available, that can be classified as acidic, basic or neutral, based on the residues of the functional groups. Electrostatically charged monomers and monomer combinations have also been described [53].

The most used monomer is methacrylic acid (Figure 15). This carboxylic acid-base monomer has several important features, such as the presence of the methyl group, that minimizes rotation and conformational flexibility, while providing van der Waals interactions. Furthermore, it can interact with the template in numerous ways, such as hydrogen bonding, ion-pair formation or weaker dipole-dipole interactions, due to the presence of the carboxylic group [53, 60]. There are some studies showing that trifluoromethacrylic acid (Figure 15) can be more efficient than methacrylic acid (MAA) due to an

enhanced acidity as a result of the three fluorine atoms that allow to stabilize the formation of the complex during polymerization and also during the rebinding process [53].

Trifluoromethacrylic acid (TfMAA) was used for imprinting nicotine and cinchona alkaloids, in comparison to MAA. Both studies revealed that the polymer obtained with TfMAA has higher affinity and increased binding strength, that resulted in an increase of the polymer selectivity. Since fluorine is the most electronegative atom in the periodic table, it has a high tendency to attract electrons. Also, there is less rotation of the bond because 3 fluorine atoms are larger than 3 hydrogens. Thus, the presence of three fluorine atoms in the monomer contributes to a better stabilization of the complex monomer-template based on ion pairing or hydrogen bonding interaction [61, 62].

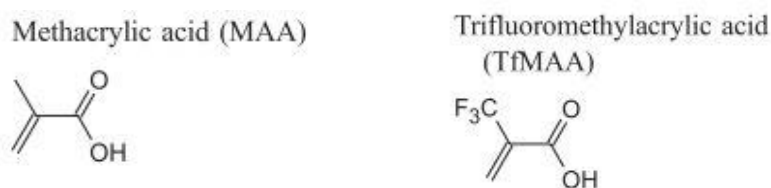


Figure 15. Structure of MAA and TfMAA [53].

F. Cross-linker

Besides the monomer, the right choice of a cross-linking agent is very important for the success of the imprinting process because it is responsible for forming a rigid polymer, fixing the functional monomers around the templates. After removal of the template, it will maintain the binding sites [59].

The cross-linker has three main functions in MIPs: to control the porosity of the polymer matrix, to stabilize the binding site formed after the imprinting process and to confer mechanical rigidity to the polymer. The cross-linker should be used in high amounts in order to generate stable recognition sites [54].

About 70-98% of the structure of the final MIP corresponds to the cross-linker. Ethylene glycol dimethacrylate (EDMA – Figure 16) is the most used cross-linker because it allows infinite conformation possibilities and is also associated to a significant degree of rigidity in the resultant polymer [53].

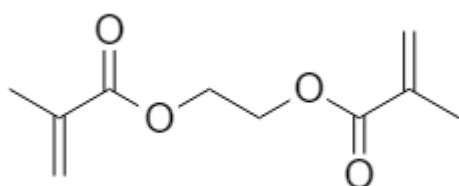


Figure 16. Structure of ethylene glycol dimethacrylate [53].

G. Solvent (porogen)

The porogenic solvent is also a very important component to obtain a MIP: it must dissolve the template molecule, the initiator, the monomer and the cross-linker; large pores should be produced to ensure a good flow through the matrix; and its polarity should be low since it is not supposed to interfere with the formation of the complex monomer-template [54]. Thus, less polar organic solvents, such as

toluene, acetonitrile or chloroform should be preferred, especially in non-covalent approaches, to improve efficiency of the imprinting process [59].

Porogenic solvents act as pore forming agents during polymerization. The most used solvents to obtain MIPs are 2-methoxyethanol, methanol, tetrahydrofuran (THF), acetonitrile, dichloromethane, chloroform, N,N-dimethylformamide (DMF) and toluene [59].

H. Initiator

Free radical polymerization, photopolymerization and electropolymerization are the most common polymerization methods to obtain MIPs [59]. In the case of free radical polymerization, the initiator can be decomposed to radicals through heating, lighting or chemical means. For example, azobisisobutyronitrile (AIBN) generates carbon-centred radicals capable of initiating the polymerization of MAA under thermal or photochemical conditions [54, 59].

Peroxy compounds and azo compounds are the most used initiators (Figure 17). These components are used at very low concentrations compared to the monomer [59].

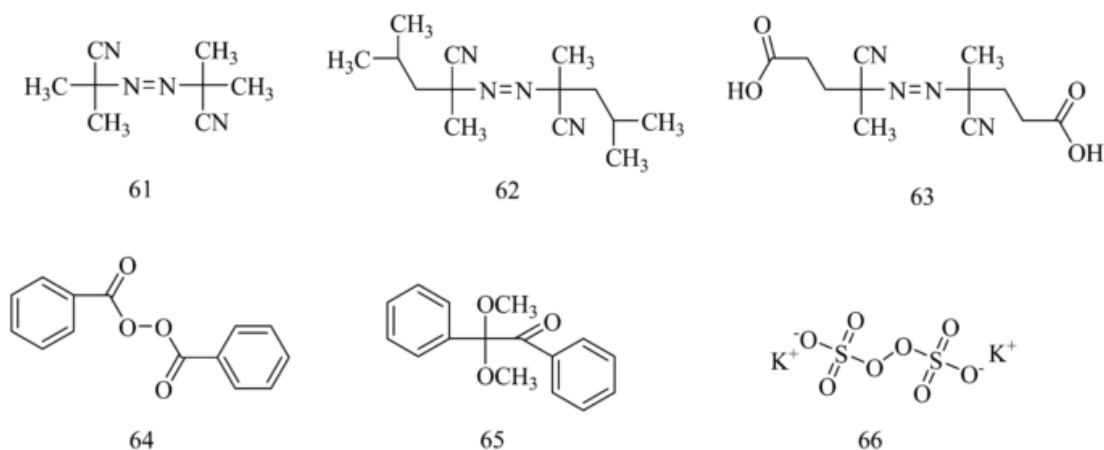


Figure 17. Chemical structure of common initiators: (61) Azobisisobutyronitrile (AIBN); (62) azobisdimethylvaleronitrile (ADV); (63) 4,4'-azobis(4-cyanovaleric acid) (ACID); (64) benzoylperoxide (BPO); (65) dimethylacetal of benzyl (BDK); (66) potassium persulfate (KPS) [59].

2.3.4.2. Chiral MIPs

There are many natural-derived chiral selectors that have been applied for chiral separation, for example, cyclodextrins, antibodies, serum albumin or quinine/quinidine derivatives. These chiral biological elements have some disadvantages, such as a complex production, which makes them very expensive, and their poor stability is also a problem since it leads to very specific handling conditions. Also, not every analyte is associated to a natural recognition element. MIPs have several advantages for chiral separation over the natural chiral selectors such as easy preparation, the materials are less expensive and they are very flexible [27].

Chiral MIPs are usually obtained using a chiral template, a functional monomer and a cross-linking agent, dissolved in a porogen. Chiral templates are used to produce cavities for only one of the two enantiomers. In this case, selectivity arises from shape-selective recognition sites generated during the imprinting process, and not from different physico-chemical properties between the two enantiomers [63, 64].

Although the conventional method to obtain chiral MIPs is based on the use of a chiral template, it is necessary to use a huge amount of the enantiomer of interest. Pure enantiomers are expensive, so a strategy used to overcome this drawback is the utilization of inexpensive enantiomers structurally related to the target (dummy templates – section 2.3.4.1. – D.) [65].

A different viable approach is the use of a chiral monomer, instead of the functional monomers commonly used. In this case, a racemic mixture of the enantiomers is introduced as template, and chirality is then induced using the chiral monomer. The racemate is more easily obtained and usually less expensive than the pure enantiomer [65].

There are many examples described in the literature, especially for chiral MIPs obtained with a chiral template, to amino acids, drugs or other organic compounds. 3 examples of chiral MIPs obtained with a racemic template and with a chiral template are described in tables 7 and 8.

Table 7. Examples of chiral MIPs produced with chiral monomers and racemic templates. Both monomer and template structures are indicated. The observations correspond to the main conclusions of the studies and the references are indicated in the last column.

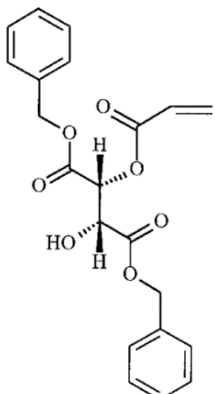
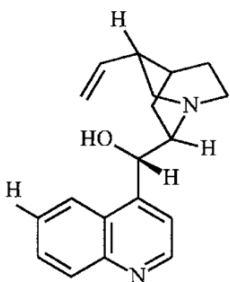
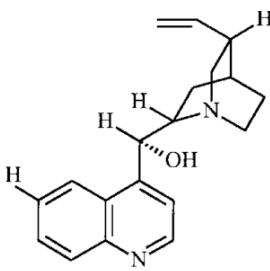
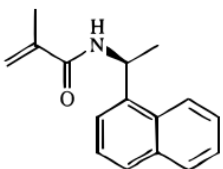
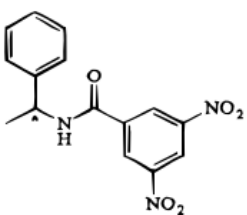
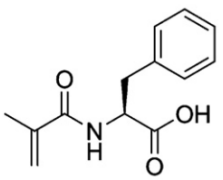
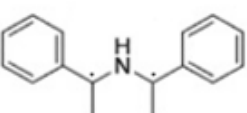
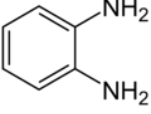
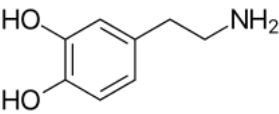
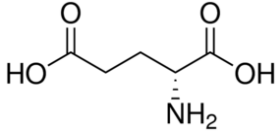
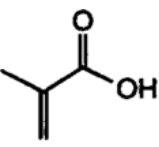
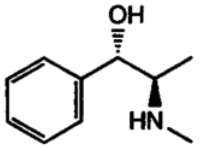
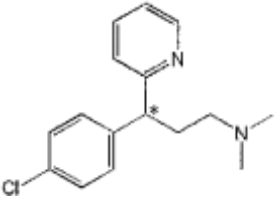
Chiral MIPs produced with chiral monomers			
Monomer Structure	Template(s) Structure	Observations	Ref.
<p>Dibenzyl (2R,3R)-O-monoacryloyl tartrate</p> 	<p>Cinchona alkaloids: Cinchonidine</p>  <p>and Cinchonine:</p> 	<ul style="list-style-type: none"> The main goal of this study was to prove the molecular recognition capacity of the polymers synthesized with the previous compounds rather than test the enantioselectivity of the MIPs. Structural analogs of the templates were tested and both polymers seemed to be selective only for the template molecules. 	[66]
<p>(S)-(-)-methacryloyl-1-naphthylethylamine ((S)-MNEA)</p> 	<p>N-(3,5-Dinitrobenzoyl)-R-methylbenzylamine (DNB)</p> 	<ul style="list-style-type: none"> Molecularly imprinted CSP prepared using chiral (S)-DNB as the template and achiral functional monomers showed to be less effective to separate both DNB enantiomers than CSP prepared with racemic DNB as template and the chiral functional monomer (S)-MNEA. 	[67]
<p>(S)-2-(2-methylacryloylamino)-3-phenyl propionic acid ((S)-MAPP)</p> 	<p>bis[(S)-1-phenylethyl]amine (R, S)-PEA</p> 	<ul style="list-style-type: none"> 3 different MIPs were prepared using the same chiral monomer ((S)-MAPP) but different templates: (R)-PEA, (S)-PEA and racemic PEA. All MIPs were able to resolve the PEA racemate, but the one obtained with (S)-PEA was the most efficient. 	[65]

Table 8. Examples of chiral MIPs produced with non-chiral monomers and chiral templates. Both monomer and template structures are indicated. The observations correspond to the main conclusions of the studies and the references are indicated in the last column.

Chiral MIPs produced with chiral template			
Monomer(s) Structure	Template(s) Structure	Observations	Ref.
<p><i>o</i>-phenylenediamine (<i>o</i>-PD)</p>  <p>Dopamine (DA)</p> 	<p>L-Glutamic acid (L-Glu)</p> 	<ul style="list-style-type: none"> • These co-polymers were obtained through electropolymerization to obtain a MIP on a gold electrode. • L-Glu imprinted copolymer was not able to bind the enantiomer D-Glu, proving the enantioselectivity. • Other amino acids were tested (L-glutamine, L-aspartic acid, L-serine, etc.) and only in the case of L-glutamine the MIP showed some binding capacitance due to the similarity of the amino acid structure, which proves the selectivity of the sensor. 	[68]
<p>MAA</p> 	<p>(S,R)-(+)-ephedrine</p> 	<ul style="list-style-type: none"> • Chiral MIPs were prepared using (S,R)-(+)-ephedrine, and it was demonstrated their significant enantioselectivity. • Also, an interesting result of this study was the capacity of these polymers to mimic natural adrenergic receptors since they were able to recognize the enantiomers of the natural ligand (epinephrine) as well as 6 adrenergic blockers. 	[69]
<p>MAA</p>	<p>D-chlorpheniramine</p> 	<ul style="list-style-type: none"> • Chlorpheniramine is an antihistaminic, and the enantiomer used as template has shown to be 200-fold more active than its enantiomer. • The chiral MIP was able to separate the enantiomers of the drug. 	[70]

2.3.4.3. Applications

MIPs have several applications in numerous fields, such as separation and purification in general (enantioselective chromatography, capillary chromatography, solid-phase extraction), sensors, drug delivery, catalysis and binding assays (artificial antibodies) [34, 55].

MIPs have some features such as chemical inertness, high stability, sensitivity and selectivity, that make these polymers appropriate to be utilized in binding assays [71]. For example, MIP nanoparticles were imprinted with an antibiotic (vancomycin) and were covalently immobilized on optical fibres to obtain a sensor. The detection was based on changes of the transmission spectrum associated to the system. The increase of vancomycin bound to the nanoparticles leads to an intensification of the changes of the spectrum [72].

These imprinted polymers can be used in high temperatures or pressures and also under acidic or basic conditions, so they can be employed for catalytic applications [71]. In this case, the template corresponds to a substrate analogue, and then, the interaction between the template and the polymer is supposed to mimic the substrate-enzyme interaction [73].

Regarding drug delivery, MIPs can be applied to induce a controlled release of a certain drug [71]. For example, tetracycline was used as both template and target molecule and it was shown that the release of the antibiotic is slower for the MIP compared to non-imprinted polymers, and more tetracycline was released. This result is important because this imprinted system can be applied to control the release of other pharmaceuticals [74].

One of the main applications of MIPs is for CSPs, especially in HPLC. MIP based CSPs are associated to high enantioselectivity and substrate-specificity [27]. Enantiomeric resolutions of different compounds such as amino acid derivatives or drugs have been reported [71].

MIPs can also be applied as chiral excipients. Enantioselective controlled delivery systems are of interest since they are supposed to release the active enantiomer while preventing the release of the non-active enantiomer. For example, three racemic drugs (ibuprofen, ketoprofen and propranolol) were introduced in MIP beads and it was demonstrated that an excess binding of the non-active enantiomer of each drug led to a weak binding of the other enantiomer that was more easily released from the chiral beads [75].

2.4. Degradation of lupanine

To date, there is only one scientific report on bacterial strains that are able to degrade lupanine. The bacterial strains were isolated from soil in which *L. albus* and *L. luteus* had been cultivated in the presence of lupanine. Two of the seven isolates were identified as *Xanthomonas oryzae* *pv.* *oryzae* and one as *Gluconobacter cerinus*. Two unidentified strains were able to degrade 99% of the lupanine present in the medium after 30 hours [2].

The hydrolysis of the lactam ring of lupanine was described in the context of the high hydrostatic pressure effects on the structure of this alkaloid. The phenomenon affects intra and intermolecular interactions, since at high pressures (1 kbar) there is self-ionization of the water, which will lead to the hydrolysis of the amide group of lupanine, as shown in Figure 18. [76].

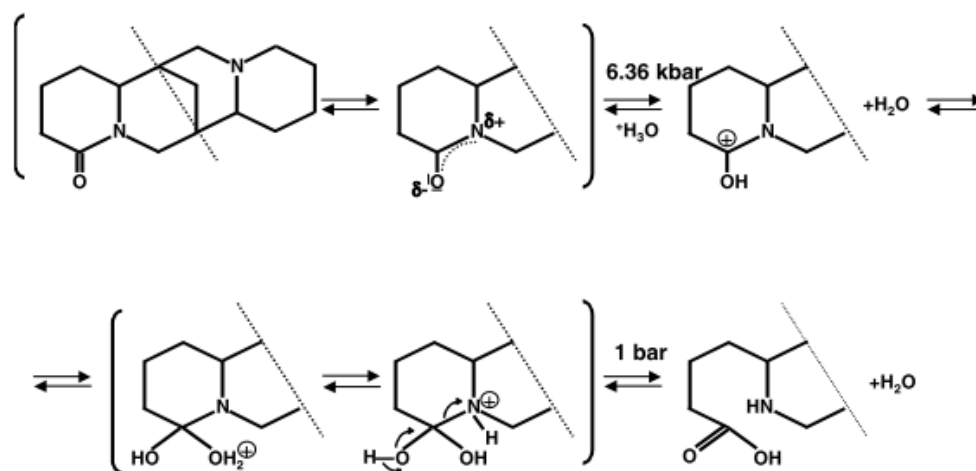


Figure 18. Predicted mechanism for lupanine hydrolysis at high hydrostatic pressure [76].

In this thesis, enzymatic degradation of lupanine was tested aiming to obtain compounds that could be of interest to the pharmaceutical industry to produce new alkaloids containing the chiral structure of lupanine.

3. Materials and Methods

3.1. Materials and Reagents

3.1.1. Lupanine quantification

For lupanine quantification, a HPLC system was used (Hitachi LaChrom). It was constituted by two pumps (Hitachi L-7100), an UV-detector (Hitachi L-7400), a programmable autosampler (Hitachi L-7250) and an interface (Hitachi D-7000) to connect the system to a computer. The column used was a core-shell organo-silica LC column from Kinetex (5 μm EVO C18 100 Å, 250 x 4.6 mm). A pre-column from Kinetex was also used.

The samples were previously basified with Potassium Hydroxide (KOH) pellets from Panreac (MW = 56.11 g/mol; CAS:1310-58-3), centrifuged using a microcentrifuge from Sigma (1-15P) and filtered into vials using nylon syringe filters from Tecnocroma (diameter = 13 mm and pore size = 0.22 μm). The pH of the samples was measured using a 691 pH meter from Metrohm.

3.1.2. Liquid-liquid extractions

9 different solvents were tested: dichloromethane, methyl *tert*-butyl ether (MTBE) from Lab-Scan (CAS: 1634-04-4), methyl isobutyl ketone (MIBK) from Acros Organics (CAS: 108-10-1), heptane from Fisher Scientific (CAS: 142-82-5), hexane from Fisher Scientific (CAS: 110-54-3), toluene from Fisher Scientific (CAS: 108-88-3), diethyl ether from Fisher Scientific (CAS: 60-29-7), 1-octanol from Merck (CAS: 111-87-5) and 1-butanol from Sigma-Aldrich (CAS: 71-36-3).

3.1.3. Resins

18 different resins were tested: Amberlite IRC 50 (Rohm and Haas; CAS: 9002-29-3), Amberlite IRC 86 (Sigma-Aldrich, CAS: 211811-37-9), Amberlite IRC 7481 (Rohm and Haas; CAS: 79620-28-3), AG-50W-X2 (Bio-Rad; CAS: 69011-20-7), AG-50W-X8 (Bio-Rad; CAS: 69011-20-7), Amberlyst 16 (Sigma-Aldrich; CAS: 125004-35-5), Amberlyst 36 (Sigma-Aldrich; CAS: 39389-20-3), Purolite PD206, Amberlite IRA 68 (Rohm and Haas; CAS: 9056-59-1), Amberlite IRA 458-Cl (Rohm and Haas; CAS: 9084-78-0), Amberlite IRA 400-Cl (Sigma-Aldrich; CAS: 9002-24-8), Amberlite IRA 410 (Sigma-Aldrich; CAS: 9002-26-0), Amberlite CG-400 (BDH Chemicals; CAS: 37247-87-3), Amberlite XAD-1 (Sigma-Aldrich), Amberlite XAD-7 (Sigma-Aldrich; CAS: 37380-43-1), Amberlite XAD-16 (Sigma-Aldrich; CAS: 104219-63-8), Dowex 1X8-50 (Alfa Aesar; CAS: 69011-19-4) and Dowex MAC-3 (Sigma Aldrich; CAS: 9052-45-3).

Reagents used during the regeneration assays were: ethanol absolute from Fisher Scientific (CAS: 64-17-5) NaOH pellets from Fisher Scientific (CAS: 1310-73-2) and HCl 37% from Fischer Scientific (CAS: 7647-01-0).

3.1.4. Nanofiltration and Ultrafiltration

NF270 (from Dow FILMTEC) membrane was used for the nanofiltration experiments and a SEPA CF TF (thin film) UF, GK, MWCO 3000 Da membrane (from Lenntech) was utilized for ultrafiltration.

A METcell cross-flow system from Evonik was utilized for all the filtration experiments. This system is constituted by a reservoir, two high-pressure cross-flow filtration cells and a gear pump. A series I HPLC pump from Scientific Systems was used for the recirculation experiments.

3.1.5. Molecularly Imprinted Polymers

Five different monomers were used: methacrylic acid (MAA) from Acros Organics (CAS: 79-41-4), itaconic acid (IA) from Acros Organics (CAS: 97-65-4), methyl methacrylate (MMA) from Sigma Aldrich (CAS: 80-62-6), styrene from Sigma Aldrich (CAS: 100-42-5) and N-isopropylacrylamide (NIPAM) from Sigma Aldrich (CAS: 2210-25-5). Azobisisobutyronitrile (AIBN) from Fluka (CAS: 78-67-1) was used as initiator, dichloromethane from Fisher Scientific (HPLC; CAS: 75-09-2) was the porogenic agent and ethylene glycol dimethacrylate (EGDMA) from Acros Organics (CAS: 97-90-5) was used as the cross-linking agent. Lupanine used as the template of MIPs was kindly supplied by Faculty of Pharmacy, University of Lisbon. A hot plate magnetic stirrer from Labnet was used during synthesis, with agitation and controlled heating.

Silicone oil from LabKem (CAS: 68083-14-7) and a hot plate magnetic stirrer from IKA RCT was used for heating the solvents, during washing of the polymers. The solvents used were HCl 37% from Fischer Scientific (CAS: 7647-01-0), methanol from Fisher Scientific (CAS: 67-56-1) and dichloromethane.

PTFE syringe filters from Tecnocroma (diameter = 13 mm and pore size = 0.20 μm) were utilized to introduce the supernatant recovered after the binding and recovery assays into new Eppendorfs.

3.1.6. Enzymatic assays

Twelve enzymes were tested for lupanine degradation:

Table 9. List of enzymes and the correspondent CAS number and company.

Enzyme	CAS	Company
Lipozyme	9001-62-1	Strem Chemicals, Inc.
Lipozyme TLIM	9001-62-1	Strem Chemicals, Inc.
Esterase	9016-18-6	Sigma
Lipase AYS	9001-62-1	Amano Enzyme Inc.
Lipase AS	9001-62-1	Amano Enzyme Inc.
Lipase PS Amano SD	9001-62-1	Amano Enzyme Inc.
Lipase AK Amano	9001-62-1	Amano Enzyme Inc.
Lipase PS Amano IM	9001-62-1	Amano Enzyme Inc.
Lipase <i>Candida cylindracea</i>	9001-62-1	Sigma
CAL-A	9001-62-1	Sigma
CAL-B (Lipase acrylic resin from <i>Candida antarctica</i>)	9001-62-1	Sigma
Penicillin amidase from <i>E. coli</i>	9014-06-6	Sigma

3.2. Methods

3.2.1. Lupanine quantification and calibration curves

Lupanine was quantified by HPLC. The mobile phase was constituted by a mixture of acetonitrile (15 %) and Na₂HPO₄ buffer (85 %), and the analysis was performed at a flow rate of 1 mL min⁻¹ for 24 minutes, at room temperature. The volume of each injection was equal to 20 µL and the detection was done at 220 nm.

Na₂HPO₄ buffer was prepared by dissolving 1.8 g of this reagent in 1 L of mili-Q water. The pH was then adjusted to 10.5 with some drops of a NaOH solution (50 g/L).

The samples were previously basified with around 1 KOH pellet (pH between 13-13.5), centrifuged at 14000 rpm for 4 minutes and filtered into vials using nylon syringe filters.

A stock solution of lupanine was prepared by dissolving 0.35 g of pure lupanine in 25 mL of mili-Q water (14 g/L). Aliquots of the stock solution were pipetted into 5 and 10 volumetric flasks to obtain solutions of lupanine with concentrations between 14 g/L and 0.00195 g/L. A 1.5 mL sample of the solutions with different concentration were transferred to HPLC vials for HPLC analysis. The calibration curves were then obtained by plotting the area of the peak correspondent to lupanine as a function of the concentration values (see annex A).

3.2.2. Chemical Oxygen Demand (COD)

COD test is based on the fact that most of the organic compounds can be oxidized in the presence of a strong oxidizing agent (in this case, potassium dichromate), under acidic conditions (sulfuric acid), at 150 °C. The organic compounds are then oxidized to carbon dioxide and water and the hexavalent dichromate (Cr₂O₇²⁻) is reduced to trivalent chromium (Cr³⁺). Silver is added to improve the oxidation of straight chain aliphatic compounds. After the reaction, ferrous ammonium sulfate (Fe(NH₄)₂(SO₄)₂·6H₂O) is used to titration of the remaining dichromate. In the end, the equivalents of oxidant consumed are converted to grams of oxygen per liter of sample (g O₂/L) [77].

The solutions needed to determine COD of an aqueous sample were prepared as follows:

(A) – Potassium dichromate (K₂Cr₂O₇) digestion solution: an aqueous solution with 10.216 g of K₂Cr₂O₇ previously dried at 103 °C for 2 hours was prepared. 167 mL of concentrated H₂SO₄ were carefully added under agitation with a magnetic stirrer. In the end, 33.3 g of HgSO₄ were added and the was completed up to 1000 mL with distilled water.

(B) – H₂SO₄ with Ag₂SO₄: this solution was bought prepared.

(C) – Concentrated ferrous ammonium sulfate solution 0.125 M: 49.01 g of Fe(NH₄)₂(SO₄)₂·6H₂O were dissolved in around 500 mL of distilled water and 20 mL of concentrated H₂SO₄ were slowly added. The solution was allowed to cool down and the volume was completed up to 1000 mL with distilled water.

(D) – Ferrous ammonium sulfate solution (FAS) 0.0125 M: 100 mL of solution (C) were diluted in distilled water up to the volume of 1000 mL.

(E) – $K_2Cr_2O_7$ standard solution: 12.26 g of $K_2Cr_2O_7$ previously dried at 103 °C for 2 hours were dissolved in distilled water. The volume was then completed up to 1000 mL.

(F) – Ferroine solution: this solution was bought prepared.

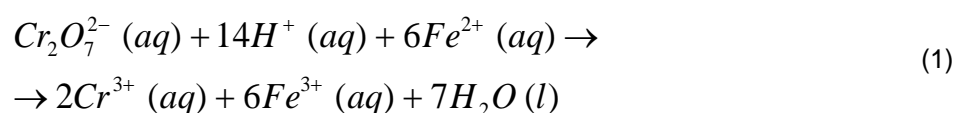
Firstly, 1.5 mL of sample, 1 mL of solution (A) and 2 mL of solution (B) were added into glass tubes. Duplicates were prepared for each sample and blanks are obtained by replacing the sample by 1.5 mL of distilled water. The mixture was carefully mixed, the tubes were closed and put into the digester at 150 °C for 2 hours.

After digestion, the tubes were allowed to cool down to room temperature in the dark. Then, the content of each tube was transferred to a 50 mL erlenmeyer, washing twice with distilled water (also transferred to the Erlenmeyer). One drop of ferroine solution (F) was added and the dichromate in excess was determined by titration with solution (D), under agitation with a magnetic stirrer. The end of titration was reached when the color of the solution changes from pale blue to strong orange/red. The volume of solution (D) spent in the titration was annotated for each sample. FAS molarity (see calculations below) was determined by titration of a standard solution that was prepared (in duplicate) as follows: 1 mL of (E) was diluted in distilled water, in an Erlenmeyer. 2 mL of concentrated H_2SO_4 were added and the solution was allowed to cool down. Then, one drop of ferroine (F) was added and the solution was titrated with solution (D).

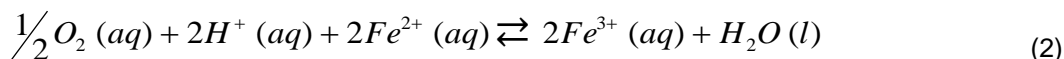
Samples collected from phase 3 and the aqueous phases of the extractions with phase 3 and organic solvents were diluted 1/100 with distilled water. The aqueous phases of the extractions with distilled water instead of phase 3 (blanks) were diluted 1/20.

COD calculation:

The chemical reaction that occurs during titration is given by:



The relation between the number of Fe^{2+} moles consumed and the number of moles of the oxygen that is dissolved in the sample is given by:



If $c(FAS)$ corresponds to FAS molarity, then it is calculated as follows:

$$c(FAS) = \frac{n(FAS)}{V(FAS)} = \frac{n(Fe^{2+})}{V(FAS)} = \frac{6 \times n(Cr_2O_7^{2-})}{V(FAS)} \quad (3)$$

Which gives:

$$c(FAS) = \frac{6 \times \frac{[K_2Cr_2O_7]}{M(K_2Cr_2O_7)} \times V(K_2Cr_2O_7)}{V(FAS)} \quad (4)$$

In this equation, $[K_2Cr_2O_7]$ is the concentration of the standard solution (0.01226 g/L), $M(K_2Cr_2O_7)$ is the molar mass of potassium dichromate (294.185 g/mol), $V(K_2Cr_2O_7)$ is the volume of the standard solution that is titrated (1 mL) and $V(FAS)$ is the volume of FAS spent in the titration of the standard.

If:

A – Volume of FAS spent in the titration of the blank (mL)

B – Volume of FAS spent in the titration of the sample (mL)

Then:

(A-B) is the volume of FAS spent in the titration of the excess dichromate.

(A-B) × c(FAS) corresponds to the number of Fe^{2+} moles consumed.

The moles of oxygen necessary for the oxidation of Fe^{2+} to Fe^{3+} are given by:

$$n(O_2) = \frac{(A - B) \times c(FAS)}{4} \quad (5)$$

Since COD values are usually expressed in mg O_2 /L, it is necessary to convert the moles of oxygen into mass by multiplying the previous value by the molar mass of O_2 (32000 mg/L):

$$m(O_2) = \frac{(A - B) \times c(FAS)}{4} \times 32000 = (A - B) \times c(FAS) \times 8000 \quad (6)$$

Considering the volume of the sample (V_s), COD values are given by:

$$COD (mg O_2 / mL) = \frac{(A - B) \times c(FAS) \times 8000}{V_s} \quad (7)$$

If the samples were previously diluted, the COD value was obtained by multiplying the value obtained with equation 7 by the dilution factor.

3.2.3. Liquid-liquid extractions

Nine different organic solvents were selected to be assessed according the criteria defined in the introduction and to provide examples of different chemical classes: dichloromethane, MTBE, MIBK, heptane, hexane, toluene, diethyl ether, 1-octanol and 1-butanol. 4 mL of phase 3 (previously basified to pH between 12-13 with approximately 0.20 g of NaOH) and 2 mL of each solvent were added to a test tube. The tubes were vortexed for 2-3 minutes, the mixture was transferred into a graduated cylinder and allowed to stand for 8-10 minutes. Then, the volumes of both organic and aqueous phase were annotated, the aqueous phase was collected with a Pasteur pipette and put in a new test tube. A second extraction was performed by adding 2 mL of the same organic solvent. The test tube was again vortexed, and the same procedure described above was done. After the two extractions, 1.5 mL of the aqueous phase was recovered, basified with KOH pellets (13-13.5) and centrifuged for 4 minutes at 14000 rpm. The samples were then filtered into vials and analyzed by HPLC for lupanine quantification. The organic phase was also recovered into small glass flasks and left in the hotte for 2 to 5 days to promote the evaporation of the organic solvent, and in the end a stream of nitrogen was used. Then, 4 mL of distilled water were added to the flasks and a sample of 1.5 mL was recovered, basified with KOH pellets (pH between 13-13.5), centrifuged for 4 minutes at 14000 rpm, filtered into vials and analyzed by HPLC.

The procedure above described was repeated using 4 mL of a solution of pure lupanine in water (3.2 g/L) instead of phase 3.

Blanks were made for the best solvents (dichloromethane, MTBE, 1-octanol, 1-butanol and toluene), by replacing phase 3 with distilled water.

3.2.4. Resins

Binding assays

Firstly, 18 different resins were tested: IRC 50, IRC 86, IRC 7481, AG-50W-X2, AG-50W-X8, Amberlyst 16, Amberlyst 36, Purolite PD206 Amberlite IRA 68, Amberlite IRA 458-Cl, Amberlite IRA 400-Cl, Amberlite IRA 410, Amberlite CG-400, Amberlite XAD-1, Amberlite XAD-7, Amberlite XAD-16, Dowex 1X8-50 and Dowex MAC-3.

Binding assays were done by adding 0.15 g of each resin and 1.5 mL of phase 3 to 2 mL Eppendorf tubes. The tubes were allowed to stand for approximately 15 hours at room temperature, under agitation (260 rpm) with magnetic stirrers. Each resin was tested in duplicate. After 15 hours, the tubes were centrifuged at 14000 rpm for 4 minutes. The supernatant was recovered and basified with KOH pellets (pH between 13 - 13.5). After this, the samples were centrifuged again, at 14000 rpm for 4 minutes and the supernatant was recovered, filtered to vials and analyzed by HPLC for lupanine quantification.

Regeneration assays

After the binding assays, the best resins (IRC 50, IRC 86, AG-50W-X2, AG-50W-X8, Amberlyst 16, Amberlyst 36, Purolite PD206 and Amberlite XAD-16) were regenerated using five different

solutions: HCl 10% (w/w) in water, NaOH 10% (w/w) in water, HCl 10% (w/w) in ethanol/water (70:30 v/v), NaOH 10% (w/w) in ethanol/water (70:30 v/v) and ethanol absolute. 1.5 mL of a regeneration solution were added to the eppendorfs containing the resins. After this, the procedure was the above-described for the binding assays, except for the regeneration solutions with ethanol. In these cases, the supernatant was recovered after the first centrifugation, filtered to new eppendorfs which were left in the fume hood for two days to promote the evaporation of the organic solvent, and then a stream of nitrogen was used. The volume was refilled with water (final volume approximately 1.5 mL), the samples were basified with KOH, centrifuged and filtered to vials for lupanine quantification.

3.2.5. Nanofiltration and Ultrafiltration

Around 400 mL (or 1500 mL) of lupin beans debittering wastewater were centrifuged at 6000 rpm and 20 °C for 30 minutes. The supernatant was recovered to be used as feed of the filtrations.

The conditioning of the membranes was done by introducing around 400 mL of distilled water into the filtration cell, applying pressure (20 bar for the nanofiltration and 5 bar for the ultrafiltration) and setting the gear pump flow rate for 420 mL/min. (or 600 mL/min.). Then, the permeate was recovered and the membranes were ready when the flux was constant.

After conditioning, the supernatant of the wastewater was introduced in the filtration cell (maximum 400 mL), the gear pump flow rate was set for 420 mL/min. (or 600 mL/min.) and the feed was left to recirculate (with no pressure) for approximately 5 minutes. After this time, two samples of 1.5 mL were recovered (initial samples) and the pressure was applied to the system (20 bar for the nanofiltration and 5 bar for the ultrafiltration).

The permeate was recovered into graduated cylinders, the flux was registered over time and some permeate and retentate samples were taken during the experiments for lupanine quantification, COD measurement, pH and conductivity control. Depressurizations were done every time a retentate sample was taken.

Concentration experiments

The filtration of 1500 mL was done by introducing the first 400 mL into the filtration cell (the maximum cell capacity), and using an HPLC pump connected to the cell, to introduce the remaining supernatant. The flux of the HPLC pump was adjusted to the permeate flux over time so that the volume inside the filtration cell was kept constant. The experiment was stopped after to collect 1200 ml in the permeate.

Recirculation experiments

The filtration was done by introducing the first 400 mL into the filtration cell and after 100 mL of permeate were recovered to a small Schott flask, maintaining a retentate volume of 300 ml, an HPLC pump was connected between the flask and the filtration cell reservoir to allow the introduction of the permeate back in the filtration cell. The flux of the HPLC pump was adjusted to the permeate flux over

time so that the volume inside the filtration cell and in the schott flask were kept constant. The experiment was stopped after 13 and 16 hours, for a flow rate equal to 420 and 600 mL/min., respectively.

3.2.6. Molecularly Imprinted Polymers

Synthesis of MIPs

MIPs were synthesized by bulk polymerization. 5 different monomers were tested: Methacrylic acid, Itaconinc acid, Methyl methacrylate, Styrene and N-isopropylacrylamide. A monomer:cross-linker:template ratio of 0.4:2.0:0.1 was used. 750 μ L of DCM were used per 0.1 mmol template, and the quantity of AIBN corresponds to 1% w/w of monomer+cross-linker weight.

Firstly, the functional monomer and the template (lupanine) were dissolved in dichloromethane, inside a glass tube, for 5 minutes under agitation with a magnetic stirrer, at room temperature. After this, the initiator (AIBN) and the cross-linker (EGDMA) were added to the polymerization solution, that was purged with a stream of nitrogen for 10 minutes at room temperature. The tube was closed and placed at 40 °C overnight (15 hours), under agitation. Then, the temperature was increased with 5 °C/20 min. increments up to 65 °C. At this temperature, the tube was left for 4 hours. In the end of the polymerization reaction, a rigid bulk polymer was obtained. The tube was opened and the polymer was crushed in a mortar. The non-imprinted polymers (NIPs) were synthesized using the same experimental conditions, except that no template was added.

After crushing, the polymers obtained with IA, MAA and MMA were transferred into a thimble to be washed using a Soxhlet-apparatus. In the case of the MIPs obtained with MAA and IA, the template molecule was removed using 70 mL of a solution of 0.1 M HCl in MeOH for 48 hours. The traces of HCl were then removed from the polymers with 70 mL of MeOH for 24 hours. NIPs obtained with methacrylic acid and itaconic acid were washed with 70 mL of MeOH for 24 hours. In the case of the MIPs obtained with MMA, the template molecule was removed using 70 mL of dichloromethane for 48 hours. NIPs obtained with MMA were washed with 70 mL of dichloromethane for 24 hours.

The polymers obtained with styrene and N-isopropylacrylamide were transferred into a glass beaker after crushing. The template was removed from MIPs with four sequential washings, using 25 mL of 0.1 M HCl in MeOH at a time, under agitation with a magnetic stirrer. Each washing step consisted of adding 25 mL of the HCl solution that was left in contact with the polymer for 3 minutes. Then, the solution was decanted and another 25 mL of the washing solution were added. This procedure was repeated four times. The traces of HCl were then removed from the polymers with three sequential washings using 25 mL of MeOH at a time, under agitation as described above for the template removal. NIPs obtained with styrene and N-isopropylacrylamide were washed with three sequential additions of 25 mL of MeOH at a time, under agitation as described above.

Two samples (1.5 mL each) of all washing solutions of MIPs were recovered into eppendorfs in the end and left in the fume hood for 5 days to promote the evaporation of the organic solvent. Then, 1.5 mL of distilled water were added, the samples were basified with KOH (13-13.5), centrifuged for 4

minutes at 14000 rpm, filtered into vials and analyzed by HPLC for lupanine quantification, to confirm that the template was removed.

After washing, the polymers were placed in a Petri dish, left in the fume hood for at least 15 hours and dried under vacuum at 40 °C.

In the end, the polymers were grounded in a mechanical mortar and sieved through sieves of 38 µm and 63 µm pore size. The fraction between 38 µm and 63 µm was used for the binding experiments.

Binding assays

Binding assays with MIPs were done by adding 0.075 g of each MIP and 1.5 mL of a solution of pure lupanine in dichloromethane (1 or 0.5 g/L) to 2 mL Eppendorf tubes. The tubes were allowed to stand for approximately 24 hours at room temperature, under magnetic agitation (60 rpm). Each MIP was tested in duplicate. After 24 hours, the tubes were centrifuged at 14000 rpm for 20 minutes. The supernatant was filtered using PTFE syringe filters to new Eppendorf tubes, and left in the fume hood for 1 day to promote the evaporation of the organic solvent. Then, the volume recovered was refilled with distilled water, the samples were basified with KOH pellets (pH between 13-13.5), centrifuged for 4 minutes at 14000 rpm, filtered into vials and analyzed by HPLC.

Regeneration assays

Regeneration assays of MIPs were done by adding 1.5 mL of 0.1 M HCl in MeOH to the Eppendorf tubes where the binding assays were performed. The tubes were allowed to stand for approximately 24 hours at room temperature, under magnetic agitation (60 rpm). After 24 hours, the tubes were centrifuged at 14000 rpm for 20 minutes. The supernatant was recovered to new Eppendorf tubes, and left in the fume hood for 1 day to promote the evaporation of the organic solvent.

Then, the volume recovered was refilled with distilled water, the samples were basified with KOH (13-13.5), centrifuged for 4 minutes at 14000 rpm, filtered into vials and analyzed by HPLC for lupanine quantification. A new regeneration cycle of 24 hours was performed after the first one, following the same steps.

3.2.7. Enantiomeric Excess

The samples for enantiomeric excess determination were analyzed by HPLC using a chiral column (Chiral Pak IC). Firstly, the supernatant recovered after the binding assays with the chiral MIP (MIP obtained with IA and L-(-)-lupanine as template) was recovered to new eppendorfs and left in the fume hood for solvent evaporation. Then, around 5 mg of lupanine were weighted and dissolved in 100 µL of isopropanol and 900 µL of hexane for HPLC injection. The mobile phase was constituted by a mixture of hexane (50%), isopropanol (25%) and hexane (with 0.1% diethanolamine (DEA); 25%). The analysis was performed at a flow rate of 1 mL/min. at room temperature and the detection was done at 230 nm.

3.2.8. Enzymatic Assays

Phosphate buffered saline (PBS) was the buffer solution utilized for the enzymatic assays. Firstly, two 1 M solutions were prepared in volumetric flasks by dissolving 17.42 g of K_2HPO_4 and 13.61 g of KH_2HPO_4 in 100 mL of distilled water. Then, 9.08 mL of K_2HPO_4 1 M and 0.920 mL of KH_2HPO_4 1 M were added into a 100-mL volumetric flask, and distilled water was added up to 100 mL to obtain a PBS solution of 0.1 M and pH 7.8.

5 mL of a solution of lupanine in PBS (0.025 g/L) were added into small glass flasks. The control flask contained only lupanine and the test flask contained lupanine and around 20 mg of enzyme used as supplied. The flasks were placed at 37 °C in an incubator, under agitation (325 rpm) with magnetic stirrers, and left to react for seven days. A sample of 1 mL was taken every day for lupanine quantification.

4. Results and discussion

4.1. Improvement of unit operations: membranes, organic solvents and resins

The first goal of this thesis was the improvement of unit operations suggested to extract lupanine from lupin beans wastewater. The main results regarding nanofiltration and ultrafiltration membranes are discussed. Then, a sub-section containing liquid-liquid extractions results is presented, including a discussion solvent selection considering several aspects (% extraction, COD retained, water contamination, environmental impact and boiling point). Section 4.1. ends with a study on the extraction of lupanine with resins, also including a discussion on resin selection based on the % binding, regeneration, COD retained and recyclability.

4.1.1. Membrane-based processes

The goal of using nanofiltration for the wastewater is to obtain pure water as permeate, and to concentrate lupanine in the retentate. Lupin beans debittering wastewater was used for concentration and recirculation studies using NF270. An ultrafiltration membrane performance was also analyzed.

Flux (J) and permeability (L_p) were calculated according to the following equations:

$$J \text{ (mL min}^{-1} \text{ m}^{-2}\text{)} = \frac{\text{Flow rate (mL min}^{-1}\text{)}}{\text{Membrane area (m}^2\text{)}} \quad (8)$$

The total membrane area is equal to 0.0026 m².

$$L_p \text{ (mL min}^{-1} \text{ m}^{-2} \text{ bar}^{-1}\text{)} = \frac{J \text{ (mL min}^{-1} \text{ m}^{-2}\text{)}}{P \text{ (bar)}} \quad (9)$$

COD and lupanine rejection were calculated using the following equations:

$$COD_{rejection} \text{ (\%)} = \frac{COD_{feed} - COD_{permeate}}{COD_{feed}} \times 100 \quad (10)$$

$$lupanine_{rejection} \text{ (\%)} = \frac{lupanine_{feed} - lupanine_{permeate}}{lupanine_{feed}} \times 100 \quad (11)$$

COD_{feed} is the COD value in the wastewater (27.85 ± 0.90 g O₂/L) and $COD_{permeate}$ is the COD value determined for the permeate recovered in the end of the filtration. $lupanine_{feed}$ is the initial concentration of lupanine, and $lupanine_{permeate}$ is the concentration of lupanine in the permeate.

4.1.1.1. Ultrafiltration and nanofiltration membranes assessment

Initial experiments were performed using a volume of wastewater of around 400 mL, concentrated until 50-60% of the initial volume. These experiments allow to obtain important parameters such as COD rejection, lupanine rejection and flux values for the membranes. The pH and the conductivity were also determined for permeate and retentate obtained in the end of the experiment. A sample of the feed was recovered before applying pressure. A SEPA CF TF (thin film) UF from Lenntech with a MWCO of 3000 Da and a NF270 nanofiltration membrane from Dow FILMTEC were used for ultrafiltration and nanofiltrations, respectively using at 5 bar and 20 bar of applied pressure. All the filtrations were performed with a tangential flow provided by a gear pump set for 420 mL/min., that corresponds to a linear velocity equal to 16.15 mL/min.cm².

Ultrafiltration is a process that can be used before the nanofiltration to retain most of the proteins, for example, while generating a permeate that is rich in lupanine. The ultrafiltration was done using a thin film membrane with a molecular weight cutoff of 3000 Da. Around 400 mL of wastewater were filtered (after centrifugation) under 5 bar, and 420 mL/min. In the end, approximately 250 mL of permeate and 150 mL of retentate were obtained. Table 10 contains the values of COD, lupanine concentration, pH and conductivity of each fraction recovered after the ultrafiltration process. The flux values were also registered during this filtration (Figure 19).

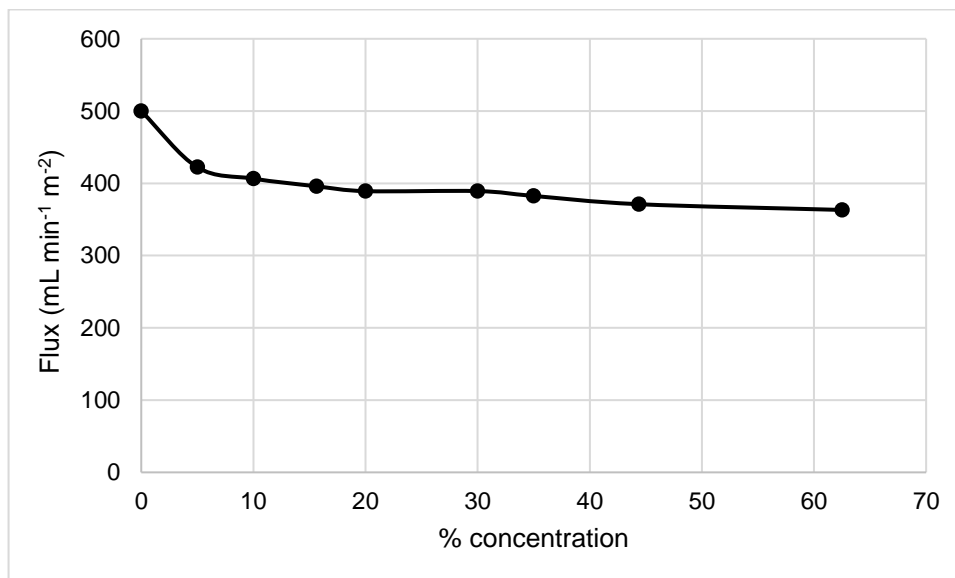


Figure 19. Variation of permeate flux with % concentration, during the ultrafiltration of 400 mL of lupin beans debittering water. The % concentration is the ratio between the volume of permeate over volume of feed.

Table 10. COD, lupanine concentration, pH and conductivity values obtained for each fraction recovered after ultrafiltration of 400 mL of lupin beans wastewater. COD rejection was calculated according to equations 8 and 9.

Fraction	Lupanine (g/L)	COD (g O ₂ /L)	% COD rejection	pH	Conductivity (μS)
Feed	4.804 ± 0.549	23.09 ± 0.41	12.46 ± 1.93	4.01	5700
Permeate	5.622 ± 0.410	20.21 ± 0.41		3.75	5460
Retentate	4.988 ± 0.505	31.17 ± 0.41		3.91	6860

The % COD rejection obtained for the ultrafiltration membrane that was utilized is very low, which means that the great majority of the macromolecules that are present in the wastewater can pass through it. This result shows the ultrafiltration membrane that was tested is inadequate to retain COD, which means that a membrane with cut-off much lower than 3000 Da is required.

The nanofiltration experiments were performed comparing the use of wastewater (phase 3, after centrifugation) directly or using around 250 mL of the ultrafiltration permeate, to mitigate fouling of the nanofiltration membrane. The flux values registered during this filtration are represented in Figure 20, along with the flux values obtained during the other nanofiltration experiment. Tables 11 and 12 contains the values of COD and lupanine concentration in each fraction recovered after the nanofiltration process. Both nanofiltration experiments were performed in similar conditions and concentration factors range, but in one case, the permeate of an ultrafiltration was used, instead of the debittering wastewater. According to Tables 11 and 12., all the parameters (lupanine, COD, pH and conductivity) are similar for both nanofiltration experiments, as expected.

Table 11. COD, lupanine concentration, pH and conductivity values obtained for each fraction recovered after nanofiltration of 400 mL of lupin beans wastewater. Lupanine and COD rejection were calculated according to equations 10 and 11.

Fraction	Lupanine (g/L)	% lupanine rejection	COD (g O ₂ /L)	% COD rejection	pH	Conductivity (μS)
Feed	4.734 ± 0.752	99.50 ± 0.31	27.85 ± 0.90	94.11 ± 0.19	4.16	5970
Permeate	0.024 ± 0.017		1.64 ± 0.06		3.36	355
Retentate	9.234 ± 0.586		60.18 ± 1.71		4.08	8510

Table 12. COD, lupanine concentration, pH and conductivity values obtained for each fraction recovered after nanofiltration of 250 mL of permeate from the ultrafiltration. Lupanine and COD rejection were calculated according to equations 10 and 11.

Fraction	Lupanine (g/L)	% lupanine rejection	COD (g O ₂ /L)	% COD rejection	pH	Conductivity (μS)
Feed	4.917 ± 0.162	99.46 ± 0.03	20.13 ± 0.33	97.28 ± 0.11	3.90	5475
Permeate	0.021 ± 0.001		0.54 ± 0.00		3.25	281
Retentate	6.199 ± 0.248		20.06 ± 3.67		4.02	9750

It is important to note that both lupanine and COD rejections are high. During nanofiltration, lupanine must stay in the retentate as much as possible and a simultaneous wastewater volume reduction should be achieved. A significant lupanine rejection was obtained with NF270 (table 11.), which means that the concentration of this compound in the permeate is low. COD rejection is also high, as expected, since most of the macromolecules present in the water will be retained by the pore size of the membrane, along with lupanine. Thus, a process prior to or after the nanofiltration is required to reduce COD.

Also, along with the concentration of lupanine in the retentate, clean water should be obtained in the permeate of the nanofiltration. According to Portuguese Legislation, the maximum COD concentration in urban wastewater discharges into receiving waters is equal to 0.125 g O₂/L [78]. The results of COD concentration for both nanofiltration experiments show that these values are higher than the reference value, which means that additional strategies are needed to reduce COD in the permeate after the nanofiltration. Ozonation or UV oxidation can be applied to the permeate to reduce COD for concentrations lower than or equal to 0.125 g O₂/L.

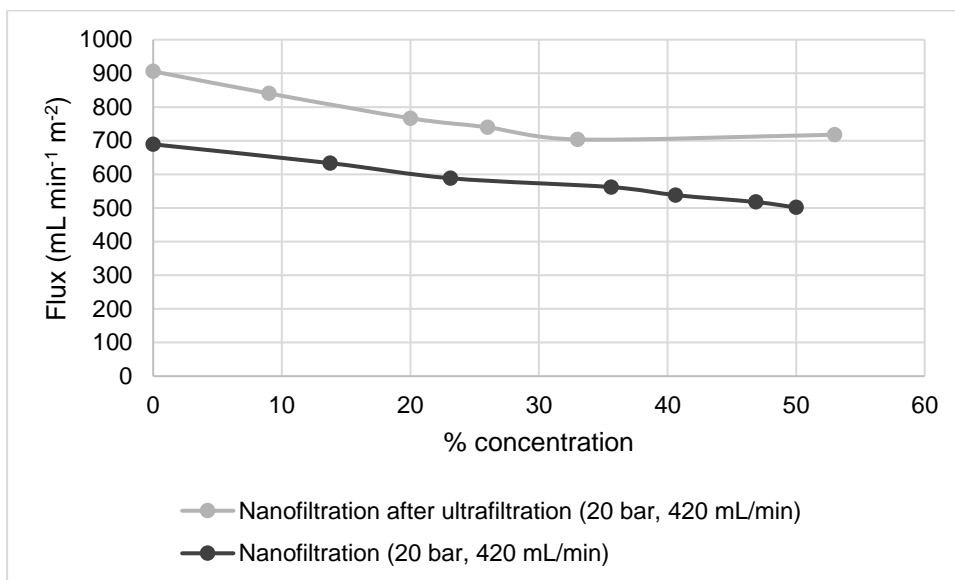


Figure 20. Variation of permeate flux with % concentration, during the nanofiltration of 400 mL of lupin beans debittering water, and the nanofiltration of 250 mL of permeate from the ultrafiltration experiment. The % concentration is the ratio between the volume of permeate over volume of feed.

The graphical representation of flux as a function of the % of concentration (Figure 20.) shows that the flux is higher for the nanofiltration that was performed after the ultrafiltration. Although the COD rejection for the ultrafiltration membrane that was tested was low, it seems to retain some macromolecules that will have an impact in the nanofiltration membrane performance.

4.1.1.2. Nanofiltration membrane performance: recirculation and concentration studies with NF270

The robustness of the nanofiltration membrane (NF270) was studied by concentration of a significant volume of lupin beans wastewater and by recirculation experiments using the centrifugation supernatant of phase 3 (i.e the solution after lupin beans cooking and resting stages, and before the beginning of the lupin beans debittering stage -which employs the larger volumes of water- by wash out of lupanine from the lupin beans solution). Note that the feed solutions were fed to the nanofiltration stage without a prior ultrafiltration process.

In case the wastewater from the lupin beans debittering stage (phase 4) is targeted, the retentate obtained from the concentration of this wastewater should be enriched to reach concentrations of lupanine and other retained aqueous matrix components at values that will be necessarily below the values found in phase 3. In this context, two recirculation experiments were performed using phase 3 (after centrifugation) to assess system flux robustness. Both recirculation experiments were done using NF270, around 400 mL of wastewater (after centrifugation) and they were performed at 20 bar, the only difference was the pump gear flow (420 mL/min and 600 mL/min). These experiments started with a simple filtration to obtain around 100 mL of permeate, leaving about 300 ml in the retentate side of the system and then the recirculation started using a HPLC pump, to introduce the permeate back in the filtration cell.

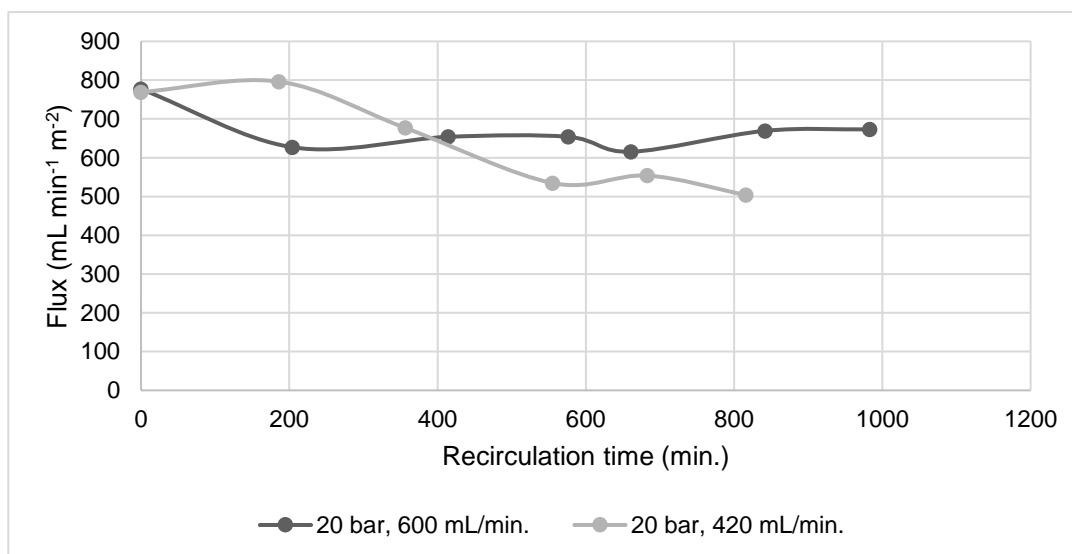


Figure 21. Variation of permeate flux with time of recirculation, after filtration of 400 mL of lupin beans wastewater to obtain 100 mL that were then recirculated. Two experiments were made: the first one for around 13 hours, at 420 mL/min. and the other one for around 17 hours at 600 mL/min. Both experiments were performed at 20 bar, using NF270.

According to Figure 21., flux decline is more significant when a lower gear pump flow is used. It seems that an increase from 420 mL/min to 600 mL/min leads to a higher and more stable flux. At this rotational speed, the flux registered after approximately 17 hours of recirculation was equal to 1346 mL min⁻¹ m⁻², and for 420 mL/min the final flux was around 1008 mL min⁻¹ m⁻², after approximately 13 hours of recirculation. The robustness of the membrane seems to be better for 600 mL/min.

Lupanine concentration (table 13.), pH and conductivity (see annex C.) were analyzed in the permeate and retentate obtained after the filtration of 400 mL of lupin beans wastewater to obtain 100 mL of permeate, and in the permeate and retentate in the end of the recirculation experiments.

Table 13. Lupanine concentration for both permeate and retentate recovered after the filtration of 100 mL and both permeate and retentate recovered after the recirculation experiments.

Sample	Lupanine (g/L)	
	Recirculation 20 bar; 420 mL/min.	Recirculation 20 bar; 600 mL/min.
Initial	4.149 ± 0.028	3.122 ± 0.055
Retentate after filtration of 100 mL	5.774 ± 0.226	4.118 ± 0.095
Retentate after recirculation	6.518 ± 0.343	5.693 ± 0.283
Permeate after filtration of 100 mL	0.003 ± 0.001	0.003 ± 0.002
Permeate after recirculation	0.002 ± 0.001	0.008 ± 0.006

Lupanine concentration is similar for both experiments which means that the rotational speed of the gear pump does not seem to interfere with lupanine retention on the membrane.

The COD obtained by the end of the experiments in the permeate was equal to 0.084 ± 0.000 g O₂/L, that is lower than the reference value (0.125 g O₂/L).

The concentration experiments described were performed using the phase 3 (i.e. the solution after lupin beans cooking and resting stages, and before the beginning of the lupin beans debittering stage), which corresponds to the more challenging case regarding the high content in organic matter and fouling agents.

The first concentration experiment consisted in the concentration of around 1500 mL of wastewater (supernatant recovered after centrifugation) using NF270 at 20 bar and a pump gear flow equal to 420 mL/min. Figure 22. shows the permeate flux as a function of the % concentration.

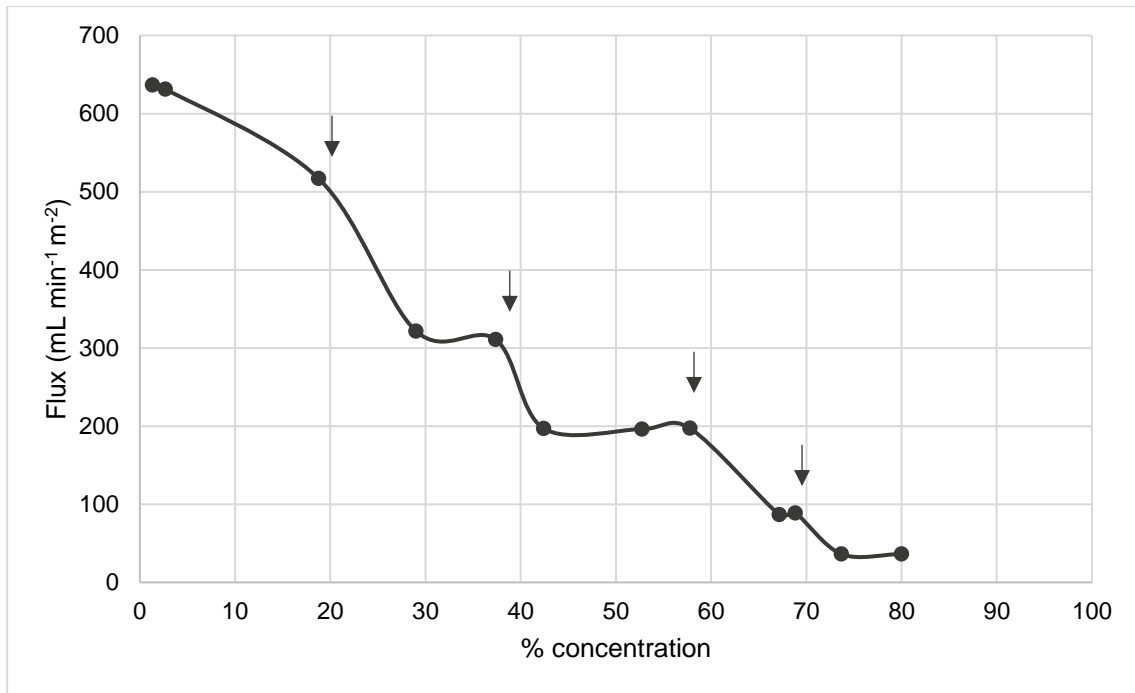


Figure 22. Variation of permeate flux with % concentration, during the nanofiltration of 1500 mL of lupin beans debittering water. The % concentration is the ratio between the volume of permeate over volume of feed. The arrows signalize the depressurizations of the filtration cell.

The abrupt flux changes signalized by the arrows in Figure 22. were caused by the depressurizations of the filtration cell overnight since the system is not automatized. During this time, the recirculation of the gear pump flow was reduced from 420 mL/min. to 180 mL/min. to avoid permeate losses, which may have contributed to an increase of fouling on the membrane. If the present experiment had been done in a continuous way (with no depressurizations or flow changes of the gear pump) maybe the flux would not have decayed so suddenly. At the end of the experiment (approximately 80 % concentrate), the flux seems to stabilize at 72.60 mL min⁻¹ m⁻².

The main goal of this filtration was to observe the flux decay over time because of fouling phenomenon. Although the wastewater is centrifuged before the nanofiltration, some particles are recovered with the supernatant and will be deposited on the membrane. Also, the macromolecules that are present in the feed contribute to fouling. COD concentration in the retentate, at the end of the experiment was high (85.28 ± 0.43 g O₂/L), as expected. Therefore, an ultrafiltration, with an appropriate membrane, before the nanofiltration would be important to retain most of the COD and prevent fouling.

The concentration of lupanine was analyzed in the permeate and retentate during the concentration experiment, and the final value in the retentate (correspondent to a % concentration of 80 %) was 12.71 ± 0.87 g/L (Figure 23.).

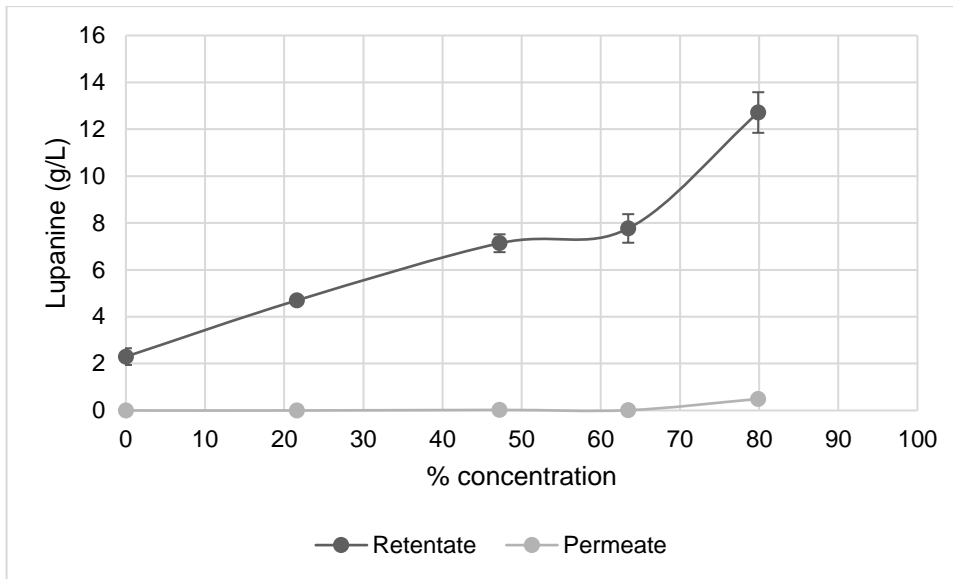


Figure 23. Lupanine concentration in the retentate and permeate during the nanofiltration of 1500 mL of lupin beans debittering water, at 20 bar and 420 mL/min.

Conductivity and pH values were also registered for both permeate and retentate (Figure 24.). It is possible to observe that, unlike conductivity, there are no significant changes in the pH. At pH between 3-4, lupanine is protonated as the pKa of this alkaloid is 9.1. The conductivity of the retentate is much higher than in the permeate which means that most of the charged molecules present in the wastewater are retained by the membrane, a phenomenon that was also noticed after the previous nanofiltration experiments. Also, from 0 to 22 % concentration, the conductivity of the retentate doubles and then only slight increases were registered until the end of the experiment.

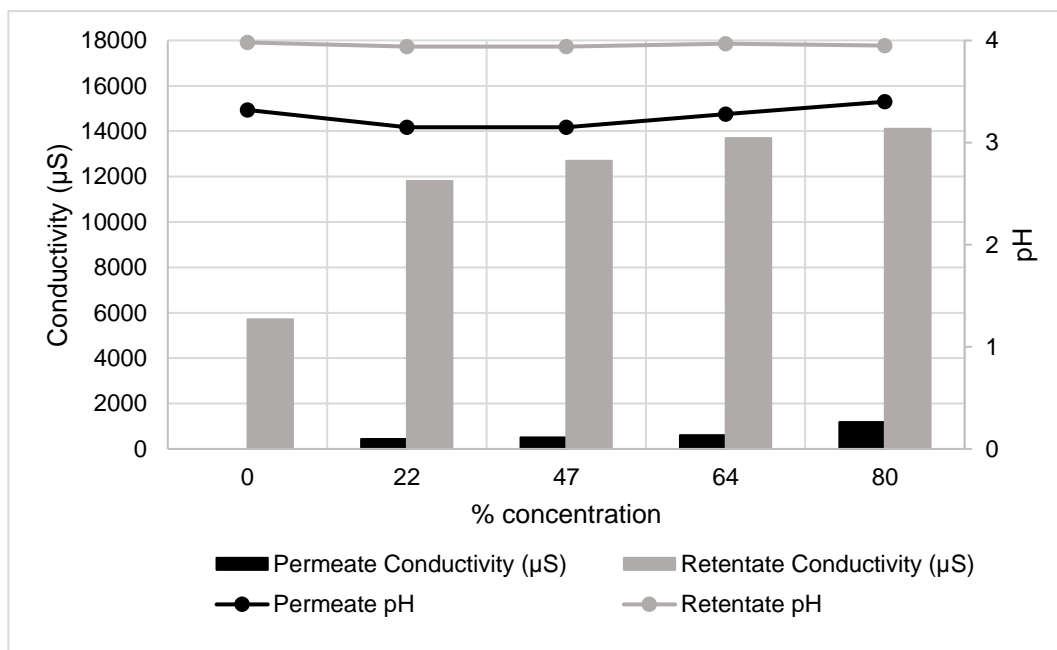


Figure 24. Conductivity and pH values registered for both permeate and retentate during the concentration of 1500 mL of lupin beans debittering wastewater.

After the recirculation experiment at 20 bar and 600 mL/min., a new concentration test (similar to the one previously described) was performed by adding around 370 mL to the retentate obtained in the end of the recirculation (total feed equal to 670 mL) and using the same membranes.

Flux values obtained during the new concentration experiment are shown in Figure 25. Again, the abrupt flux changes signaled by the arrows in the figure were caused by the depressurizations of the filtration cell overnight and the subsequent reduction of the rotational speed from 600 to 180 mL/min. The flux results of this nanofiltration can be compared with the ones shown in Figure 22. It is possible to say that the increase of the rotational speed seems to have a positive impact because in general, for the same % concentration, the flux is higher in this case than when the experiment is performed at 420 mL/min.

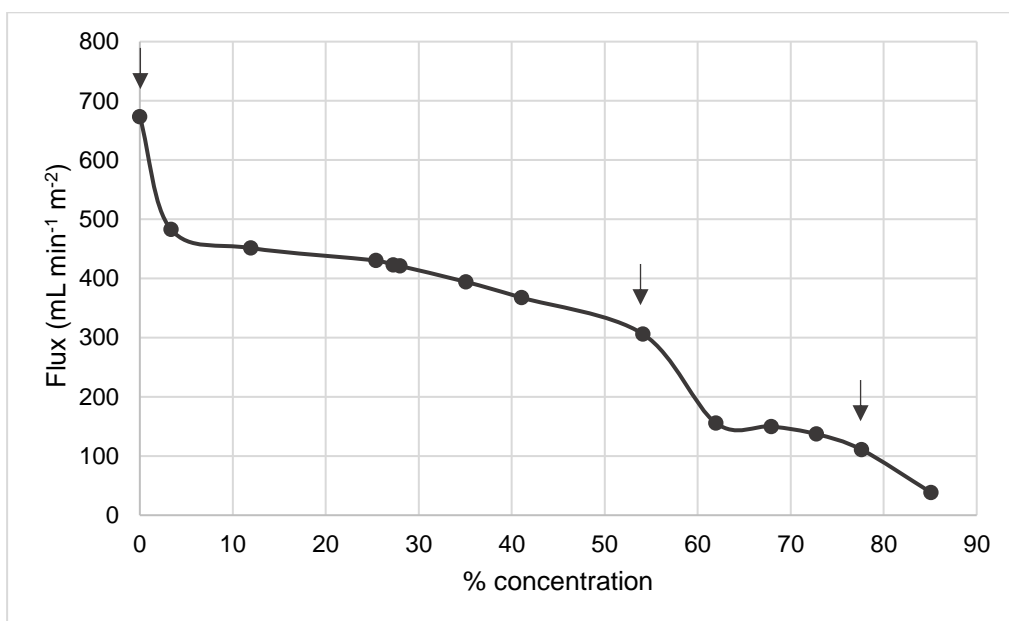


Figure 25. Variation of permeate flux with % concentration, during the nanofiltration of 670 mL of lupin beans debittering water, immediately after the recirculation experiment at 20 bar and 600 mL/min. The % concentration is the ratio between the volume of permeate over volume of feed. The arrows signalize the depressurizations of the filtration cell.

The graphical representations of flux vs % concentration for both concentration experiments show that there is a significant flux drop with overnight stops. This observation shows that the organic matter has a significant influence in membrane performance. Thus, clean in place (CIP) operations should be added to the process.

The concentration of lupanine was analyzed in the permeate and retentate during the concentration experiment (Figure 26.).

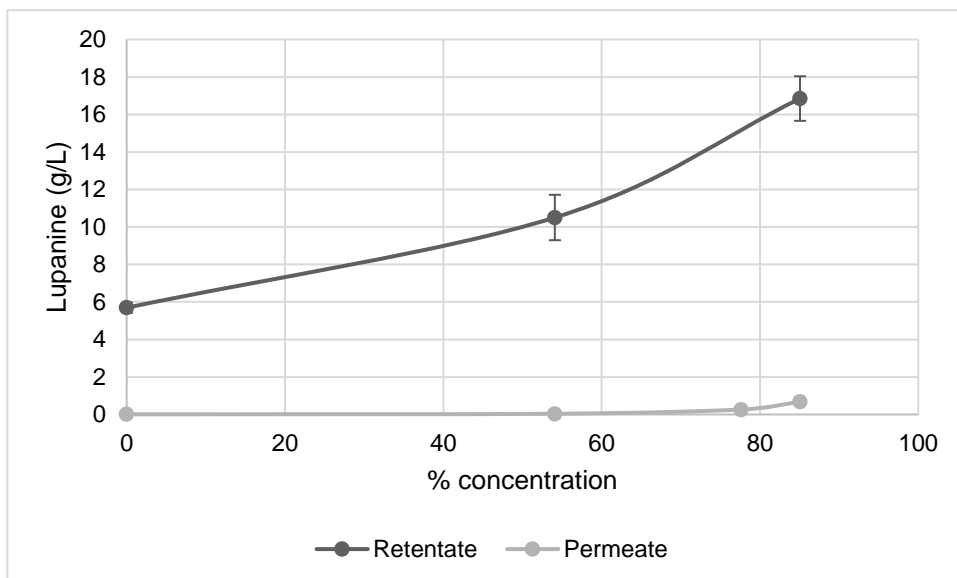


Figure 26. Lupanine concentration in the retentate and permeate during the nanofiltration of 670 mL of lupin beans debittering water, at 20 bar and 420 mL/min.

The final value in the retentate (correspondent to a % concentration of 85 %) was 16.85 ± 1.19 g/L, which is slightly higher than the final concentration of the value of 12.71 ± 0.87 g/L, obtained on previous concentration experiment.

Although these preliminary results seem interesting, the total feed volume differences (that have probably different fouling issues) and the depressurizations (that were done for different % concentration and in an unequal number of times) must be taken into account. Both experiments should be repeated using the same feed volumes and under the same depressurization conditions, varying only the gear pump flow for reliable conclusions.

4.1.2. Extraction of lupanine with organic solvents

The solvents for liquid-liquid extractions must be selected essentially according to five parameters: the percentage of extraction (% extraction), COD retained, water contamination with extraction solvent, solvent inherent environmental impact (GSK guide) and the boiling point for easy recover of lupanine and extraction solvent recycling.

4.1.2.1. Screening of the best solvents: % extraction

The % extraction was obtained by quantifying lupanine in the organic and aqueous phases after two successive extractions with 4 mL of lupin beans wastewater and 2 mL of the organic solvent (twice). The % extraction for two successive extractions is given by the following equation:

$$\% \text{ extraction (2 successive extractions)} = \frac{c_{org\ 1} \times V_{org\ 1} + c_{org\ 2} \times V_{org\ 2}}{c_{aq\ 0} \times V_{aq\ 0}} \times 100 \quad (12)$$

In this equation, $c_{org\ 1}$ and $c_{org\ 2}$ correspond to the concentration of lupanine in the organic phase of the first and second extraction, respectively. $V_{org\ 1}$ and $V_{org\ 2}$ are the volumes of the organic phase of the first and second extraction, respectively. c_{aq} and V_{aq} are the concentration of lupanine in the aqueous phase and the volume of the aqueous phase after the two extractions, respectively.

If $c_{aq\ 0}$ and $V_{aq\ 0}$ represent the initial concentration of lupanine in lupin beans wastewater and the initial volume of the aqueous phase, respectively, then the mass balance equation for these extractions is given by:

$$c_{aq\ 0} \times V_{aq\ 0} = c_{org\ 1} \times V_{org\ 1} + c_{org\ 2} \times V_{org\ 2} + c_{aq} \times V_{aq} \quad (13)$$

Substituting equation (13) in equation (12), then:

$$\% \text{ extraction} = \frac{c_{aq\ 0} \times V_{aq\ 0} - c_{aq} \times V_{aq}}{V_{aq\ 0} \times c_{aq\ 0}} \times 100 \quad (14)$$

The % extraction was obtained for each solvent was determined using wastewater (previously basified) and using a solution of lupanine in water (3.2 g/L) to study matrix effects. The concentration of lupanine in the wastewater is approximately 3.235 g/L.

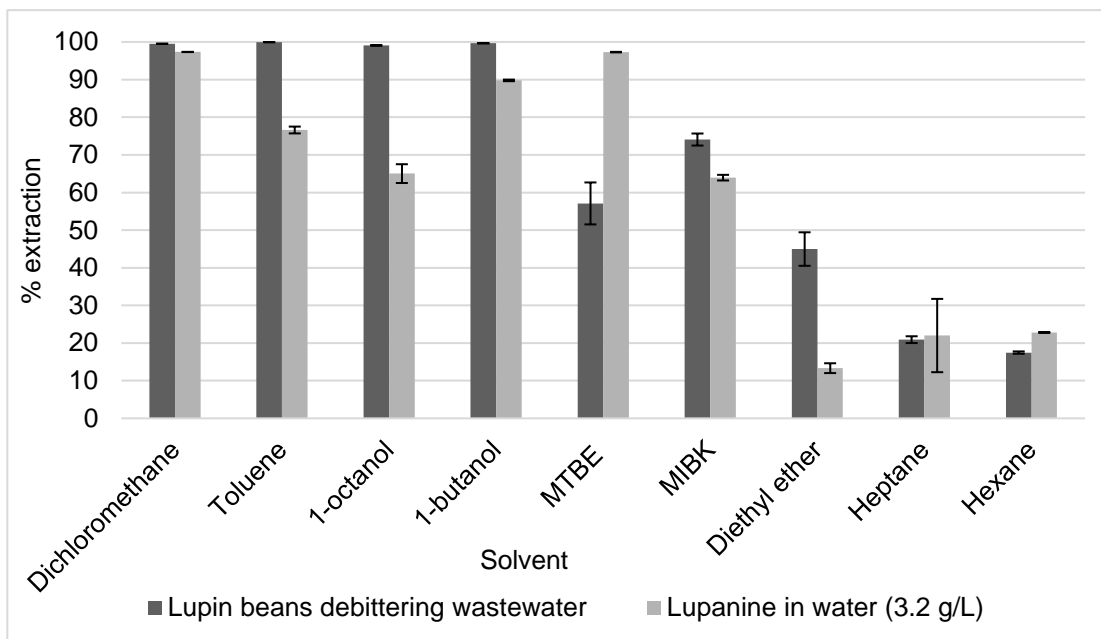


Figure 27. % extraction calculated according to equation 14 for lupin beans debittering wastewater and a solution of pure lupanine.

The solvents to extract lupanine showing higher efficiency on lupanine extraction were dichloromethane, toluene, 1-octanol, 1-butanol and MTBE.

Extraction of lupanine from aqueous wastewater using toluene, 1-octanol, diethyl ether and MTBE seems to be influenced by the matrix. MTBE appears to be more efficient if lupanine is dissolved in water. The other three solvents appear to work better if the debittering water is used. If the % extraction for a given solvent depend on the aqueous matrix, there might be some ions in the wastewater which presence will interfere with the passage of lupanine from de aqueous to the organic phase during the extractions. Depending on the concentration of the ions in solution, salting in or salting out phenomena might occur. Salting in occurs when the ions weak the attractive forces between the molecules, then increasing the solubility of lupanine in water. On the other hand, if the concentration of ions becomes higher, there will be a competition between these small molecules and lupanine for molecules of the aqueous solvent. In this case, lupanine will move to the organic phase.

In the case of MTBE, salting in in phenomenon seems to be occurring when the aqueous matrix is the lupin beans wastewater because the efficiency of the extraction is better when a solution of lupanine in water is used. On the contrary, for toluene, 1-octanol and diethyl ether salting out phenomenon seems to facilitate the passage of lupanine from the aqueous to the organic phase for lupin beans wastewater.

4.1.2.2. COD retained

In the context of the experiments that were performed, COD retained is defined as the capability of a given organic solvent to separate COD from lupanine. When doing liquid-liquid extractions, COD is supposed to remain in the aqueous phase so that the organic phase contains lupanine and as less COD as possible. Thus, a good choice would be a solvent that is able to extract a high amount of lupanine while keeping most of the organic matter in the aqueous phase.

The percentage of COD retained (% COD retained) was obtained by using the following equation:

$$\% \text{ COD retained} = \left(\frac{COD_{aq} - COD_{blank}}{COD_{aq0}} \right) \times 100 \quad (15)$$

In this equation, COD_{aq0} is the COD value determined for lupin beans wastewater (27.85 ± 0.90 g O₂/L), COD_{aq} is the COD value determined for each aqueous phase recovered after the two successive extractions with the wastewater and COD_{blank} represents the COD value of the aqueous phase recovered after two successive extractions with water instead of wastewater (blanks).

Figure 28 contains the COD retained, that was determined for the solvents with higher % extraction: dichloromethane, 1-octanol, 1-butanol, toluene and MTBE, and the values obtained for the aqueous phase recovered after the extractions.

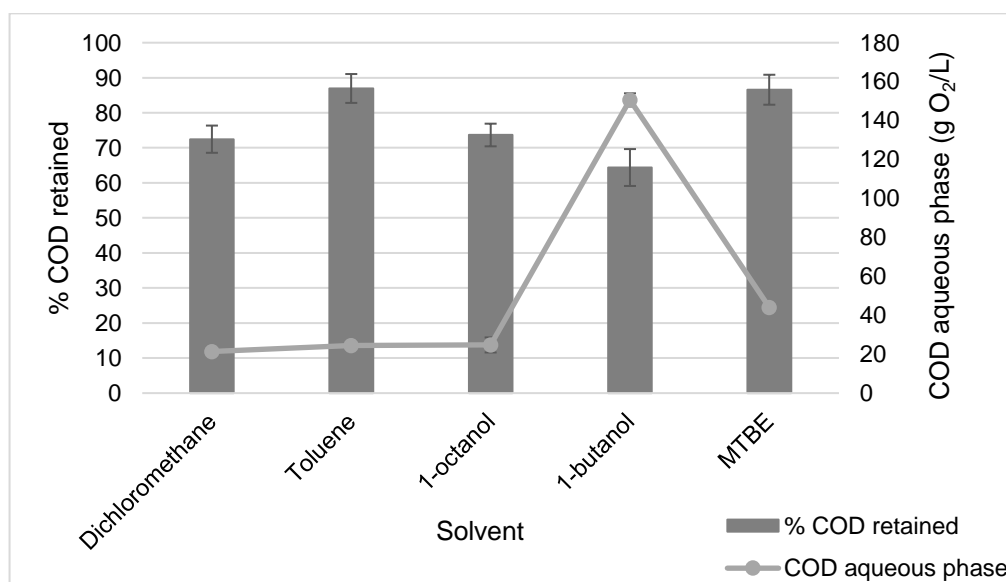


Figure 28. % COD retained calculated according to equation 15, for the extractions with the best five solvents and lupin beans debittering wastewater. COD values determined for the aqueous phase recovered after the two successive extractions.

Toluene and MTBE seem to be a little more efficient than the other solvents to remove COD, which means that, if one of these two solvents are chosen, then around 90% of the organic matter that can be found in the wastewater will remain in the aqueous phase, after both extractions. It is important

to note that the COD of the aqueous phase of the extractions with 1-butanol is high mainly due to the contamination of the solvent.

4.1.2.3. Water contamination

COD was determined for “blank extractions”. These extractions were done by adding 2 mL of each of the best organic solvents to 4 mL of distilled water, twice. The aqueous phase was recovered to determine how much COD was present due to contamination of the organic solvent. Higher COD values mean that a significant amount of the organic solvent dissolved in water during the extractions. The results are shown in table 14:

Table 14. COD values obtained for the aqueous phase recovered after two extractions with 4 mL of distilled water and 2 mL of each organic solvent (twice).

Solvent	COD (g O ₂ /L)	Solubility in water (25 °C; w/w) [46]	Log ₁₀ Kow (w/w) [46]
Dichloromethane	1.20 ± 0.56	1.3	1.25
Toluene	0.28 ± 0.12	0.052	2.69
1-octanol	0.97 ± 0.01	0.6	-
1-butanol	160.52 ± 10.40	7.3	0.88
MTBE	19.94 ± 0.84	4.3	0.94

Water contamination by each organic solvent is related with the capability of the solvent to be dissolved in water. Besides the COD values presented in table 14, there are other important parameters to discuss the possibility of a given solvent to be dissolved in water. Polarity, the solubility of each solvent in water and the n-octanol/water partition coefficient (Kow) are important values.

Both alcohols have high polarity values, and 1-butanol along with MTBE have the highest solubility in water values. Both parameters are low for toluene. Regarding log₁₀ Kow, if Kow gives the ratio between the concentration of the solvent in octanol and in water, then high values of this parameter indicate that the solvent has low affinity for water.

1-octanol has a high polarity but its solubility in water is low which may explain the significant value of log₁₀ Kow. 1-butanol, on the other hand, has high solubility in water so its log₁₀ Kow is low. In fact, this solvent showed to be a substantial water contaminant due to the huge COD value, and it must not be chosen to integrate the extraction process.

Dichloromethane, toluene and 1-octanol seem to be the most reasonable solvents to choose considering the low COD values for the blank extractions.

4.1.2.4. Environmental impact, waste and human health

The environmental impact of each solvent should be analyzed based on the tables 4, 5 and 6 (section 2.3.3.).

About the aquatic impact, it is important to note that 1-octanol has the lowest score in this parameter and it is considered to be harmful and toxic for fishes and invertebrates, respectively. On the other hand, butanol, MTBE and dichloromethane are not harmful to both invertebrates and fishes, and both butanol and dichloromethane have a significant overall aquatic score.

Regarding the air impact, and even though the values of POCP and odor threshold could not be found for MTBE, this solvent, along with dichloromethane seem to be the solvents with lower air impact. However, it is important to recall that the best score value, i.e., the score value that indicates the greenest solvent is 10 for both aquatic and air impact. For air impact, the maximum value indicated for these solvents was 6 (for dichloromethane). This means that all the best solvents to extract lupanine have significant air impact.

In addition, waste and human health scores can be found in table 6, section 2.3.3. for all the solvents that were tested. It is important to highlight that dichloromethane has very low scores for the human health parameters, which means that it is an extremely hazardous solvent. Regarding waste scores, this solvent has maximum recycling score, but the other three parameters (incineration, biotreatment and VOC emissions) contribute to the fact that dichloromethane is one of the less green solvents of the list.

1-octanol and 1-butanol seem to be the most suitable solvents regarding both waste and human health scores, according to the GSK solvent guide.

4.1.2.5. Final decisions for liquid-liquid extractions

Besides the four topics already discussed (% extraction, % COD retained, water contamination and environmental impact), there is another relevant parameter that must be considered to choose the most adequate solvent for the extraction of lupanine: the boiling point (see section 2.3.3., table 4).

It is possible to foresee three different possible routes for further lupanine purification after solvent extraction: (i) evaporation of the extraction solvent to directly recover lupanine, (ii) further lupanine purification using a solid adsorber, such as a MIP (see section 4.4) and (iii) solvent exchange of lupanine in a recrystallization solvent, after addition of a resolving chiral acid for diastereomeric resolution. In the first case and third, the solvent will be evaporated after the extractions, so the boiling point should be as low as possible. If, after the extractions, a recrystallization step is needed, then methanol will be added. In this case, the boiling point of the chosen organic solvent must be lower than the boiling point of these solvents to allow its evaporation, while keeping lupanine dissolved in methanol. In case liquid-liquid extraction is made by a polymer different of the optimum solvent for MIP binding (DCM), lupanine should be dissolved in the work solvent or there is the possibility of a swapping step from the other organic solvent to DCM.

1-octanol has a high boiling point. In fact, when this extracting solvent was used and the organic phase recovered and left to evaporate. The solvent would not evaporate, even using nitrogen flow or a vacuum line. Therefore, although 1-octanol seems to be efficient to extract lupanine, recovery of this compound will then be challenging due to difficulties on evaporating this extracting solvent.

All five solvents showed similar results regarding COD retained, so the final decision should rely on water contamination, the boiling point and the environmental, waste and human health impact. 1-butanol and 1-octanol should be excluded because the first one causes substantial water contamination and octanol cannot be easily evaporated due to its high boiling point. Toluene has a significant environmental impact, and DCM is a very hazardous solvent (considering waste and human health issues) which leaves MTBE as the most suitable solvent for lupanine extraction. Both MTBE and DCM have low boiling points (40 and 55 °C, respectively), so they can be easily evaporated. DCM would be more appropriate because there would be no need for a solvent swap operation and lupanine dissolved in this solvent could be directly used for MIPs assays.

4.1.3. Extraction of lupanine with resins

% binding, regeneration and lupanine recovery, COD retained and recyclability will be analyzed to decide what are the most suitable resins to include in a unit operation of the process to extract lupanine.

4.1.3.1. Screening of the best resins: % binding

Binding assays were performed for each of the eighteen available resins (see section 2.3.2., table 2) by using 1.5 mL of lupin beans debittering wastewater, without any treatment, and 0.15 g of each resin. Two parameters were calculated: % binding (equation 16) and the adsorption capacity (Q – equation 17):

$$\% \text{ binding} = \frac{(c_i - c_e)}{c_i} \times 100 \quad (16)$$

$$Q = \frac{(c_i - c_e)}{M} \times V \quad (17)$$

In these equations, c_i corresponds to the concentration of lupanine in the wastewater (3.235 g/L) and c_e is the equilibrium concentration of lupanine (obtained by quantifying lupanine in the supernatant recovered after the binding assays). V is the volume of the lupin beans wastewater (1.5 mL) and M is the mass of resin (0.15 g).

Figure 29. contains the results obtained for % binding and Q for each resin:

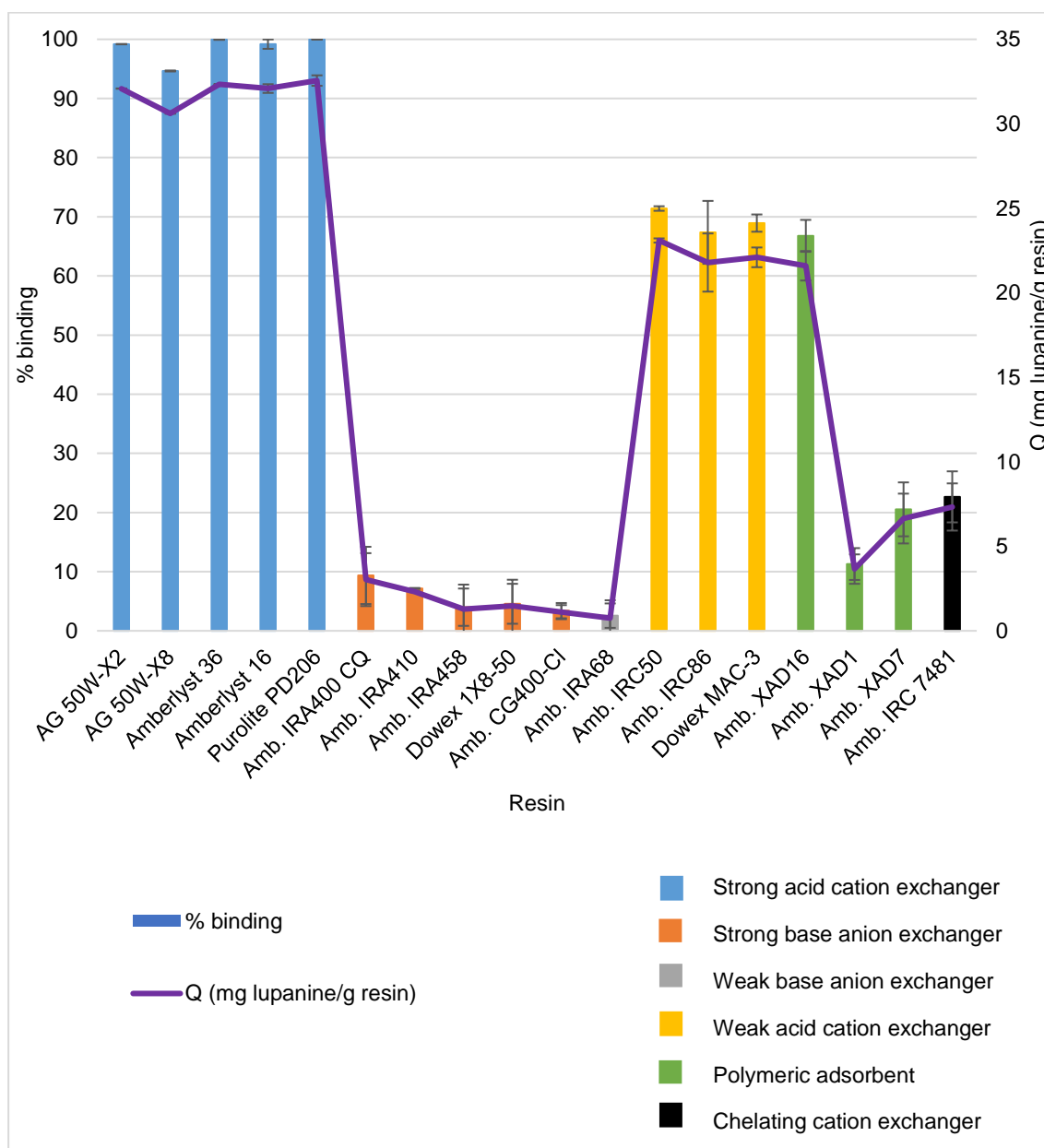


Figure 29. % binding and Q values obtained for each resin. Each different color represents the classification of each resin (15 ion exchangers and 3 polymeric adsorbents). Amb. is an abbreviation for Amberlite.

From the resins assessed, the ones with higher binding efficient for lupanine were the strong and weak acid cation exchangers: AG 50W-X2, AG 50W-X8, Amberlyst 36, Amberlyst 16, Purolite PD206, Amberlite IRC 86, Amberlite IRC 50 and Dowex MAC-3. Lupin beans wastewater contains lupanine in the acidic form, which means that this molecule is protonated (because the pH of the wastewater is between 3 and 4 and the pKa of lupanine is 9.1). Thus, lupanine will have a positive charge and the strong sulfonic acid or weak carboxylic groups cation exchange resins will exchange the hydrogen ions for the lupanine molecules.

As expected, the anion exchanger resins were not efficient for lupanine binding because the functional groups have positive charges (see table 2, section 2.3.2.) and there is a repulsion between

these groups and the positively charged lupanine molecules. However, a low % binding was obtained in some cases, which may be a result of non-ionic interactions between lupanine and the polymeric matrix of the resins. Acrylic polymers are able to form hydrogen bonds and styrene cross-linked with divinylbenzene copolymers can interact through hydrophobic effects.

The polymeric resin that promotes higher adsorption of lupanine is the one with a hydrophobic polymeric chain, XAD-16. It interacts with organic compounds (like lupanine) through hydrophobic and polar effects, due to the presence of the aromatic rings. XAD-7 is composed of an acrylic polymer which means that there is the possibility of hydrogen bonding between lupanine and this resin. Since hydrogen bonds are stronger interactions than hydrophobic or polar interactions, a higher % binding would be expected for XAD-7. It is important to note that there is a difference between these two adsorbent resins that probably affects their binding capacity: the surface area that is indicated by the manufacturers. In this case, it is important to discuss the surface area and the pore size of these resins. The pore diameter is similar for both resins (90 Å for XAD-7 and 100 Å for XAD-16), but the surface area of XAD-16 is 900 m²/g whereas the surface area of XAD-7 is 450 m²/g, according to the information given by the manufacturers. Since these two resins have similar pore size the larger surface area of XAD-16 may explain the better performance of this resin to bind lupanine in comparison with XAD-7.

Binding assays were also done using a solution of lupanine in water with similar concentration to lupin beans wastewater (3.2 g/L), to study matrix effects (Figure 30):

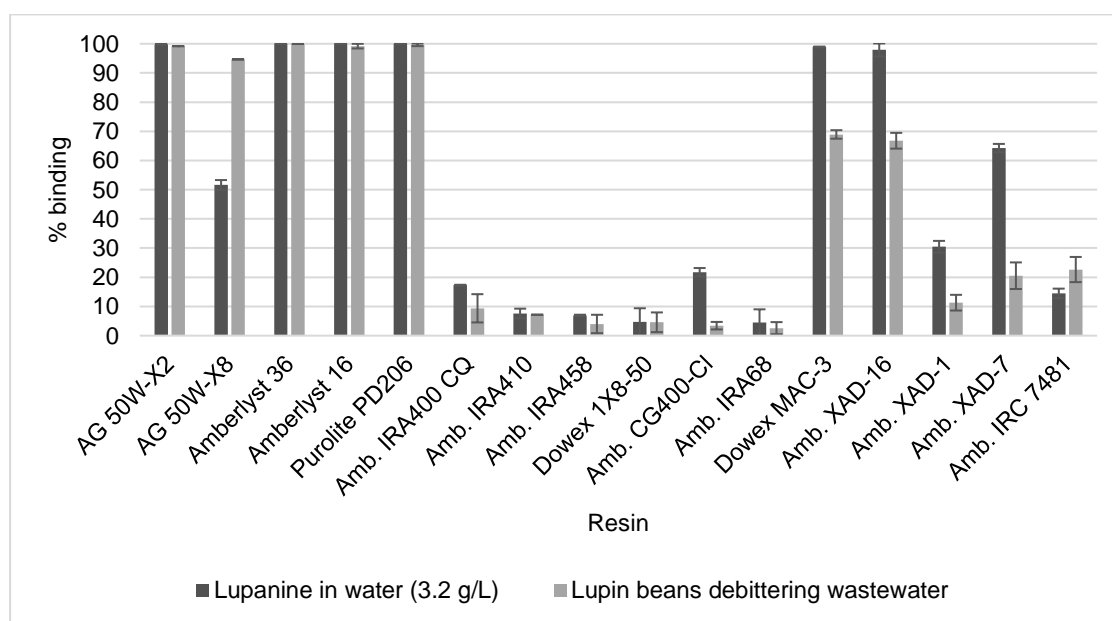


Figure 30. % binding for the eighteen resins that were tested using a solution of pure lupanine in water (3.2 g/L) and lupin beans debittering wastewater. IRC50 and IRC86 were not included because these resins are no longer commercially available and Dowex MAC-3 has analogous characteristics (binding and regeneration results were similar), so it was used to replace the other two.

AG 50W-X8 higher binding for lupanine in lupin beans wastewater matrix than when dissolved in pure water. This observation may be explained by salting out, in which the ions that are present in the wastewater are in sufficiently high concentration to compete with lupanine for the interaction with water

molecules. Thus, lupanine becomes less soluble in water and it will be more available to interact with the resin.

On the other hand, salting in phenomenon seems to occur for the polymeric resins (XAD-16, XAD-1 and XAD-7), the weak acid cation exchangers (IRC50, IRC86 and MAC-3) and for a strong base anion exchanger (CG400-Cl), since they seem to be more efficient for a solution of pure lupanine in water. In these cases, more lupanine molecules will stay in the water due to the presence of ions. The ions will promote the interaction of lupanine with molecules of the solvent, which means that these molecules will be less available to interact with the resins. In particular, the non-ionic interactions established between lupanine and XAD resins will be decreased because the interaction between lupanine molecules is favored.

AG 50W-X8 and MAC-3 are both cation exchanger resins and different effects are occurring. Non-ionic interactions can also occur between the matrix of the ionic resins and lupanine or other compounds that are present in the wastewater. In fact, these two resins have different polymeric matrixes (polystyrene and polyacrylic, respectively) which may explain the different behavior. For example, a polymer of polyacrylic nature is able to establish hydrogen bonds, so some compounds that are present in the wastewater will compete with lupanine to bind the resin.

4.1.3.2. Regeneration assays and lupanine recovery

The best resins to extract lupanine from phase 3 were selected to regeneration assays with lupanine recovery: strong and weak acid cation exchangers and a polymeric adsorbent.

Five different regeneration solutions were tested: HCl 10 % (w/w) in water, NaOH 10 % (w/w) in water, HCl 10 % (w/w) in ethanol/water (70:30 v/v), NaOH 10 % (w/w) in ethanol/water (70:30 v/v) and ethanol absolute. In all cases, the % recovery was calculated according to the following equation:

$$\% \text{ recovery} = \frac{c_r}{(c_i - c_e)} \times 100 \quad (18)$$

In this equation, c_r corresponds to the concentration of lupanine recovered after the regeneration assays, c_i is the concentration of lupanine in phase 3 (3.235 g/L) and c_e is the concentration of lupanine in the supernatant recovered after the binding assays.

Figure 31. contains the results obtained for % recovery of lupanine for the best resins, and all regeneration solutions tested:

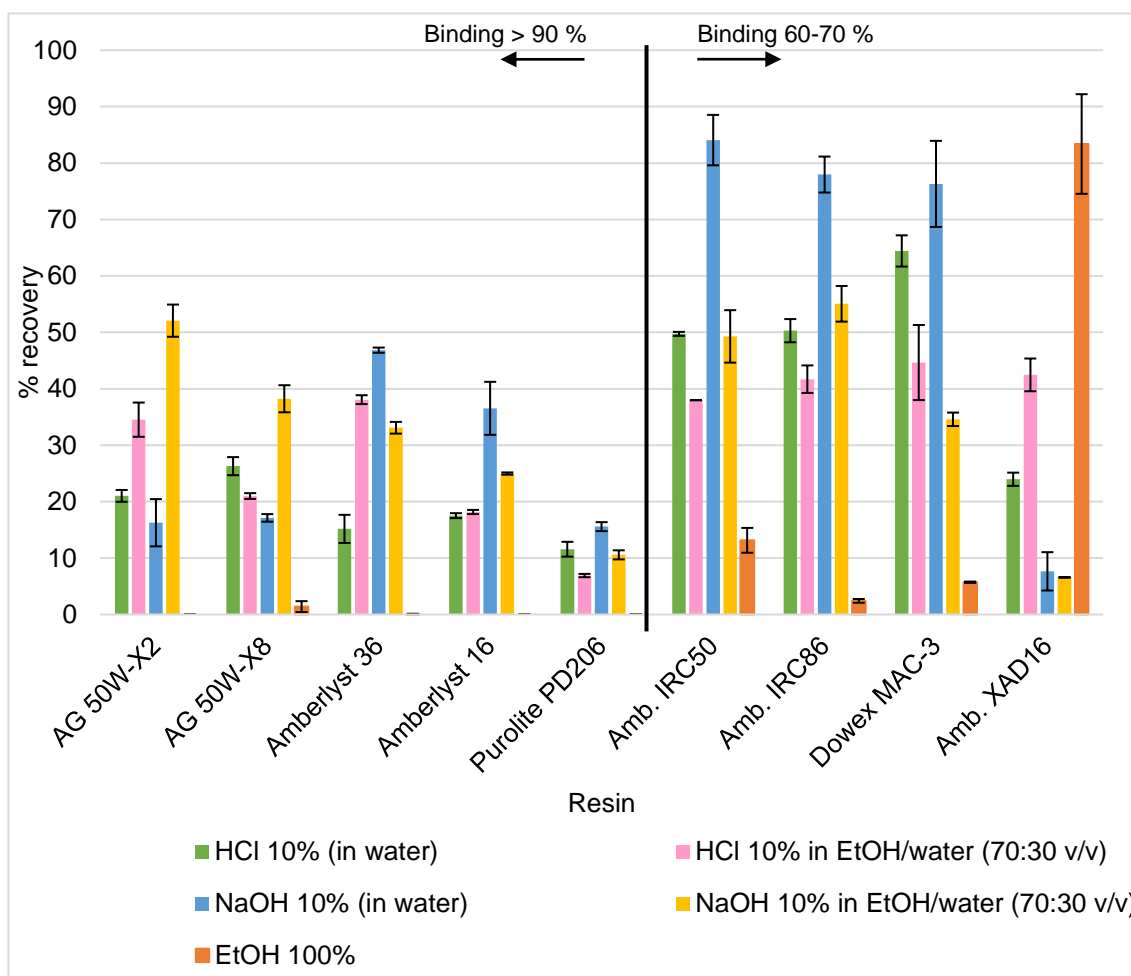


Figure 31. % recovery for the acidic resins and the polymeric one, using five different solutions. The vertical line signalizes the resins with % binding higher than 90% (on the left) and the resins with % binding between 60 and 70% (on the right).

Regeneration with NaOH and HCl is mainly based on ionic interactions, while the regeneration with ethanol is based on weaker interactions (dipole-dipole or hydrophobic interactions). Thus, as expected, the regeneration of ion exchange resins with ethanol is not efficient. On the contrary, ethanol seems to be useful to recover lupanine that was adsorbed on XAD-16.

In general, regeneration of the acidic resins with NaOH in water seems to be more efficient than with HCl. Na⁺ ions will compete with protonated lupanine to bind the resin, lupanine will dissociate from the resin and it will move to the solution. In the case of HCl, it will dissociate in the water, and the H⁺ will protonate the sulfonic or carboxylic groups, allowing lupanine to be recovered.

Aqueous solutions of HCl and NaOH with ethanol were also tested aiming to increase the % of recovery of lupanine that may be adsorbed to the ion exchange resins, which was not verified.

Considering the results of binding and regeneration, the best option seems to be choosing the weak acid cation exchanger resin (Dowex MAC-3) or the polymeric adsorbent resin (XAD 16) to recover lupanine. Although the strong acid cation exchanger resins have a % binding closer to 100, lupanine

recovery is more efficient for the weak acid cation exchanger resins (around 80 % of lupanine recovery for a % binding of about 70).

4.1.3.3. Binding isotherms

Binding assays for the isotherms were done using quantities of resin (XAD-16 and MAC-3) from 37.5 to 450 mg, and the same lupin beans wastewater volume (1.5 mL).

Two models were utilized to analyze the binding isotherms obtained with the resins: Langmuir and Freundlich. These two isotherms are based on different assumptions: Langmuir model assumes that a monolayer of solute molecules (in this case, lupanine) is formed uniformly on the sorbent surface (resin), and there is a finite number of adsorption sites; Freundlich model assumes that a multilayer of solute molecules is formed on heterogeneous surfaces.

Freundlich isotherm is given by the following equation:

$$q_e = K_F c_e^{1/n} \quad (19)$$

In this equation, q_e is the amount of lupanine adsorbed per unit mass of resin (mg/g), K_F is a Freundlich constant (related to the relative adsorption capacity of the adsorbent (mg/g)), c_e is the equilibrium concentration of lupanine (g/L) and $1/n$ is a heterogeneity factor.

Equation 19 can be linearized, to obtain both K_F and $1/n$ (see annex, section D.), and q_e is represented as a function of c_e , for each resin.

Langmuir isotherm is given by the following equation:

$$q_e = \frac{q_{\max} \times K_L \times c_e}{1 + K_L \times c_e} \quad (20)$$

In this equation, q_e is the amount of lupanine adsorbed per unit mass of resin (mg/g), q_{\max} is the maximum adsorption capacity and K_L is a Langmuir constant (related to the free energy of adsorption (L/mg)).

Equation 20 can be linearized, to obtain both K_L and q_{\max} (see annex, section D), and q_e is represented as a function of c_e , for each resin.

Figures 32. and 33. contain the adsorption, Langmuir and Freundlich isotherms for XAD-16 and Dowex MAC-3, respectively. Adsorption isotherms were obtained by calculating q_e for each c_e , according to equation 17 (see section 4.1.3.1.).

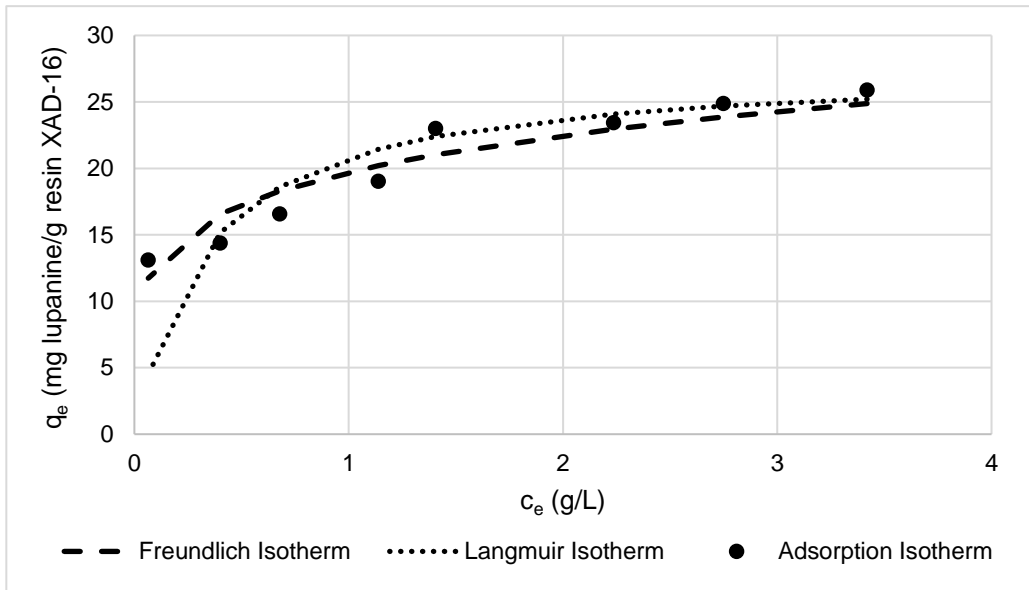


Figure 32. Freundlich, Langmuir and adsorption isotherms obtained for XAD-16.

According to Figure 32, the adsorption isotherm obtained for XAD-16, Freundlich isotherm seems to be more adequate to fit the values than Langmuir isotherm. Then, it is possible to assume that lupanine may form a multilayer on XAD-16 heterogeneous surface.

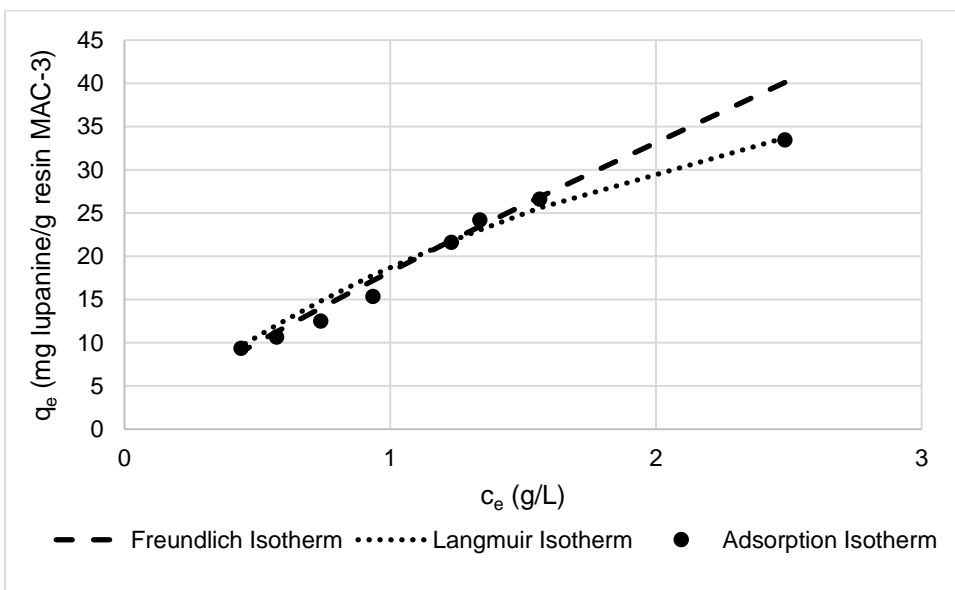


Figure 33. Freundlich, Langmuir and adsorption isotherms obtained for Dowex MAC-3.

According to Figure 33., the adsorption isotherm obtained for XAD-16, Langmuir isotherm seems to be more adequate to fit the values than Freundlich isotherm. In this case, it is possible to assume that lupanine may form a monolayer on Dowex MAC-3 resin, that is described as a homogeneous surface with identical adsorption sites.

4.1.3.4. COD retained

Similarly to the strategy what was indicated for the solvent extractions, in the context of the experiments that were performed, COD retained is defined as the capability of a given resin to separate COD from lupanine. When doing binding assays, COD is supposed to remain in the supernatant so that the resin contains lupanine and as less COD as possible.

COD values were also determined for the supernatant recovered after the binding assays, for two different quantities of Dowex MAC-3 and XAD 16 (100 and 300 mg/mL) and 1.5 mL of lupin beans debittering wastewater, after binding experiments with the wastewater. % COD retained was obtained by using the following equation:

$$\% \text{ COD retained} = \left(\frac{\text{COD}_{\text{sup}}}{\text{COD}_{\text{wastewater}}} \right) \times 100 \quad (21)$$

In this equation, $\text{COD}_{\text{wastewater}}$ is the COD value determined for phase 3 ($27.85 \pm 0.90 \text{ gO}_2/\text{L}$), COD_{sup} is the COD value determined for the supernatant recovered after the binding assays.

The values obtained for both resins are presented in table 15:

Table 15. % COD retained and absolute values of COD for Dowex MAC-3 and XAD-16 (100 and 300 mg/mL).

Resin (mg/mL)		COD_{sup} (g O ₂ /L)	% COD retained
Dowex MAC-3	100	23.41 ± 1.45	81.94 ± 3.69
	300	18.37 ± 1.26	65.97 ± 4.51
XAD-16	100	22.37 ± 0.30	80.34 ± 1.06
	300	20.20 ± 0.75	72.52 ± 2.68

The % COD retained is similar for both resins, but for higher resin concentrations, XAD-16 seems to be slightly more efficient to remove COD from phase 3.

4.1.3.5. Recyclability

To test the recyclability of the two best resins to extract lupanine, 3 binding/regeneration cycles were performed for XAD-16 and MAC-3. 450 mg of each resin and 1.5 mL of debittering wastewater were utilized for the binding assays, and 1.5 mL of the corresponding regeneration solution were used for the regeneration assays. The results are shown in the figure below.

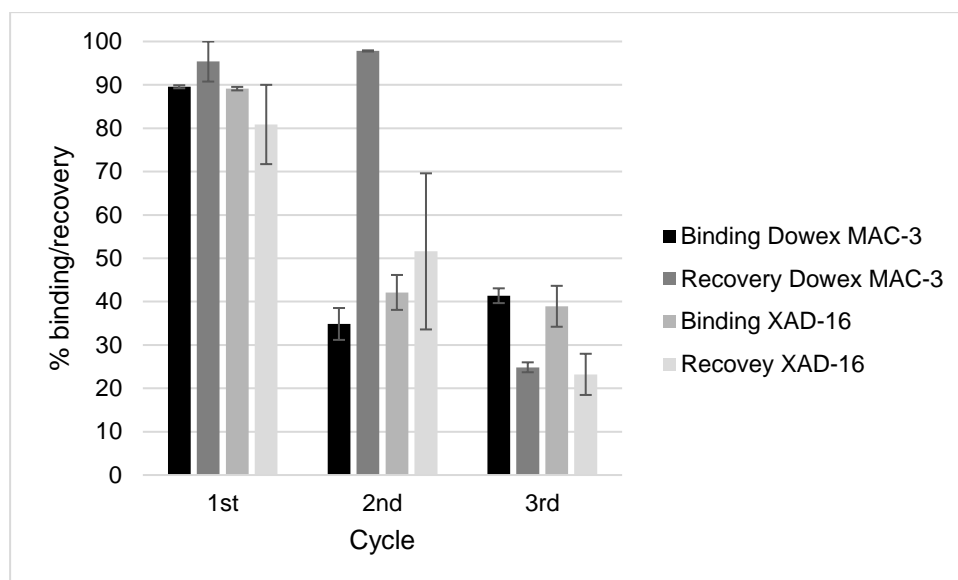


Figure 34. % binding and % recovery for the XAD-16 and MAC-3 assays with debittering wastewater, for 3 cycles.

According to Figure 34., the % binding significantly decreases after the first binding/regeneration cycle, for both resins. Lupanine recovery from MAC-3 is done using NaOH in water: the Na⁺ ions will exchange lupanine and will stay in the polymeric matrix. Thus, after this step, a second wash with HCl in water should have been done to swap Na⁺ ions back to H⁺, promoting the protonation and consequent regeneration of the resin.

Regarding XAD-16, lupanine recovery is done using ethanol, that have high affinity to the polymer. By the end of the recovery assays, the resin will be full of ethanol molecules. Thus, in this case a second wash step should also have been done, using water, to remove the ethanol molecules and improve the results.

It is important to say that the binding assays are performed using debittering wastewater with no previous treatment (it is directly applied in the tubes containing the resins). This means that the COD is very high, and there are many compounds that may be interacting with the resins, along with lupanine. These organic compounds will contribute to the fouling of the resin. In fact, the previous section showed that around 30-35 % of the COD that is present in the wastewater will be adsorbed to the resin, thus decreasing resin performance for lupanine purification. A process to isolate lupanine includes an ultrafiltration step to remove most of the macromolecules, which may help to improve recyclability of the resins.

4.1.3.6. Final remarks on resins selection to isolate lupanine

Eighteen resins were tested for lupanine binding and nine were selected for regeneration and lupanine recovery. In the end of this screening process, two resins showed to be useful for lupanine extraction: XAD-16 (adsorbent) and Dowex MAC-3 (ion exchanger, that substituted both IRC50 and IRC86 which are no longer commercially available). The performance of these two resins is similar, the difference are the regeneration solutions (ethanol for XAD-16 and NaOH in water for MAC-3). These differences allow distinct approaches in a process to isolate lupanine from the wastewater, which will be discussed in section 4.4.

4.2. Molecularly Imprinted Polymers for lupanine

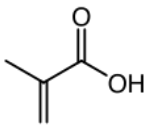
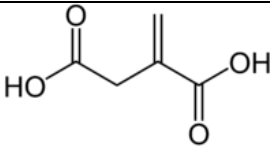
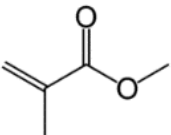
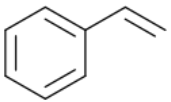
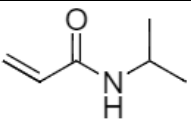
Besides membrane-based processes, liquid-liquid extractions and resins, an additional unit operation consisting in the isolation or, ideally, the chiral resolution of lupanine using molecularly imprinted polymers (MIPs) was tested.

Firstly, five monomers with different chemical properties were used to obtain MIPs, using racemic lupanine as template. The goal of this part of the work was to select the monomer that was more efficient to produce a specific MIP to extract lupanine. Then a chiral MIP was synthesized with the selected monomer to evaluate the enantiomeric resolution capacity of the polymer for lupanine.

4.2.1. Screening of monomers using racemic lupanine

The structure of each monomer used in this study, and their molecular weight, are indicated in the following table:

Table 16. Structure and molecular weight of the five monomers used to synthesize MIPs with racemic lupanine.

Monomer	Structure	Molecular weight (g/mol)	Observations
Methacrylic acid (MAA)		86.06	Monomer with one carboxylic group
Itaconic acid (IA)		130.10	Monomer with two carboxylic groups
Methyl methacrylate (MMA)		100.12	Monomer with an ester group
Styrene		104.15	Aromatic monomer, containing a benzene ring
N-isopropylacrylamide (NIPAM)		113.16	Monomer with an amide group

The interactions between lupanine and the monomers are based on non-covalent forces, essentially, hydrogen bonds, electrostatic, hydrophobic and van der Waals interactions (that include dipole-dipole and dipole-induced dipole interactions).

Considering the chemical structure of lupanine (Figure 35.), it is possible to see that this molecule is able to form hydrogen bonds because it has two electronegative atoms that work as hydrogen acceptors (the nitrogen and oxygen atoms indicated in Figure 35.). Hydrogen bonds will then

be formed between these atoms and the hydrogens that are covalently bond to an electronegative atom (hydrogen donor). The carboxylic groups of methacrylic acid and itaconic acid can act as hydrogen donors since they contain a hydroxyl group. It was expected that the polymers obtained with itaconic acid could be more efficient to extract lupanine because this compound contains two hydroxyl groups, which means that each molecule of IA can form two hydrogen bonds.

Ionic interactions are possible between IA and MAA. These monomers contain carboxylic groups that are able to lose the acidic protons to the tertiary amine of lupanine, as indicated in Figure 35. Thus, lupanine acquires a positive charge that will be electrostatically attracted by the carboxylic acid groups.

NIPAM contains an amide group that is capable of forming hydrogen bonds with lupanine. Considering that nitrogen is less electronegative than oxygen, then it is expected that the interaction between lupanine and NIPAM through hydrogen bonding is weaker than between MAA and IA. Also, this monomer is not able to establish ionic interactions.

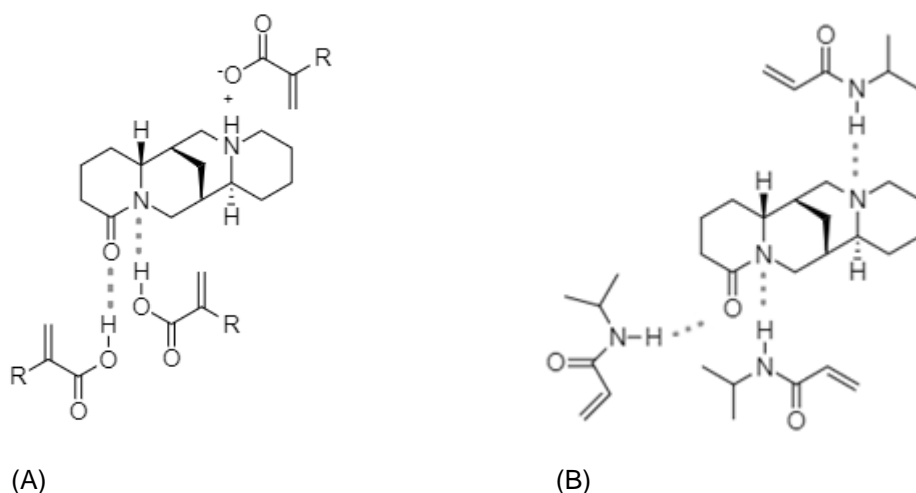


Figure 35. Possible hydrogen bonding (dashed lines) and ionic interactions between lupanine and IA, MAA (A) and possible hydrogen bonding (dashed lines between lupanine and NIPAM (B). For MAA, R = CH₃ and for IA R = H₂C-COOH.

Styrene is a derivative of benzene, which means that the establishment of hydrogens bonds or dipole-dipole interactions is not possible, since there are only carbon and hydrogen atoms. Dipole-induced dipole forces are the only possible intermolecular forces between styrene and lupanine.

MMA contains an ester group, which means that it cannot establish hydrogen bonds or ionic interactions with lupanine, only weaker forces (dipole-dipole and dipole-induced dipole).

The preliminary results were obtained using a 0.1 g/L solution of pure lupanine in dichloromethane. After the preliminary assays, new binding experiments were performed with all polymers using a more concentrated solution of lupanine in DCM (1 g/L) (Figure 36.). The % binding was calculated according to equation 22:

$$\% \text{ binding} = \frac{(c_i - c_e)}{c_i} \times 100 \quad (22)$$

In this equation, c_i corresponds to the concentration of lupanine in the stock solution and c_e is the equilibrium concentration of lupanine (obtained by quantifying lupanine in the supernatant recovered after the binding assays).

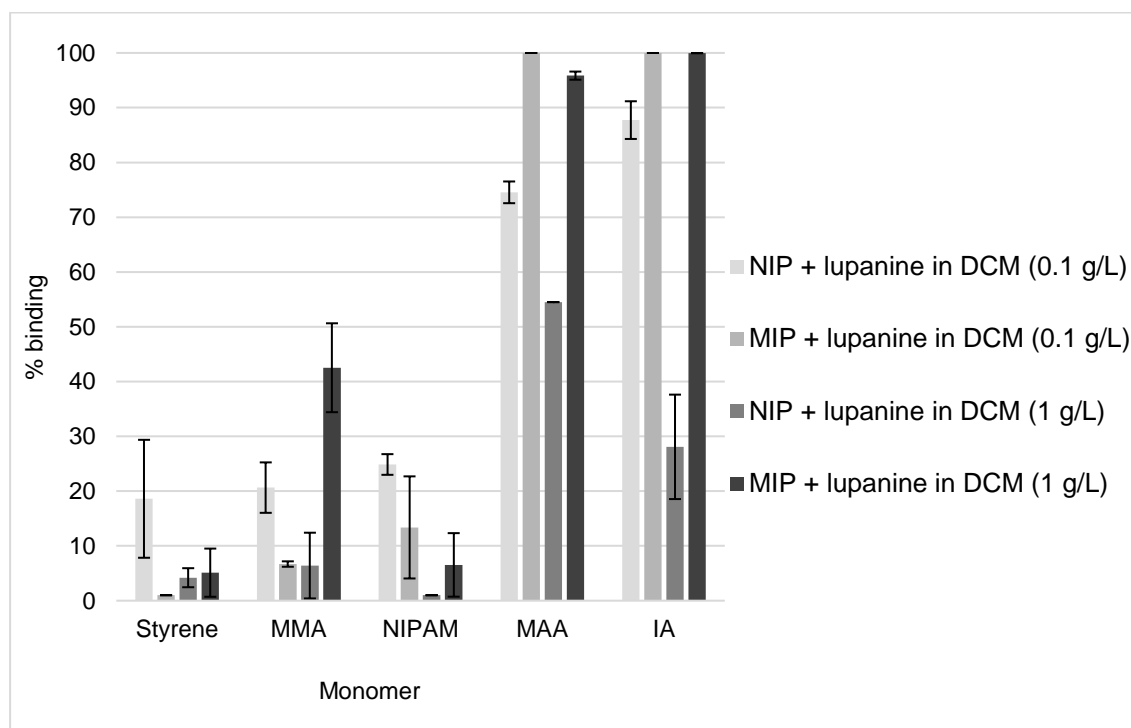


Figure 36. Binding results for NIPs and MIPs obtained with the monomers indicated and two solutions of racemic lupanine in dichloromethane (0.1 and 1 g/L).

A polymer is efficient if there is a significant difference of the % binding between the MIP and the NIP. It is also expected a lower % binding for NIPs than MIPs. In the case of NIPs there is no template during the polymerization, which means that the monomers will be distributed in a random way. On the other hand, the presence of the template molecule during the synthesis of MIPs allow the arrangement of the monomers around lupanine, producing pockets that will have the three-dimensional shape of lupanine.

For low target concentration, non-specific binding may be favored, and the target molecules will not fill in the cavities of the MIPs. For an ideal concentration, most of the binding sites will be occupied by lupanine molecules (specific binding) and the non-specific interactions will be negligible, leading to a significant difference between the % binding for the MIP and the correspondent NIP. When the target concentration is higher than the ideal, then no more cavities will be available and most of the molecules will remain in the solution, which will induce low binding % for the polymers.

Regarding styrene, MMA and NIPAM, the NIPs showed higher % binding than the correspondent MIPs, using the solution of lower concentration (0.1 g/L). This unexpected situation may

have happened eventually due to the arrangement of the monomers in the NIP, that favored the interaction with lupanine more than in MIPs, since a low concentration was used.

Although there is no significative difference between the % binding for the MIPs and NIPs obtained with MAA and IA, these two seem to be the most promising monomers to produce MIPs for lupanine, according to the results obtained with the solution of 0.1 g/L.

When a more concentrated solution of lupanine was utilized (1 g/L), it was possible to confirm that styrene and NIPAM are not adequate to produce MIPs for lupanine as the % binding is very low. The polymers obtained with MMA show an improvement when the concentration of lupanine is increased, but the MIP has a % binding that is lower than MAA and IA MIPs. The more efficient MIPs to bind lupanine seem to be the ones synthesized with MAA and IA. In this case, the lupanine solution was 10 times more concentrated than in the previous assays, and a significant % binding can be observed between the NIP and the MIP, especially for IA. These results are in agreement with the predicted interactions that were previously analyzed.

4.2.2. Chiral MIP for lupanine resolution

IA was the selected monomer to synthesize a MIP using L(-)-lupanine as template to obtain a chiral MIP. Binding assays with the chiral MIP were performed using a solution of racemic lupanine in DCM (5 g/L, so that there would be sufficient lupanine for HPLC injection, that requires a minimum weight of 5 mg). Both % binding and enantiomeric excess (calculated according to equation 23.) are presented in Table 17.

$$Enantiomeric\ excess\ (ee\ \%) = \frac{Area_{D-(+)-lupanine} - Area_{L-(-)-lupanine}}{Area_{D-(+)-lupanine} + Area_{L-(-)-lupanine}} \times 100 \quad (23)$$

In equation 23, $Area_{D-(+)-lupanine}$ is the area of the peak correspondent to D-(+)-lupanine and $Area_{L-(-)-lupanine}$ is the area of the peak correspondent to L(-)-lupanine obtained in the chromatogram of each sample (see annex, Figures 47. and 48.)

Table 17. Binding and enantiomeric excess results obtained after the binding assays with the chiral MIP produced with IA and L(-)-lupanine as template.

IA Polymer	% binding	% ee
NIP	38.87 ± 1.66	9.92 ± 2.98
MIP	60.95 ± 5.88	7.41 ± 2.32

The results presented in Table 17. show that the MIP obtained with IA and L-(-)-lupanine did not seem to be able to separate lupanine enantiomers.

Although it was expected that the use of an enantiomer as template would induce enantioselectivity of the polymer, it is important to recall that lupanine interacts with IA essentially through two hydrogen bonds (see Figure 35.). These interactions may not be sufficient to produce cavities that are specific for just one enantiomer.

An interesting and perhaps more viable alternative to obtain a functional enantioselective MIP would be the use of a chiral monomer, along with the chiral template, for the polymerization reaction.

4.2.3. MIPs regeneration and lupanine recovery

Besides MIPs binding capacity, its regeneration is also an important step to recover lupanine and to reuse the polymer. A solution of 0.1 M HCl in MeOH was utilized to regenerate the MIPs obtained with IA and MAA, and recover lupanine. MeOH is characterized by its high polarity that enables the disruption of the hydrogen bonds formed between the template and the functional monomer. The presence of HCl promotes the protonation of certain atoms, such as the carboxylic group of IA or MAA that is supposed to establish an electrostatic interaction (see Figure 35.), breaking these interactions with lupanine. In fact, the solution of 0.1 M HCl in MeOH was successfully applied to remove the lupanine that was used as template to produce the MIPs during the polymerization reaction.

The MIPs with higher % binding, obtained after the assays with racemic lupanine, were subjected to two successive cycles of regeneration (24 hours each), using 0.1 M HCl in MeOH. The % recovery was calculated according to equation 24, and the results are shown in Figure 37.

$$\% \text{ recovery} = \frac{c_r}{(c_i - c_e)} \times 100 \quad (24)$$

In this equation, c_r corresponds to the concentration of lupanine recovered after the regeneration assays, c_i is the concentration of lupanine in the feed solution and c_e is the concentration of lupanine in the supernatant recovered after the binding assays.

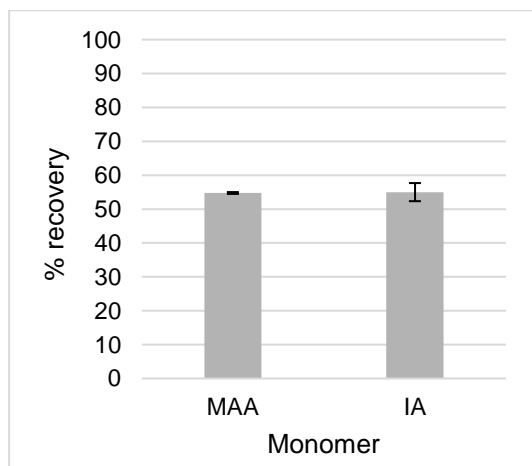


Figure 37. % regeneration obtained for the MIPs obtained with MAA and IA.

According to the results shown in Figure 37., the % regeneration is around 55 % for both polymers, after two regeneration cycles of 24 hours each. It is important to mention that a new regeneration cycle using only MeOH would be essential to neutralize the polymers by promoting the removal of protons. This third regeneration cycle would also probably allow to recover some of the lupanine that was not recuperated during the other two cycles.

It is difficult to obtain a total separation between the supernatant and the polymer as there are always polymer particles that remain in the solution, even after centrifugation. When the supernatant is recovered either after the binding or the regeneration assays, some polymer particles are lost. To minimize these losses, it would be more efficient to do a single regeneration cycle with 0.1 M HCl in MeOH for 48 hours than the two successive cycles that were done, followed by the regeneration with MeOH for 24 hours.

The regeneration assays were done at room temperature. Heating should also be explored to increase regeneration efficiency, since hydrogen bonds should be more easily disrupted.

4.3. Enzymatic transformation of lupanine

An interesting process that could follow the lupanine purification would be the transformation of this alkaloid by enzymes. The degradation of lupanine molecule could allow the synthesis of other molecules, while keeping intact the chiral structure. Several lipases, an esterase and a penicillin acylase were introduced in a test tube containing lupanine dissolved in PBS, and a sample was taken every day for lupanine quantification (Figure 38).

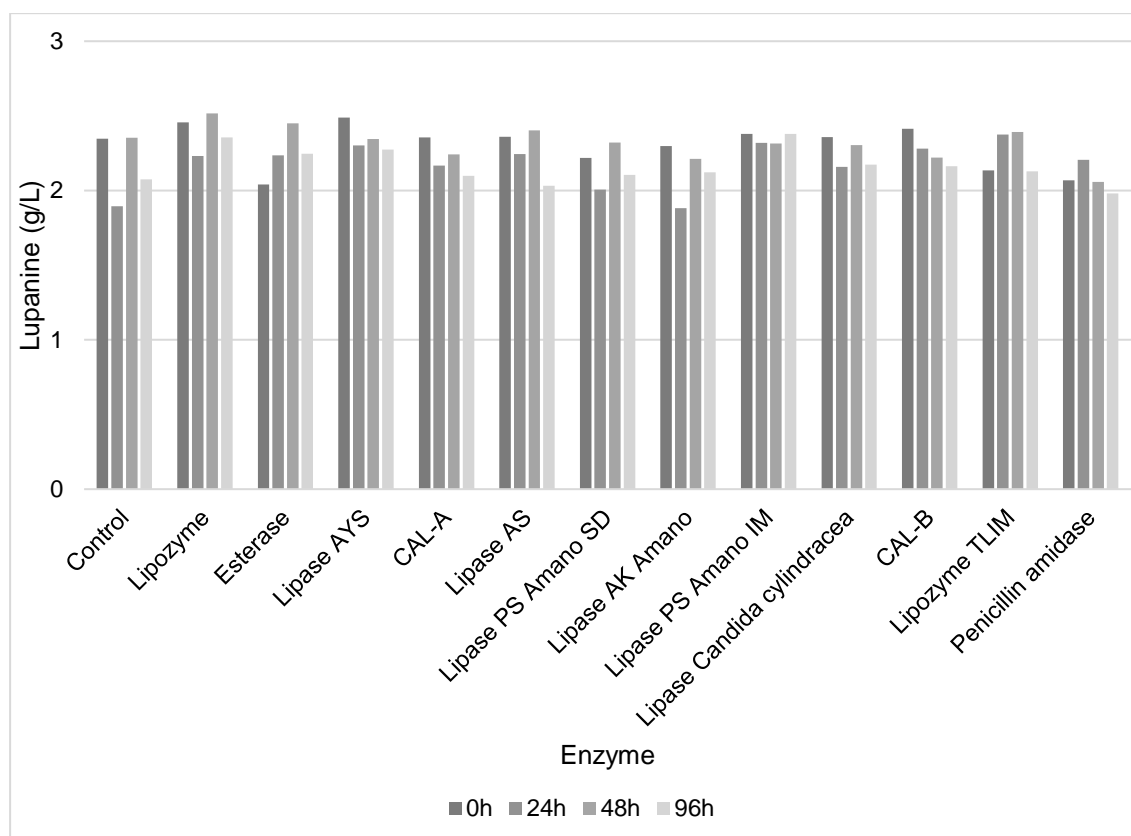


Figure 38. Results from the enzymatic assays with lupanine in PBS. The reactions were allowed to occur for approximately 5 days, and a sample was recovered every day for lupanine quantification. A control test tube containing only lupanine dissolved in PBS was placed in the same conditions as the tubes containing the enzymes.

According to Figure 38., the enzymes that were tested were not able to degrade lupanine. There are some oscillations in lupanine concentration since it was possible to recover only one sample each day due to the small volume of the solutions.

Considering that lupanine contains a δ -lactam ring (Figure 39. – (A)), another type of enzymes that could be tested in the future are β -lactamases. These group of enzymes hydrolyze the amide group of β -lactam ring (Figure 39. – (B)).

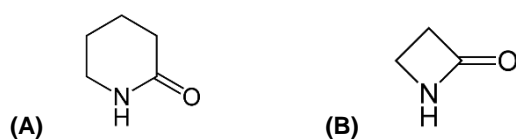


Figure 39. (A) δ -lactam ring structure (present in lupanine) and (B) β -lactam ring hydrolyzed by β -lactamases.

4.4. Lupanine Recovery Process

Considering the different unit operations assessed based on membranes, liquid-liquid extractions, resins and MIPs, two simple approaches could be considered: direct extraction of lupanine with organic solvents or resins.

(i) Direct extraction of lupanine with organic solvents would imply a large contamination of water with the solvent. Even if the contamination is minimal, the water must be treated after the extraction when considering its re-use.

(ii) Regarding resins, water contamination with solvent is most probably not a problem. When considering treatment of the lupin beans debittering wastewater by the resin, the challenge found is the large amount of resin needed to direct extract of lupanine from the water to relevant low levels.

In both cases, the solution requires to reduce the water volume using a nanofiltration to obtain clean water in the permeate and a filtration retentate rich in lupanine, which will then be fed to a solvent extraction or resin step. An efficient process to extract lupanine was assessed using wastewater from phase 3 and it should start with a centrifugation to eliminate as much solid particles as possible, followed by an ultrafiltration to remove the macromolecules and the resultant permeate will then be subjected to a nanofiltration. This sequence of steps allows to reduce the amount of water from which lupanine will be extracted, while concentrating this alkaloid.

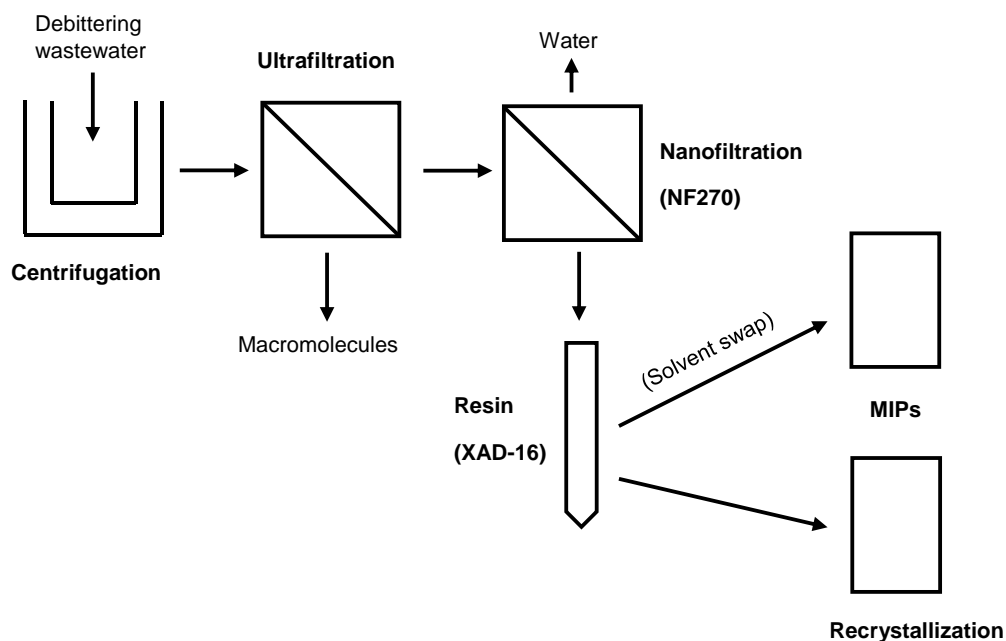


Figure 40. Suggested process to extract lupanine from lupin beans debittering wastewater. This process starts with a centrifugation to remove the solid particles, then the supernatant is subjected to an ultrafiltration to reduce the concentration of macromolecules. The resultant permeate will be used as feed of a nanofiltration, and the resultant retentate is applied to XAD-16, that is regenerated with ethanol.

After nanofiltration, a retentate rich in lupanine is obtained, and it can be fed to a resin step. Considering that there are two resins that can be integrated in the process, an adsorbent (XAD-16) and an ion exchanger (MAC-3), two processes can be created (Figure 40 and 41). If XAD-16 is used, then the lupanine is recovered by elution with ethanol, resulting in a lupanine rich solution in ethanol. The lupanine enantiomers can then be isolated by diastomeric resolution by recrystallization directly from this lupanine solution in methanol, or the methanol can be evaporated to obtain the racemate. Alternatively, solvent swap step of lupanine from methanol to DCM can be performed, placing the lupanine in a solvent which would allow to use MIPs for a fine isolation of pure racemic lupanine isolation or for enantiomeric resolution, if chiral MIPs are developed (Figure 40). This process does not include solvent extractions.

The other suggested process differs from the previous one because it uses the ion exchanger resin (MAC-3), which regeneration is made with NaOH 10% in water, followed by a liquid-liquid extraction with DCM. For the organic extractions, lupanine must be deprotonated, and the use of a strong base for regeneration of the resin makes this sequence of steps very suitable. After the extraction, the organic phase (that contains lupanine) will be used for binding assays with MIPs to obtain racemic lupanine or chiral MIPs for the enantiomeric resolution of this alkaloid (Figure 41).

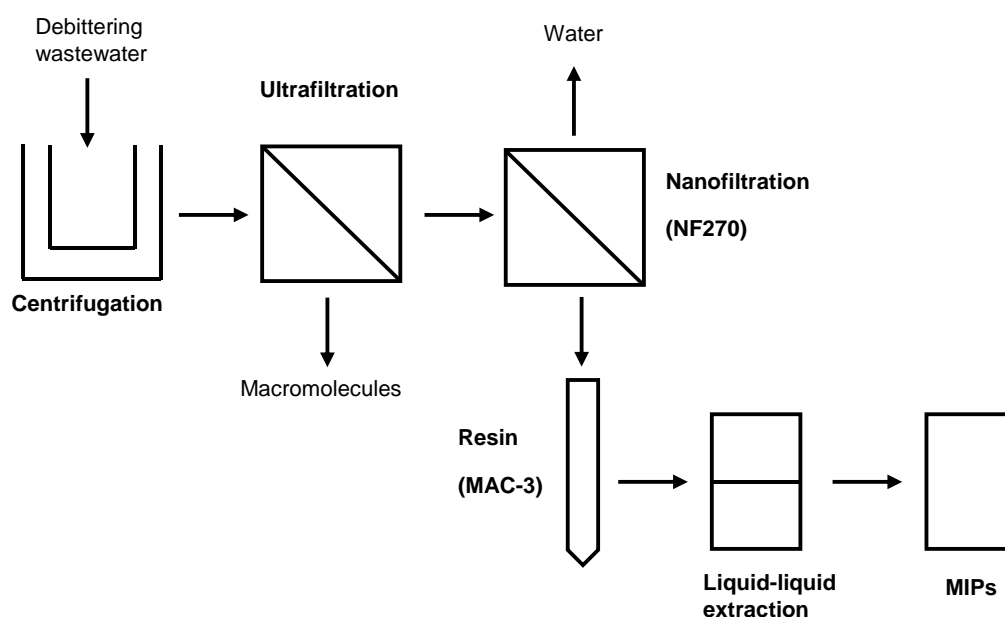


Figure 41. Suggested process to extract lupanine from lupin beans debittering wastewater. This process starts with a centrifugation to remove the solid particles, then the supernatant is subjected to an ultrafiltration to reduce the concentration of macromolecules. The resultant permeate will be used as feed of a nanofiltration, and the retentate is the applied to MAC-3, that is regenerated with NaOH 10% in water. After regeneration, a liquid-liquid extraction with DCM is done, and the organic phase is applied to MIPs.

It is important to note that, except for the MIPs, none of the unit operations are specific for lupanine. They are based, essentially, on molecular size (membranes), solvent affinity (liquid-liquid extractions) or adsorption/ionic interactions (resins). Lupin beans debittering wastewater contains macromolecules, such as proteins, hydrocarbons or lipids, and other alkaloids that may be carried out

along with lupanine. The introduction of an ultrafiltration process will reduce the presence of macromolecules, but it is possible that the other alkaloids remain in the water. Thus, the use of MIPs as the last unit operation would provide the molecular specificity that is required to obtain pure lupanine by the end of the process.

Comparing the two suggested processes, it is possible to say that the introduction of an organic extraction implies the contamination of the resultant aqueous phase. However, in this part of the process, the water volume should be much reduced due to the nanofiltration. Another important aspect is the use of a strong base for regeneration of MAC-3, that will imply the posterior neutralization of the solution, possibly with HCl. In conclusion, the second process seems to be more adequate for MIPs isolation, since there is no need for solvent swapping (which implies the evaporation of one solvent and posterior addition of the other organic solvent). Also, even though there is an extra unit operation (the liquid-liquid extraction), this extraction with DCM allows to eliminate the remaining COD (that may not have been retained during ultrafiltration), or some organic matter from the resin itself.

Some improvements must still be done, starting with an adequate ultrafiltration membrane to retain most of the macromolecules present in the wastewater, that will help to prevent or retard fouling on the nanofiltration membrane. More specific progresses should be made regarding MIPs. Firstly, if these polymers will be used for racemic lupanine isolation, then an effective regeneration methodology should be investigated. Secondly, a more useful application of MIPs by the end of the process would be the enantiomeric separation of lupanine with chiral MIPs. The chiral MIP produced with IA and a lupanine enantiomer did not seem to work. An alternative would be the use of a chiral monomer.

Considering the two processes suggested, some calculations can be done in terms of membrane area for NF, quantity of resins and volume of organic solvents.

Considering 3500 L per batch of wastewater, a UF is used first to concentrate the wastewater up to 90%, and then the 3150 L permeate obtained are subjected to nanofiltration. Two nanofiltration operations should be done: in the first one, the feed is concentrated up to 50% (1575 L of permeate and retentate). Then, the retentate is subjected to another NF and concentrated up to 70%. By the end of both NF processes, 2677.5 L of clean water are obtained, and 472.5 L of retentate are available for lupanine recovery. For the first NF, a flux equal to $11.53 \text{ L h}^{-1}\text{m}^{-2}$ and a 24 hours process to filtrate 3150 L gives a membrane area equal to 11.38 m^2 . For the second NF, a flux equal to $5.34 \text{ L h}^{-1}\text{m}^{-2}$ and a 24 hours process to filtrate 1575 L gives a membrane area equal to 12.29 m^2 (Figure 42).

If, after the filtration processes, 472.5 L of retentate are obtained for lupanine recovery, then 141.75 kg of resin are needed and 472.5 L of organic solvent are necessary for liquid-liquid extractions.

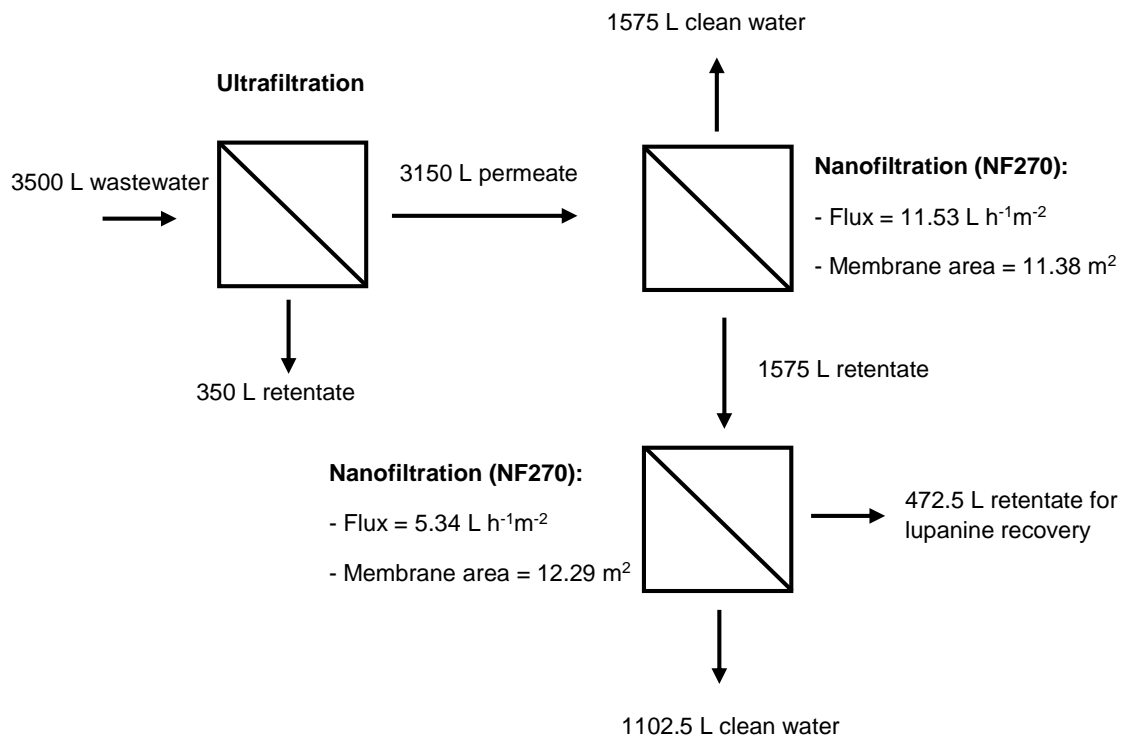


Figure 42. Sequence of filtrations that compose the first part of the process to recover lupanine. The approximate volume values obtained in each fraction are indicated, considering an initial value of 3500 L. membrane areas were calculated for 24 hours and considering the fluxes indicated.

5. Conclusions and Future Work

It was possible to suggest two membrane-based processes to isolate lupanine from lupin beans debittering wastewater, that include also resins, liquid-liquid extractions and MIPs. The processes are composed by a centrifugation, ultrafiltration, nanofiltration, and the resultant retentate can be applied to either a polymeric resin (XAD-16) or to an ion exchange resin (Dowex MAC-3), followed by a liquid-liquid extraction. MIPs constitute the last unit operation of the processes.

A different ultrafiltration membrane, with MWCO lower than 3000 Da should be tested for organic matter retention and fouling mitigation, since the flux decay of the nanofiltration concentration experiments was significant.

MIPs obtained with IA and MAA, showed promising results for racemic lupanine. IA was selected to synthesize a chiral MIP, using a lupanine enantiomer as template, but the polymer did not exhibit enantioselectivity. An alternative to be explored is the synthesis of a chiral using a chiral monomer, to be included in the process as an enantioselective unit. MIPs regeneration protocol should also be improve for efficient lupanine recovery and polymer reuse.

6. References

- [1] I. I. Koleva, T. A. van Beek, A. E. M. F. Soffers, B. Dusemund, and I. M. C. M. Rietjens, "Alkaloids in the human food chain - natural occurrence and possible adverse effects," *Mol. Nutr. Food Res.*, vol. 56, no. 1, pp. 30–52, 2012.
- [2] F. M. C. Santana, A. M. Fialho, I. Sá-Correia, and J. M. A. Empis, "Isolation of bacterial strains capable of using lupanine, the predominant quinolizidine alkaloid in white lupin, as sole carbon and energy source," *J. Ind. Microbiol. Biotechnol.*, vol. 17, no. 2, pp. 110–115, 1996.
- [3] H. Reinhard, H. Rupp, F. Sager, M. Streule, and O. Zoller, "Quinolizidine alkaloids and phomopsins in lupin seeds and lupin containing food," *J. Chromatogr. A*, vol. 1112, no. 1–2, pp. 353–360, 2006.
- [4] D. J. Hopper and M. A. Kaderbhai, "The quinohaemoprotein lupanine hydroxylase from *Pseudomonas putida*," *Biochim. Biophys. Acta - Proteins Proteomics*, vol. 1647, no. 1–2, pp. 110–115, 2003.
- [5] M. Ganzera, A. Krüger, and M. Wink, "Determination of quinolizidine alkaloids in different *Lupinus* species by NACE using UV and MS detection," *J. Pharm. Biomed. Anal.*, vol. 53, no. 5, pp. 1231–1235, 2010.
- [6] A. Aiello, E. Fattorusso, M. Menna, and O. Tagliatalata-Scafati, *Modern Alkaloids*. Wiley-VCH, 2007.
- [7] T. Aniszewski, *Alkaloids - Secrets of Life*. Elsevier, 2007.
- [8] M. Wink, "Interference of alkaloids with neuroreceptors and ion channels," *Stud. Nat. Prod. Chem.*, vol. 21, no. PART B, pp. 3–122, 2000.
- [9] K. Saito, Y. Koike, H. Suzuki, and I. Murakoshi, "Biogenetic implication of lupin alkaloid biosynthesis in bitter and sweet forms of *Lupinus luteus* and *L. albus*," *Phytochemistry*, vol. 34, no. 4, pp. 1041–1044, 1993.
- [10] S. Bunsupa, M. Yamazaki, and K. Saito, "Quinolizidine alkaloid biosynthesis: recent advances and future prospects," *Front. Plant Sci.*, vol. 3, no. October, p. 239, 2012.
- [11] M. Wiedemann, C. M. Gurrola-Díaz, B. Vargas-Guerrero, M. Wink, P. M. García-López, and M. Düfer, "Lupanine Improves Glucose Homeostasis by Influencing KATP Channels and Insulin Gene Expression," *Molecules*, vol. 20, no. 10, pp. 19085–19100, 2015.
- [12] C. Barbeitos, 2016, "Towards the development of a process for lupin beans detoxification wastewater with lupanine recovery." Master thesis in Biological Engineering, Instituto Superior Técnico, Universidade de Lisboa.
- [13] T. Bobkiewicz-Kozłowska, M. Dworacka, S. Kuczyński, M. Abramczyk, R. Kolanoś, W. Wysocka, P. M. Garcia Lopez, and H. Winiarska, "Hypoglycaemic effect of quinolizidine alkaloids - lupanine and 2-thionosparteine on non-diabetic and streptozotocin-induced diabetic rats," *Eur. J. Pharmacol.*, vol. 565, no. 1–3, pp. 240–244, 2007.
- [14] P. M. García López, P. G. De La Mora, W. Wysocka, B. Maiztegui, M. E. Alzugaray, H. Del Zotto, and M. I. Borelli, "Quinolizidine alkaloids isolated from *Lupinus* species enhance insulin secretion," *Eur. J. Pharmacol.*, vol. 504, no. 1–2, pp. 139–142, 2004.

- [15] A. K. Przybył and M. Kubicki, "Simple and highly efficient preparation and characterization of (-)-lupanine and (+)-sparteine," *Tetrahedron*, vol. 67, no. 40, pp. 7787–7793, 2011.
- [16] N. M. Clark, P. García-Álvarez, A. R. Kennedy, C. T. O'Hara, and G. M. Robertson, "Reactions of (-)-sparteine with alkali metal HMDS complexes: conventional meets the unconventional," *Chem. Commun.*, no. 39, p. 5835, 2009.
- [17] A. R. Kennedy and C. T. O'Hara, "Isolation and characterisation of a (-)-sparteine coordinated mixed alkyl/amido sodium magnesiate, a chiral variant of an important utility ate base," *Dalt. Trans.*, no. 37, p. 4975, 2008.
- [18] H. Maheswaran, K. L. Prasanth, G. G. Krishna, K. Ravikumar, B. Sridhar, and M. L. Kantam, "Enantioselective nitroaldol (Henry) reaction using copper(II) complexes of (-)-sparteine.," *Chem. Commun. (Camb)*, pp. 4066–4068, 2006.
- [19] C. M. McSweeney, V. M. Foley, and G. P. McGlacken, "The asymmetric alkylation of dimethylhydrazones; intermolecular chirality transfer using sparteine as chiral ligand," *Chem. Commun.*, vol. 50, no. 94, pp. 14817–14819, 2014.
- [20] A. S. Batsanov, C. Grosjean, T. Schütz, and A. Whiting, "A (-)-sparteine-directed highly enantioselective synthesis of boroproline. Solid- and solution-state structure and properties," *J. Org. Chem.*, vol. 72, no. 16, pp. 6276–6279, 2007.
- [21] S. K. Ritter, "Where has all the sparteine gone?," *Chem. Eng. News*, vol. 95, no. 17, pp. 18–20, 2017.
- [22] J.-P. R. Hermet, M. J. McGrath, P. O'Brien, D. W. Porter, and J. Gilday, "Concise asymmetric synthesis of (-)-sparteine.," *Chem. Commun. (Camb)*, vol. 44, no. 16, pp. 1830–1, 2004.
- [23] J. D. Firth, P. O'Brien, and L. Ferris, "Revisiting the sparteine surrogate: development of a resolution route to the (-)-sparteine surrogate.," *Org. Biomol. Chem.*, vol. 12, no. 46, pp. 9357–65, 2014.
- [24] C. E. Housecroft and E. C. E. C. Constable, *Chemistry: An Introduction to Organic, Inorganic and Physical Chemistry*, 4th ed. Prentice Hall, 2010.
- [25] R. Chang, *Chemistry*, 10th ed. McGraw-Hill Education, 2010.
- [26] G. Gübitz and M. G. Schmid, "Chiral separation by chromatographic and electromigration techniques. A review," *Biopharm. Drug Dispos.*, vol. 22, no. 7–8, pp. 291–336, 2001.
- [27] M. P. Tiwari and A. Prasad, "Molecularly imprinted polymer based enantioselective sensing devices: A review," *Anal. Chim. Acta*, vol. 853, no. 1, pp. 1–18, 2015.
- [28] J. McConathy and M. J. Owens, "Stereochemistry in Drug Action," *Prim Care Companion J Clin Psychiatry*, vol. 5, no. 2, pp. 70–73, 2003.
- [29] M. D. Armstrong, "An Observation on a Partial Resolution of Racemic Compounds," *J. Am. Chem. Soc.*, vol. 1, no. 2, pp. 4456–4457, 1943.
- [30] A. Ghanem and H. Y. Aboul-Enein, "Application of lipases in kinetic resolution of racemates," *Chirality*, vol. 17, no. 1, pp. 1–15, 2005.
- [31] F. C. Ferreira, H. Macedo, U. Cocchini, and A. G. Livingston, "Development of a Liquid-Phase Process for Recycling Resolving Agents within Diastereomeric Resolution," 2006.
- [32] D. Perdicchia, M. S. Christodoulou, G. Fumagalli, F. Calogero, C. Marucci, and D. Passarella,

- “Enzymatic kinetic resolution of 2-piperidineethanol for the enantioselective targeted and diversity oriented synthesis,” *Int. J. Mol. Sci.*, vol. 17, no. 1, 2015.
- [33] K. M. Koeller and C. Wong, “Enzymes for chemical synthesis,” *Nature*, vol. 409, pp. 232–240, 2001.
- [34] S. Yang, Y. Wang, Y. Jiang, S. Li, and W. Liu, “Molecularly imprinted polymers for the identification and separation of chiral drugs and biomolecules,” *Polymers (Basel)*, vol. 8, no. 6, 2016.
- [35] J. Shen, T. Ikai, and Y. Okamoto, “Synthesis and application of immobilized polysaccharide-based chiral stationary phases for enantioseparation by high-performance liquid chromatography,” *J. Chromatogr. A*, vol. 1363, pp. 51–61, 2014.
- [36] M. Michaud, E. Jourdan, A. Villet, A. Ravel, C. Grosset, and E. Peyrin, “A DNA aptamer as a new target-specific chiral selector for HPLC,” *J. Am. Chem. Soc.*, vol. 125, no. 28, pp. 8672–8679, 2003.
- [37] J. Zhou, J. Tang, and W. Tang, “Recent development of cationic cyclodextrins for chiral separation,” *TrAC - Trends Anal. Chem.*, vol. 65, pp. 22–29, 2015.
- [38] S. Carmalia, V. D. Alves, I. M. Coelho, L. M. Ferreira, and A. M. Lourenço, “Recovery of lupanine from *Lupinus albus* L. leaching waters,” *Sep. Purif. Technol.*, vol. 74, no. 1, pp. 38–43, 2010.
- [39] H. K. Shon, S. Phuntsho, D. S. Chaudhary, S. Vigneswaran, and J. Cho, “Nanofiltration for water and wastewater treatment - A mini review,” *Drink. Water Eng. Sci.*, vol. 6, no. 1, pp. 47–53, 2013.
- [40] M. Mulder, *Basic Principles of Membrane Technology*. Springer, 1991.
- [41] a. W. Mohammad, Y. H. Teow, W. L. Ang, Y. T. Chung, D. L. Oatley-Radcliffe, and N. Hilal, “Nanofiltration membranes review: Recent advances and future prospects,” *Desalination*, vol. 356, pp. 226–254, 2015.
- [42] D. Alchin, “Ion Exchange Resins,” pp. 1–5, 2015.
- [43] P. Gogoi, N. N. Dutta, and P. G. Rao, “Adsorption of catechin from aqueous solutions on polymeric resins and activated carbon,” *Indian J. Chem. Technol.*, vol. 17, no. 5, pp. 337–345, 2010.
- [44] W. S. Miller, C. J. Castagna, and A. W. Pieper, “Understanding ion-exchange resins for water treatment systems,” *GE Water Process Technol.*, p. 1, 2009.
- [45] J. Zhang and B. Hu, “Liquid-Liquid Extraction (LLE),” in *Separation and Purification Technologies in Biorefineries*, 2013, pp. 61–78.
- [46] I. M. Smallwood, *Handbook of organic solvent properties*. 1996.
- [47] C. M. Alder, J. D. Hayler, R. K. Henderson, A. M. Redman, L. Shukla, L. E. Shuster, and H. F. Sneddon, “Updating and further expanding GSK’s solvent sustainability guide,” *Green Chem.*, vol. 18, no. 13, pp. 3879–3890, 2016.
- [48] R. K. Henderson, C. Jiménez-González, D. J. C. Constable, S. R. Alston, G. G. a. Inglis, G. Fisher, J. Sherwood, S. P. Binks, and A. D. Curzons, “Expanding GSK’s solvent selection guide – embedding sustainability into solvent selection starting at medicinal chemistry,” *Green Chem.*, vol. 13, pp. 854–862, 2011.

- [49] Y. Andersson-Sköld and L. Holmberg, "Photochemical ozone creation potentials (POCP) and replacement of solvents in Europe," *Atmos. Environ.*, vol. 34, no. 19, pp. 3159–3169, 2000.
- [50] A. Levet, C. Bordes, Y. Clément, P. Mignon, C. Morell, H. Chermette, P. Marote, and P. Lantéri, "Acute aquatic toxicity of organic solvents modeled by QSARs," *J. Mol. Model.*, vol. 22, no. 12, 2016.
- [51] A. McCluskey, C. I. Holdsworth, and M. C. Bowyer, "Molecularly imprinted polymers (MIPs): sensing, an explosive new opportunity?," *Org. Biomol. Chem.*, vol. 5, no. 20, pp. 3233–44, 2007.
- [52] a. Beltran, F. Borrell, R. M. Marcé, and P. a G. Cormack, "Molecularly-imprinted polymers: Useful sorbents for selective extractions," *TrAC - Trends Anal. Chem.*, vol. 29, no. 11, pp. 1363–1375, 2010.
- [53] a. G. Mayes and M. J. Whitcombe, "Synthetic strategies for the generation of molecularly imprinted organic polymers," *Adv. Drug Deliv. Rev.*, vol. 57, no. 12, pp. 1742–1778, 2005.
- [54] H. Yan and K. Ho Row, "Characteristic and Synthetic Approach of Molecularly Imprinted Polymer," *Int. J. Mol. Sci.*, vol. 7, pp. 155–178, 2006.
- [55] N. M. Maier and W. Lindner, "Chiral recognition applications of molecularly imprinted polymers: A critical review," *Anal. Bioanal. Chem.*, vol. 389, no. 2, pp. 377–397, 2007.
- [56] W. Ji, X. Ma, H. Xie, L. Chen, X. Wang, H. Zhao, and L. Huang, "Molecularly imprinted polymers with synthetic dummy template for simultaneously selective removal and enrichment of ginkgolic acids from Ginkgo biloba L. leaves extracts," *J. Chromatogr. A*, vol. 1368, pp. 44–51, 2014.
- [57] J. Matsui, K. Fujiwara, and T. Takeuchi, "Atrazine-selective polymers prepared by molecular imprinting of Trialkylmelamines as dummy template species of atrazine," *Anal. Chem.*, vol. 72, no. 8, pp. 1810–1813, 2000.
- [58] Y. M. Yin, Y. P. Chen, X. F. Wang, Y. Liu, H. L. Liu, and M. X. Xie, "Dummy molecularly imprinted polymers on silica particles for selective solid-phase extraction of tetrabromobisphenol A from water samples," *J. Chromatogr. A*, vol. 1220, pp. 7–13, 2012.
- [59] L. Chen, X. Wang, W. Lu, X. Wu, and J. Li, "Molecular imprinting: perspectives and applications," *Chem. Soc. Rev.*, vol. 45, no. 8, pp. 2137–2211, 2016.
- [60] M. Kempe, L. Fischert, and K. Mosbach, "Chiral Separation Using Molecularly Imprinted Heteroaromatic Polymers," vol. 6, pp. 25–29, 1993.
- [61] J. Matsui, I. A. Nicholls, and T. Takeuchi, "Molecular recognition in cinchona alkaloid molecular imprinted polymer rods," *Anal. Chim. Acta*, vol. 365, no. 1–3, pp. 89–93, 1998.
- [62] J. Matsui, O. Doblhoff-Dier, and T. Takeuchi, "2-(Trifluoromethyl)acrylic acid: A novel functional monomer in non-covalent molecular imprinting," *Anal. Chim. Acta*, vol. 343, no. 1–2, pp. 1–4, 1997.
- [63] B. Sellergren, "Imprinted chiral stationary phases in high-performance liquid chromatography.," *J. Chromatogr. A*, vol. 906, pp. 227–252, 2001.
- [64] R. J. Ansell, "Molecularly imprinted polymers for the enantioseparation of chiral drugs," *Adv. Drug Deliv. Rev.*, vol. 57, no. 12, pp. 1809–1835, 2005.
- [65] J. J. Torres, N. Gsponer, C. L. Ramírez, D. M. a Vera, H. a. Montejano, and C. a. Chesta, "Experimental and theoretical studies on the enantioselectivity of molecularly imprinted polymers

- prepared with a chiral functional monomer," *J. Chromatogr. A*, vol. 1266, pp. 24–33, 2012.
- [66] M. Knutsson, H. S. Andersson, and I. a Nicholls, "Novel chiral recognition elements for molecularly imprinted polymer preparation.," *J. Mol. Recognit.*, vol. 11, no. 1–6, pp. 87–90, 1998.
- [67] K. Hosoya, Y. Shirasu, K. Kimata, and N. Tanaka, "Molecularly Imprinted Chiral Stationary Phase Prepared with Racemic Template," *Anal. Chem.*, vol. 70, no. 5, pp. 943–945, 1998.
- [68] R. Ouyang, J. Lei, H. Ju, and Y. Xue, "A molecularly imprinted copolymer designed for enantioselective recognition of glutamic acid," *Adv. Funct. Mater.*, vol. 17, no. 16, pp. 3223–3230, 2007.
- [69] O. Ramstrom, C. Yu, K. Mosbach, and O. Ramström, "Chiral Recognition in Adrenergic Receptor Binding Mimics Prepared by Molecular Imprinting," *J. Mol. Recognit.*, vol. 9, no. 5–6, pp. 691–696, 1996.
- [70] J. Haginaka and C. Kagawa, "Uniformly sized molecularly imprinted polymer for Evaluation of retention and molecular recognition properties in an aqueous mobile phase," *J. Chromatogr. A*, vol. 948, pp. 77–84, 2002.
- [71] G. Vasapollo, R. Del Sole, L. Mergola, M. R. Lazzoi, A. Scardino, S. Scorrano, and G. Mele, "Molecularly imprinted polymers: Present and future prospective," *Int. J. Mol. Sci.*, vol. 12, no. 9, pp. 5908–5945, 2011.
- [72] S. Korposh, I. Chianella, A. Guerreiro, S. Caygill, S. Piletsky, S. W. James, and R. P. Tatam, "Selective vancomycin detection using optical fibre long period gratings functionalised with molecularly imprinted polymer nanoparticles," *Analyst*, vol. 139, no. 9, pp. 2229–2236, 2014.
- [73] W. J. Cheong, S. H. Yang, and F. Ali, "Molecular imprinted polymers for separation science: A review of reviews," *J. Sep. Sci.*, vol. 36, no. 3, pp. 609–628, 2013.
- [74] W. Cai and R. B. Gupta, "Molecularly-imprinted polymers selective for tetracycline binding," *Sep. Purif. Technol.*, vol. 35, no. 3, pp. 215–221, 2004.
- [75] R. Suedee, "Enantioselective Release of Controlled Delivery Granules Based on Molecularly Imprinted Polymers," *Drug Deliv.*, vol. 9, no. 1, pp. 19–30, 2002.
- [76] M. Giel-Pietraszuk, Z. Gdaniec, T. Brukwicki, and J. Barciszewski, "Molecular mechanism of high pressure action on lupanine," *J. Mol. Struct.*, vol. 826, no. 2–3, pp. 120–125, 2007.
- [77] R. R. Himebaugh and M. J. Smith, "Semi-Micro Tube Method for Chemical Oxygen Demand," *Anal. Chem.*, vol. 51, no. 7, pp. 1085–1087, 1979.
- [78] H. M. Do Monte, M. T. Santos, A. M. Barreiros, and A. Albuquerque, *Tratamento de Águas Residuais - Operações e Processos de Tratamento Físico e Químico*. 2016.

Annexes

A. Calibration curves

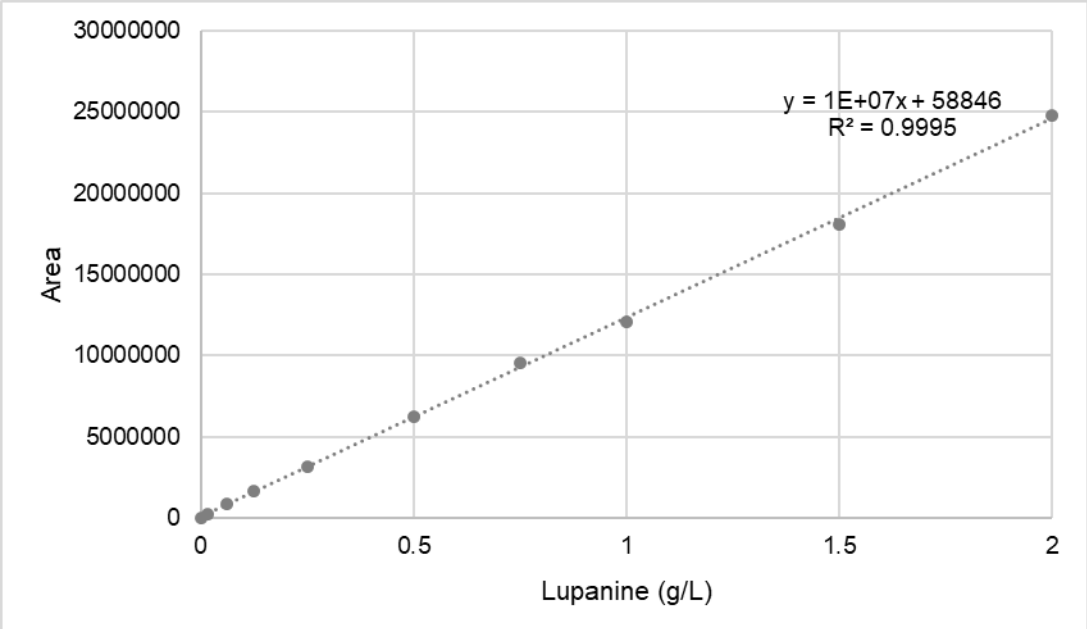


Figure 43. Calibration curve for concentrations between 0.00145 and 2 g/L.

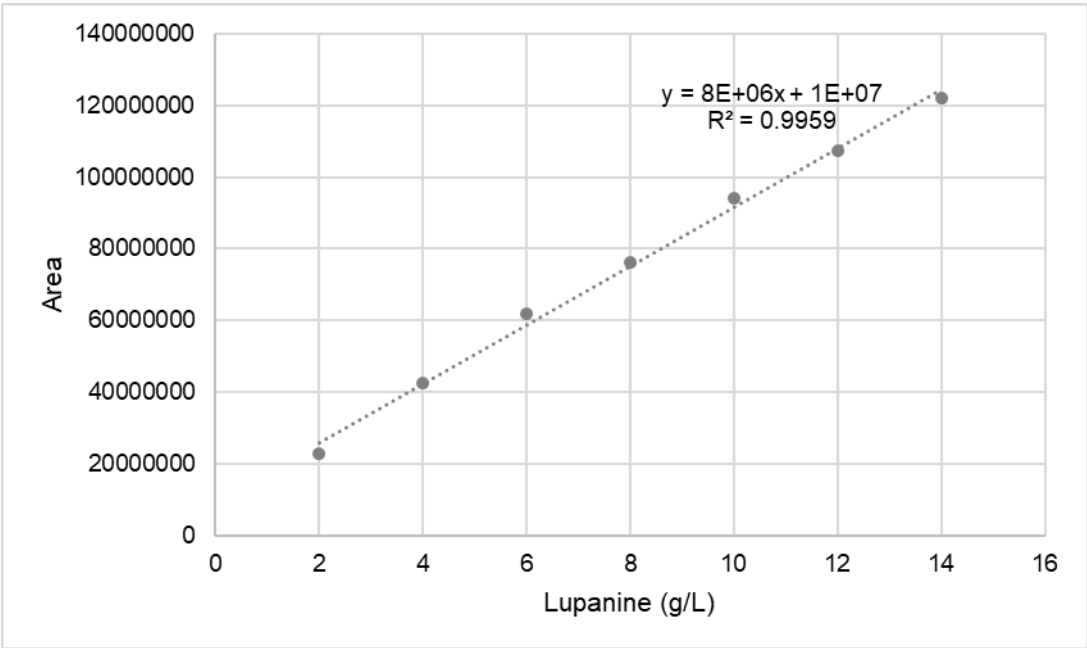


Figure 44 Calibration curve for concentrations higher than 2 g/L and equal or lower than 14 g/L..

B. Chromatograms

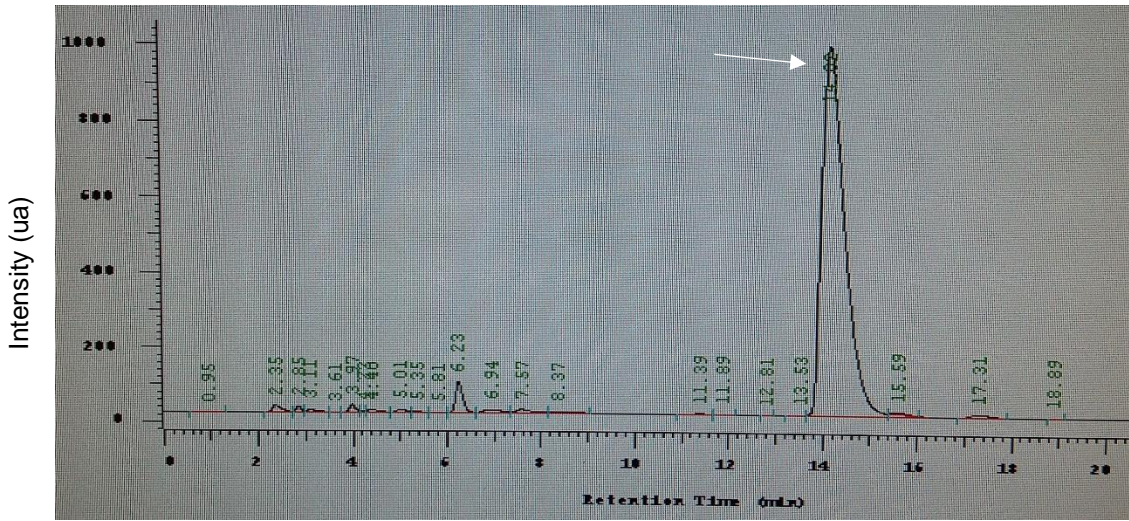


Figure 45. Typical chromatogram obtained for a solution of lupanine in water (approximately 3 g/L). the arrow signalizes the peak correspondent to lupanine.

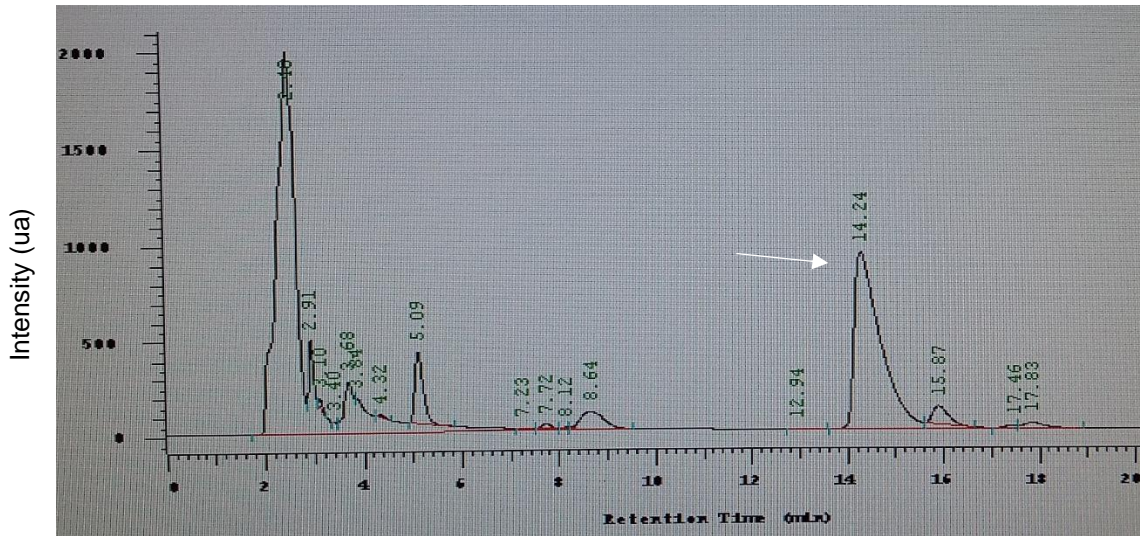


Figure 46. Typical chromatogram obtained for phase 3. The arrow signalizes the peak correspondent to lupanine.

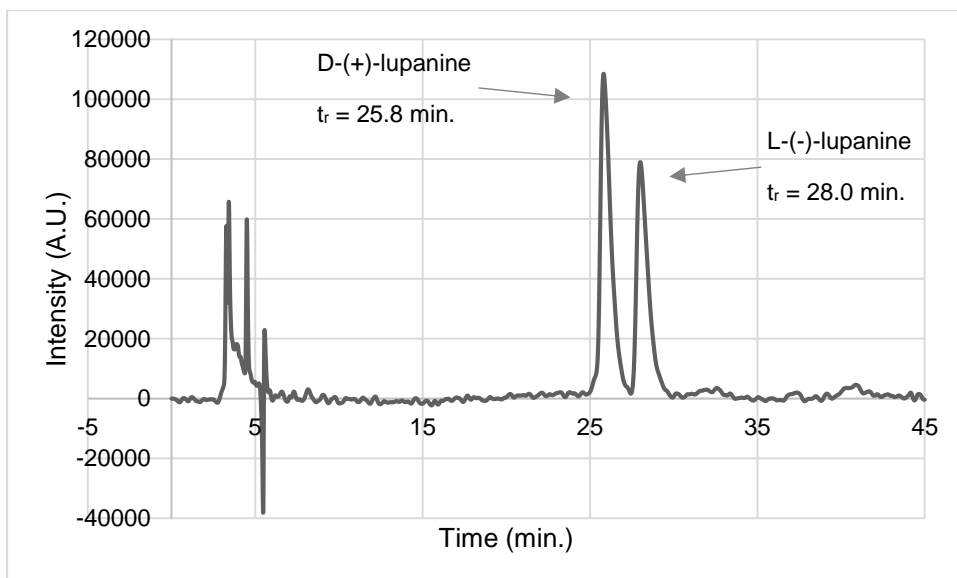


Figure 47. Chromatogram obtained for the injection of a sample after the binding assays with the IA NIP. Both (L)-(-)- and (D)-(+)-lupanine retention times (t_r) are indicated.

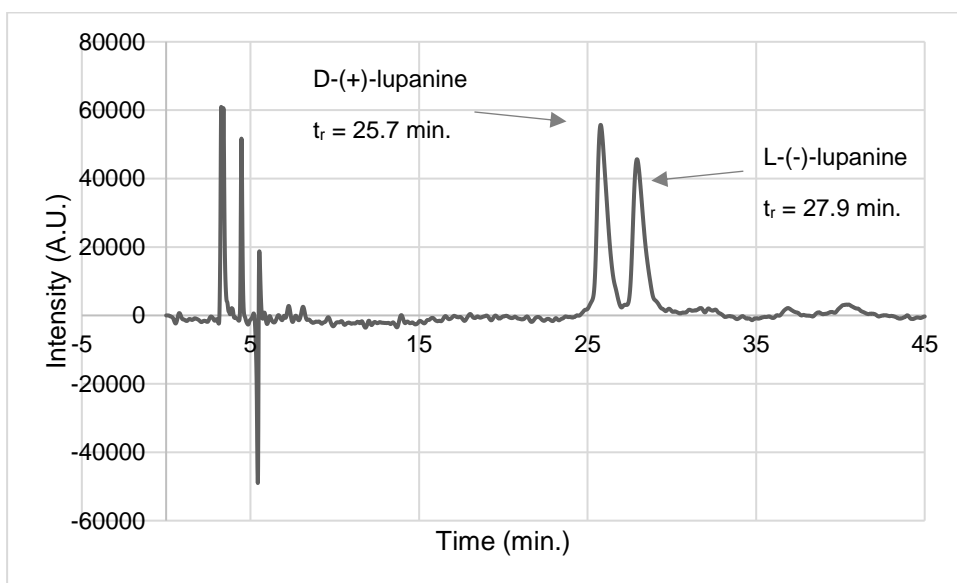


Figure 48. Chromatogram obtained for the injection of a sample after the binding assays with the IA chiral MIP. Both (L)-(-)- and (D)-(+)-lupanine retention times (t_r) are indicated.

C. Recirculation experiments

Table 18. Conductivity and pH values for both permeate and retentate recovered after the filtration of 100 mL and both permeate and retentate recovered after the recirculation experiments.

Sample	Recirculation 20 bar; 420 mL/min.		Recirculation 20 bar; 600 mL/min.	
	pH	Conductivity (μS)	pH	Conductivity (μS)
Initial	5.94	4300	4.40	5900
Retentate after filtration of 100 mL	5.99	6180	4.39	6850
Retentate after 13 h of recirculation	5.23	7070	4.40	7000
Permeate after filtration of 100 mL	5.03	124.5	3.49	250
Permeate after 13 h of recirculation	4.10	152.2	3.40	229

D. Langmuir and Freundlich Isotherms

The Langmuir model rely on four conditions that must be satisfied by the adsorption system: all adsorption sites are independent and of equal adsorption energy; only one molecule of solute can bind each adsorption site; there is no interaction between the solute molecules and the adsorption process must be reversible. This model is based on the formation of a monolayer of solutes adsorbed on the sorbent surface, that contains a finite number of adsorption sites.

The amount of lupanine adsorbed per unit mass of adsorbent (resin) (mg/g) is given by the following equation:

$$q_e = \frac{q_{\max} \times K_L \times c_e}{1 + K_L \times c_e} \quad (25)$$

In this equation q_{\max} is the maximum adsorption capacity (mg/g) and K_L is a Langmuir constant (related to the free energy of adsorption (g/L)).

The previous equation is linearized, and both q_{\max} and K_L can be found using the linear regression of the model:

$$\frac{c_e}{q_e} = \frac{1}{q_{\max} \times K_L} + \frac{c_e}{q_{\max}} \quad (26)$$

q_e in the previous equation was calculated by equation 16 for each c_e . Then, the linear regression was obtained for each resin (Figures 49 and 50) and the slope corresponds to $1/q_{\max}$ whereas

the intersection of the y-axis gives the value of $1/(q_{\max} + K_L)$. q_{\max} and K_L values obtained for each resin are indicated in table 19.

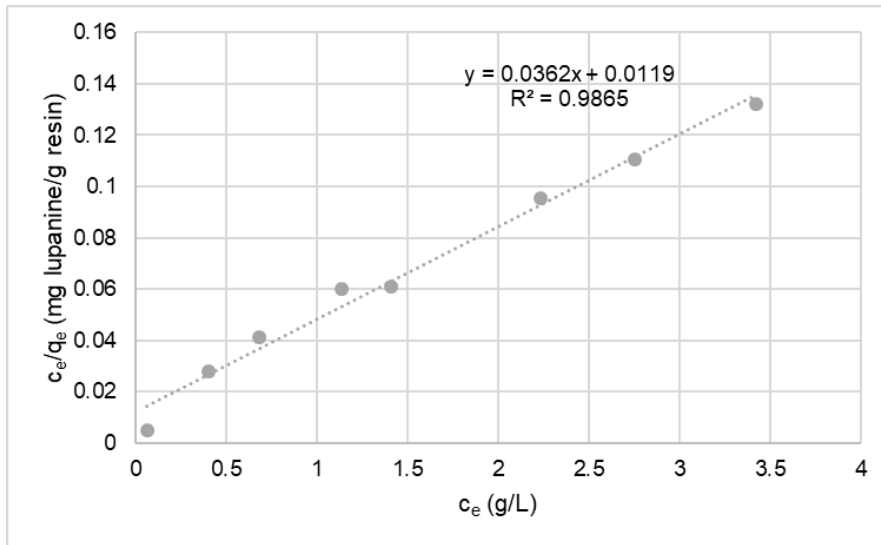


Figure 49. Langmuir linear regression obtained for XAD-16, by representing each c_e/q_e values as a function of c_e values. The equation of the linear regression and the value of R^2 are also indicated.

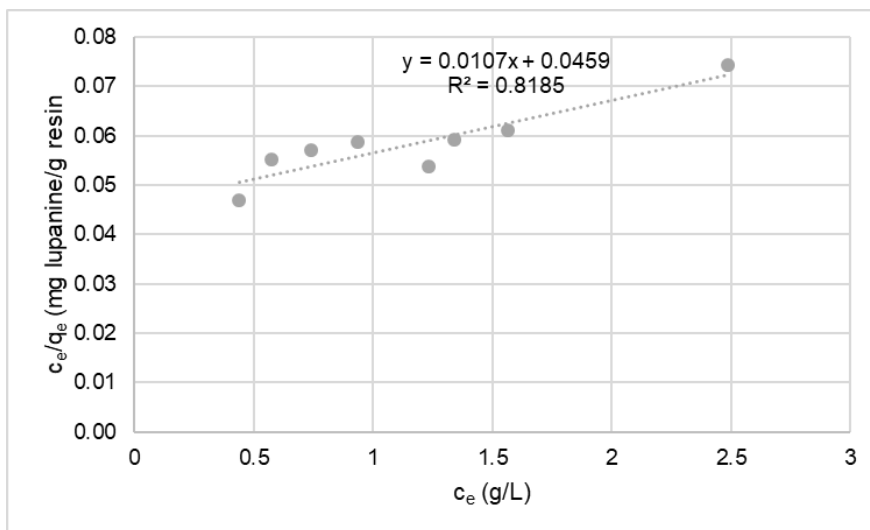


Figure 50. Langmuir linear regression obtained for Dowex MAC-3, by representing each c_e/q_e values as a function of c_e values. The equation of the linear regression and the value of R^2 are also indicated.

Table 19. Langmuir parameters (q_{\max} and K_L) for both XAD-16 and Dowex MAC-3, calculated from the equation of the linear regressions (Figures 49 and 50).

Resin/Parameter	q_{\max} (mg/g)	K_L (g/L)
XAD-16	27.62	3.04
Dowex MAC-3	72.99	0.35

The values contained in table 19 were then utilized to obtain q_e values for each c_e according to equation 25, and the results are presented in Figure 32, section 4.1.3.3.

Freundlich model assumes that a multilayer of solute molecules is formed on heterogeneous surfaces, and it is given by the following equation:

$$q_e = K_F c_e^{1/n} \quad (27)$$

In this equation, q_e is the amount of lupanine adsorbed per unit mass of resin (mg/g), K_F is a Freundlich constant (related to the relative adsorption capacity of the adsorbent (mg/g)), c_e is the equilibrium concentration of lupanine (g/L) and $1/n$ is a heterogeneity factor.

The previous equation is linearized, and both n and K_F can be found using the linear regression of the model:

$$\ln(q_e) = \ln(K_F) + \frac{1}{n} \times \ln(c_e) \quad (28)$$

q_e in the previous equation was calculated by equation 17 (see section 4.1.3.1.) for each c_e . Then, the linear regression was obtained for each resin (Figures 51 and 52) and the slope corresponds to $1/n$ whereas the intersection of the y-axis gives the value of $\ln(K_F)$. $1/n$ and K_F values obtained for each resin are indicated in table 20.

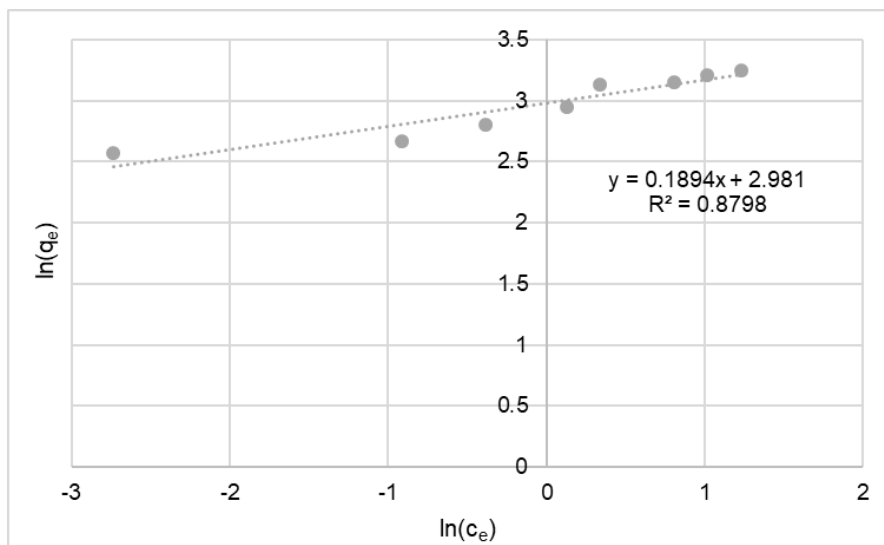


Figure 51. Freundlich linear regression obtained for XAD-16, by representing each c_e/q_e values as a function of c_e values. The equation of the linear regression and the value of R^2 are also indicated.

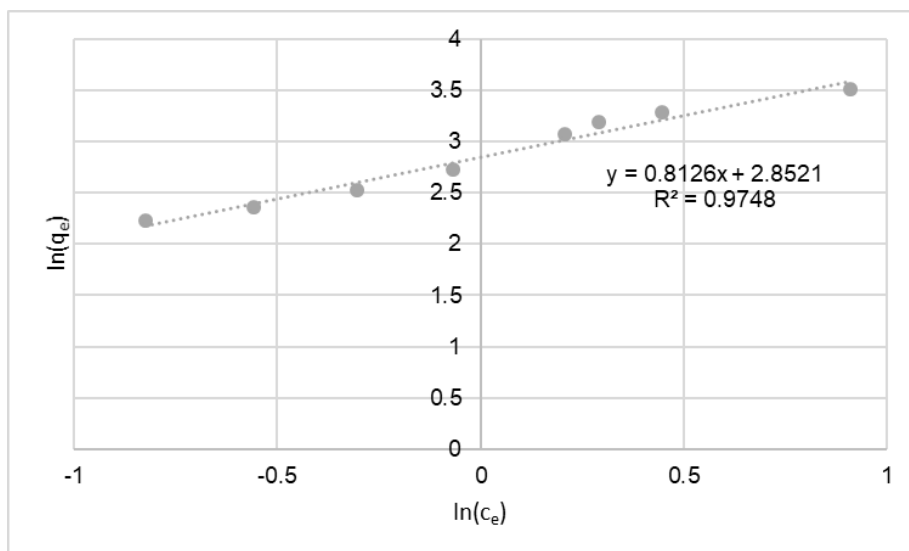


Figure 52. Freundlich linear regression obtained for Dowex MAC-3, by representing each c_e/q_e values as a function of c_e values. The equation of the linear regression and the value of R^2 are also indicated.

Table 20. Freundlich parameters (n and K_F) for both XAD-16 and Dowex MAC-3, calculated from the equation of the linear regressions (Figures 51 and 52).

Resin/Parameter	n	K_F
XAD-16	5.28	19.71
Dowex MAC-3	1.15	18.23

The values contained in table 20 were then utilized to obtain q_e values for each c_e according to equation 27, and the results are presented in Figure 33, section 4.1.3.3.